

# Recommendations for Cardiac Chamber Quantification by Echocardiography in Adults: An Update from the American Society of Echocardiography and the European Association of Cardiovascular Imaging

Roberto M. Lang, MD, FASE, FESC, Luigi P. Badano, MD, PhD, FESC, Victor Mor-Avi, PhD, FASE, Jonathan Afilalo, MD, MSc, Anderson Armstrong, MD, MSc, Laura Ernande, MD, PhD, Frank A. Flachskampf, MD, FESC, Elyse Foster, MD, FASE, Steven A. Goldstein, MD, Tatiana Kuznetsova, MD, PhD, Patrizio Lancellotti, MD, PhD, FESC, Denisa Muraru, MD, PhD, Michael H. Picard, MD, FASE, Ernst R. Rietzschel, MD, PhD, Lawrence Rudski, MD, FASE, Kirk T. Spencer, MD, FASE, Wendy Tsang, MD, and Jens-Uwe Voigt, MD, PhD, FESC, *Chicago, Illinois; Padua, Italy; Montreal, Quebec and Toronto, Ontario, Canada; Baltimore, Maryland; Créteil, France; Uppsala, Sweden; San Francisco, California; Washington, District of Columbia; Leuven, Liège, and Ghent, Belgium; Boston, Massachusetts*

The rapid technological developments of the past decade and the changes in echocardiographic practice brought about by these developments have resulted in the need for updated recommendations to the previously published guidelines for cardiac chamber quantification, which was the goal of the joint writing group assembled by the American Society of Echocardiography and the European Association of Cardiovascular Imaging. This document provides updated normal values for all four cardiac chambers, including three-dimensional echocardiography and myocardial deformation, when possible, on the basis of considerably larger numbers of normal subjects, compiled from multiple databases. In addition, this document attempts to eliminate several minor discrepancies that existed between previously published guidelines. (J Am Soc Echocardiogr 2015;28:1-39.)

**Keywords:** Adult echocardiography, Transthoracic echocardiography, Ventricular function, Normal values

From the University of Chicago Medical Center, Chicago, Illinois (R.M.L., V.M.-A., K.T.S.); the University of Padua, Padua, Italy (L.P.B., D.M.); Jewish General Hospital, McGill University, Montreal, Quebec, Canada (J.A., L.R.); Johns Hopkins University, Baltimore, Maryland (A.A.); INSERM U955 and Hôpital Henri Mondor, Créteil, France (L.E.); Uppsala University, Uppsala, Sweden (F.A.F.); the University of California, San Francisco, San Francisco, California (E.F.); Medstar Washington Hospital Center, Washington, District of Columbia (S.A.G.); University Hospital Leuven, Leuven, Belgium (T.K., J.-U.V.); the University of Liège Hospital, Liège, Belgium (P.L.); Massachusetts General Hospital and Harvard Medical School, Boston, Massachusetts (M.H.P.); Ghent University Hospital, Ghent, Belgium (E.R.R.); and the University of Toronto, Toronto, Ontario, Canada (W.T.).

The following authors reported no actual or potential conflicts of interest in relation to this document: Jonathan Afilalo, MD, MSc, Anderson Armstrong, MD, MSc, Laura Ernande, MD, PhD, Frank A. Flachskampf, MD, FESC, Steven A. Goldstein, MD, Tatiana Kuznetsova, MD, PhD, Patrizio Lancellotti, MD, PhD, FESC, Victor Mor-Avi, PhD, FASE, Michael H. Picard, MD, FASE, Ernst R. Rietzschel, MD, PhD, Kirk T. Spencer, MD, FASE, Wendy Tsang, MD, and Jens-Uwe Voigt, MD, PhD, FESC. The following authors reported relationships with one or more commercial interests: Luigi P. Badano, MD, PhD, FESC, received grants from GE Healthcare, Siemens, and Esaote and serves on the speakers' bureau for GE

Healthcare. Elyse Foster, MD, FASE, received grant support from Abbott Vascular Structural Heart. Roberto M. Lang, MD, FASE, FESC, received grants from and serves on the speakers' bureau and advisory board for Philips Medical Systems. Denisa Muraru, MD, received research equipment from and served as a consultant for GE Healthcare. Lawrence Rudski, MD, FASE, holds stock in GE.

#### Attention ASE Members:

The ASE has gone green! Visit [www.aseuniversity.org](http://www.aseuniversity.org) to earn free continuing medical education credit through an online activity related to this article. Certificates are available for immediate access upon successful completion of the activity. Nonmembers will need to join the ASE to access this great member benefit!

Drs Lang and Badano co-chaired the Writing Group.

Reprint requests: American Society of Echocardiography, 2100 Gateway Centre Boulevard, Suite 310, Morrisville, NC 27560 (E-mail: [ase@asecho.org](mailto:ase@asecho.org)).

0894-7317/\$36.00

Copyright 2015 by the American Society of Echocardiography.

<http://dx.doi.org/10.1016/j.echo.2014.10.003>

## Abbreviations

<b>AP</b> = Anteroposterior
<b>ASE</b> = American Society of Echocardiography
<b>BSA</b> = Body surface area
<b>CMR</b> = Cardiac magnetic resonance
<b>DTI</b> = Doppler tissue imaging
<b>EACVI</b> = European Association of Cardiovascular Imaging
<b>EDV</b> = End-diastolic volume
<b>EF</b> = Ejection fraction
<b>ESV</b> = End-systolic volume
<b>FAC</b> = Fractional area change
<b>GLS</b> = Global longitudinal strain
<b>I-I</b> = Inner edge-to-inner edge
<b>IVC</b> = Inferior vena cava
<b>LA</b> = Left atrial
<b>L-L</b> = Leading edge-to-leading edge
<b>LV</b> = Left ventricular
<b>MDCT</b> = Multidetector computed tomography
<b>PW</b> = Pulsed-wave
<b>RA</b> = Right atrial
<b>RIMP</b> = Right ventricular index of myocardial performance
<b>RV</b> = Right ventricular
<b>RWT</b> = Relative wall thickness
<b>STE</b> = Speckle-tracking echocardiography
<b>TAPSE</b> = Tricuspid annular plane systolic excursion
<b>TAVI</b> = Transcatheter aortic valve implantation
<b>TAVR</b> = Transcatheter aortic valve replacement
<b>TEE</b> = Transesophageal echocardiography
<b>3D</b> = Three-dimensional
<b>3DE</b> = Three-dimensional echocardiography
<b>TTE</b> = Transthoracic echocardiography
<b>2D</b> = Two-dimensional
<b>2DE</b> = Two-dimensional echocardiography

## TABLE OF CONTENTS

I. The Left Ventricle	3
1. Measurement of LV Size	3
1.1. Linear Measurements	3
1.2. Volumetric Measurements	3
1.3. Normal Reference Values for 2DE	6
1.4. Normal Reference Values for 3DE	6
Recommendation	6
2. LV Global Systolic Function	6
2.1. Fractional Shortening	6
2.2. EF	7
2.3. Global Longitudinal Strain (GLS)	7
2.4. Normal Reference Values	7
Recommendations	10
3. LV Regional Function	10
3.1. Segmentation of the Left Ventricle	10
3.2. Visual Assessment	11
3.3. Regional Wall Motion during Infarction and Ischemia	11
3.4. Regional Abnormalities in the Absence of Coronary Artery Disease	11
3.5. Quantification of Regional Wall Motion Using Doppler and STE	11
Recommendations	12
4. LV Mass	13
Recommendations	16
II. The Right Ventricle	16
5. General Recommendations for RV Quantification	16
6. Essential Imaging Windows and Views	16
7. RV Measurements	17
7.1. Linear Measurements	17
7.2. Volumetric Measurements	17
Recommendations	17
8. RV Systolic Function	19
8.1. RIMP	19
8.2. TAPSE	19
8.3. RV 2D FAC	19
8.4. DTI-Derived Tricuspid Lateral Annular Systolic Velocity	20
8.5. RV Strain and Strain Rate	20
Recommendations	20
8.6. RV 3D EF	20
Recommendation	20
III. The Left and Right Atria	20
9. LA Measurements	24
9.1. General Considerations for LA Size	24
9.2. Linear Dimensions and Area Measurements	25
9.3. Volume Measurements	25
9.4. Normal Values of LA Measurements	25
Recommendations	28
10. Right Atrial measurements	28
Recommendations	28
IV. The Aortic Annulus and Aortic Root	28
11. The Aortic Annulus	28
12. The Aortic Root	30
13. Identification of Aortic Root Dilatation	32
Recommendations	32
V. The Inferior Vena Cava	32
Notice and Disclaimer	33
References	33
Appendix	39.e1
Methods	39.e1
Echocardiographic Measurements	39.e1
Statistical Analysis	39.e1

The quantification of cardiac chamber size and function is the cornerstone of cardiac imaging, with echocardiography being the most commonly used noninvasive modality because of its unique ability to provide real-time images of the beating heart, combined with its availability and portability. Standardization of the methodology used to quantify cardiac chambers is maintained by creating and disseminating official recommendations, which when followed by practitioners provides uniformity and facilitates communication. Recommendations for echocardiographic chamber quantification were last published in 2005 by the American Society of Echocardiography (ASE) and the European Association of Echocardiography (renamed the European Association of Cardiovascular Imaging [EACVI]).<sup>1,2</sup>

Since then, echocardiographic technology has continued evolving, with two major developments being real-time three-dimensional (3D) echocardiography (3DE) and myocardial deformation imaging. The goal of this document is to provide an update to the previously published guidelines, as well as recommendations and reference values, while eliminating the minor discrepancies that existed between previous guidelines. The normal values in this update include 3DE and myocardial deformation, when possible. Importantly, compared with the previous guidelines, this update is based on considerably larger numbers of normal subjects, compiled from multiple databases, to improve the reliability of the reference values.

Although most issues covered in this document reflect a broad consensus among the members of the writing group, one important issue the group debated was partition values for severity of abnormalities. Most often, in addition to describing a parameter as normal or abnormal (reference values), clinical echocardiographers qualify the degree of abnormality with terms such as *mildly*, *moderately*, and

*severely* abnormal, which reflect the degree to which measurements deviate from normal. In addition to providing normative data, it would be beneficial to standardize cutoffs for severity of abnormality for all parameters across echocardiography laboratories, such that the term *moderately abnormal*, for example, would have the same meaning universally. However, different approaches may be used for determining cutoff values for the different degrees of abnormality, all of which have significant limitations.

The first approach would be to empirically define cutoffs for mild, moderate, and severe abnormalities on the basis of SDs above or below the reference limit derived from a group of healthy people. The advantage of this method is that these data readily exist for most echocardiographic parameters. However, this approach is fundamentally flawed. First, not all echocardiographic parameters are normally distributed (or Gaussian), even in a normal population. Second, even if a particular parameter is normally distributed in normal subjects, most echocardiographic parameters, when measured in the general population, have a significant asymmetric distribution in one direction (abnormally large for size or abnormally low for function parameters). An alternative method would be to define abnormalities on the basis of percentile values (e.g., 95th, 99th) of measurements derived from a population that includes both healthy people and those with disease. Although these data would still not be normally distributed, they would account for the asymmetric distribution and the range of abnormality present within the general population. The major limitation of this approach is that such population data sets simply do not exist for most echocardiographic variables.

Ideally, an approach that predicts outcomes or prognosis would be preferred. That is, defining a variable as moderately deviated from normal would imply that there is a moderate risk for a particular adverse outcome for a patient. Although sufficient data linking risk and cardiac chamber sizes exist for several parameters (e.g., left ventricular [LV] size and ejection fraction [EF], left atrial [LA] volume), outcomes data are lacking for many other parameters. Unfortunately, this approach also has limitations. The first obstacle is how to best define risk. The cutoffs suggested for the same parameter vary broadly for different risks in different patient populations and disease states.

Last, cutoff values may be determined by experience-based consensus of expert opinions. An extensive debate arose among the members of the writing group, some of whom felt that providing partition values on the basis of this scientifically less-than-rigorous approach would be a disservice to the echocardiography community and that a disease-specific approach might be required to achieve meaningful clinical categorization of the severity of abnormality. Others felt that such cutoffs would provide a uniform reference for echocardiographic reporting, which would be easier to interpret by referring clinicians. The compromise was to provide experience-based partition values only for LV EF and LA volume, while suggested partition values for additional parameters of LV size and mass are listed in the [Appendix](#). All partition values should be interpreted with caution in this perspective.

For parameters other than LV size, function, and mass as well as LA volume, only the mean value and the SD of gender-, age-, and body surface area (BSA)-normalized cutoffs or upper and lower limits are reported in the appropriate sections of this document. For these parameters, measurements exceeding  $\pm 1.96$  SDs (i.e., the 95% confidence interval) should be classified as abnormal. Any description of the degree of deviation from normality in the

echocardiographic report should remain at the discretion of the individual laboratory, and the writing group does not recommend specific partition values.

Quantification using transesophageal echocardiography (TEE) has advantages and disadvantages compared with transthoracic echocardiography (TTE). Although visualization of many cardiac structures is improved with TEE, some differences in measurements have been found between TEE and TTE, particularly for chamber dimensions and thickness. These differences are primarily attributable to the inability to obtain from the transesophageal approach the standardized imaging planes and views used when quantifying chamber dimensions transthoracically. It is the recommendation of this writing group that the same range of normal values for LV and right ventricular (RV) chamber dimensions and volumes apply for both TEE and TTE. For details on specific views for optimal measurements, please refer to the recently published TEE guidelines.<sup>3</sup>

All measurements described in this document should be performed on more than one cardiac cycle to account for interbeat variability. The committee suggests the average of three beats for patients in normal sinus rhythm and a minimum of five beats in patients with atrial fibrillation. Because the committee acknowledges that the implementation of this recommendation is time consuming, the use of representative beats is acceptable in the clinical setting.

## I. THE LEFT VENTRICLE

### 1. Measurement of LV Size

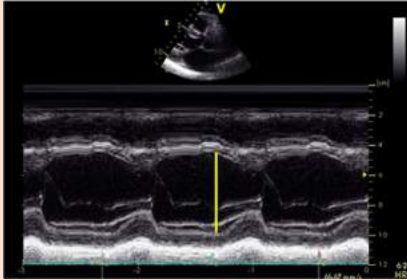

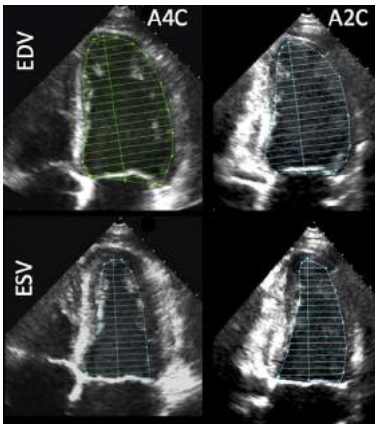
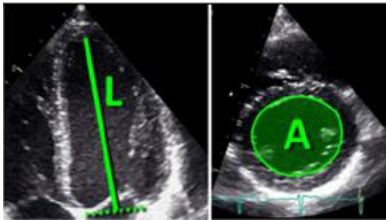
The most commonly used parameters to describe LV cavity size include linear internal dimensions and volumes. Measurements are commonly reported for end-diastole and end-systole, which are then used to derive parameters of global LV function. To allow comparison among individuals with different body sizes, chamber measurements should be reported indexed to BSA.

**1.1. Linear Measurements.** It is recommended that linear internal measurements of the left ventricle and its walls be performed in the parasternal long-axis view. Values should be carefully obtained perpendicular to the LV long axis and measured at or immediately below the level of the mitral valve leaflet tips. In this regard, the electronic calipers should be positioned on the interface between the myocardial wall and cavity and the interface between the wall and the pericardium. Internal dimensions can be obtained with a two-dimensional (2D) echocardiography (2DE)-guided M-mode approach, although linear measurements obtained from 2D echocardiographic images are preferred to avoid oblique sections of the ventricle ([Table 1](#)).

**1.2. Volumetric Measurements.** LV volumes are measured using 2DE or 3DE. Volume calculations derived from linear measurements may be inaccurate, because they rely on the assumption of a fixed geometric LV shape such as a prolate ellipsoid, which does not apply in a variety of cardiac pathologies. Accordingly, the Teichholz and Quinones methods for calculating LV volumes from LV linear dimensions are no longer recommended for clinical use.

Volumetric measurements are usually based on tracings of the interface between the compacted myocardium and the LV cavity.

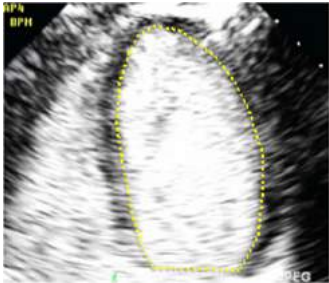
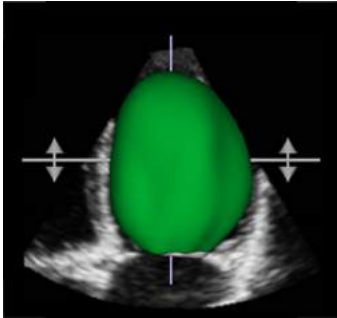
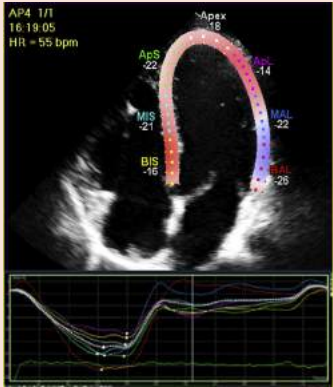
**Table 1** Recommendations for the echocardiographic assessment of LV size and function

Parameter and method	Technique	Advantages	Limitations
<b>Internal linear dimensions.</b> Linear internal measurements of the LV should be acquired in the parasternal long-axis view carefully obtained perpendicular to the LV long axis, and measured at the level of the mitral valve leaflet tips. Electronic calipers should be positioned on the interface between myocardial wall and cavity and the interface between wall and pericardium ( <i>orange arrows</i> ).	M-mode tracing 	<ul style="list-style-type: none"> <li>• Reproducible</li> <li>• High temporal resolution</li> <li>• Wealth of published data</li> </ul>	<ul style="list-style-type: none"> <li>• Beam orientation frequently off axis</li> <li>• Single dimension, i.e., representative only in normally shaped ventricles</li> </ul>
	2D-guided linear measurements 	<ul style="list-style-type: none"> <li>• Facilitates orientation perpendicular to the ventricular long axis</li> </ul>	<ul style="list-style-type: none"> <li>• Lower frame rates than M-mode</li> <li>• Single dimension, i.e., representative only in normally shaped ventricles</li> </ul>
<b>Volumes.</b> Volume measurements are usually based on tracings of the blood-tissue interface in the apical four- and two-chamber views. At the mitral valve level, the contour is closed by connecting the two opposite sections of the mitral ring with a straight line. LV length is defined as the distance between the middle of this line and the most distant point of the LV contour.	Biplane disk summation 	<ul style="list-style-type: none"> <li>• Corrects for shape distortions</li> <li>• Less geometrical assumptions compared with linear dimensions</li> </ul>	<ul style="list-style-type: none"> <li>• Apex frequently foreshortened</li> <li>• Endocardial dropout</li> <li>• Blind to shape distortions not visualized in the apical two- and four-chamber planes</li> </ul>
	Area-length 	<ul style="list-style-type: none"> <li>• Partial correction for shape distortion</li> </ul>	<ul style="list-style-type: none"> <li>• Apex frequently foreshortened</li> <li>• Heavily based on geometrical assumptions</li> <li>• Limited published data on normal population</li> </ul>

(Continued)



Table 1 (Continued)

Parameter and method	Technique	Advantages	Limitations
	Endocardial border enhancement 	<ul style="list-style-type: none"><li>• Helpful in patients with suboptimal acoustic window</li><li>• Provides volumes that are closer to those measured with cardiac magnetic resonance</li></ul>	<ul style="list-style-type: none"><li>• Same limitations as the above non-contrast 2D techniques</li><li>• Acoustic shadowing in LV basal segments with excess contrast</li></ul>
	3D data sets 	<ul style="list-style-type: none"><li>• No geometrical assumption</li><li>• Unaffected by foreshortening</li><li>• More accurate and reproducible compared to other imaging modalities</li></ul>	<ul style="list-style-type: none"><li>• Lower temporal resolution</li><li>• Less published data on normal values</li><li>• Image quality dependent</li></ul>
<b>Global Longitudinal Strain.</b> Peak value of 2D longitudinal speckle tracking derived strain (%).		<ul style="list-style-type: none"><li>• Angle independent</li><li>• Established prognostic value</li></ul>	<ul style="list-style-type: none"><li>• Vendor dependent</li></ul>

2D, two-dimensional; 3D, three-dimensional; A2C, apical 2-chamber view; A4C, apical 4-chamber view; EDV, end-diastolic volume; ESV, end-systolic volume; LV, left ventricular.

At the mitral valve level, the contour is closed by connecting the two opposite sections of the mitral ring with a straight line. LV length is defined as the distance between the bisector of this line and the apical point of the LV contour, which is most distant to it. The use of the longer LV length between the apical two- and four-chamber views is recommended.

LV volumes should be measured from the apical four- and two-chamber views. Two-dimensional echocardiographic image acquisition should aim to maximize LV areas, while avoiding foreshortening of the left ventricle, which results in volume underestimation. Acquiring LV views at a reduced depth to focus on the LV cavity will reduce the likelihood of foreshortening and

minimize errors in endocardial border tracings (Table 1). Because the issue of foreshortening is less relevant in 3D data sets, 3D image acquisition should focus primarily on including the entire left ventricle within the pyramidal data set. To ensure reasonably accurate identification of end-systole, the temporal resolution of 3D imaging should be maximized without compromising spatial resolution.

Contrast agents should be used when needed to improve endocardial delineation when two or more contiguous LV endocardial segments are poorly visualized in apical views, as per published guidelines.<sup>4</sup> Contrast-enhanced images may provide larger volumes than unenhanced images that are closer to those obtained with cardiac

magnetic resonance (CMR) in head-to-head comparison.<sup>5</sup> Care should be taken to avoid acoustic shadowing, which may occur in LV basal segments in the presence of high concentrations of contrast. Normal reference values for LV volumes with contrast enhancement are not well established.

The most commonly used method for 2D echocardiographic volume calculations is the biplane method of disks summation (modified Simpson's rule), which is the recommended 2D echocardiographic method by consensus of this committee (Table 1). An alternative method to calculate LV volumes when apical endocardial definition precludes accurate tracing is the area-length method, in which the LV is assumed to be bullet shaped. The mid-LV cross-sectional area is computed by planimetry in the parasternal short-axis view and the length of the ventricle taken from the midpoint of the annular plane to the apex in the apical four-chamber view (Table 1). The shortcoming of this method is that the bullet-shape assumption does not always hold true. One of the advantages of 3D echocardiographic volume measurements is that they do not rely on geometric assumptions. In patients with good image quality, 3D echocardiographic measurements are accurate and reproducible and should therefore be used when available and feasible.<sup>6</sup> The advantages and disadvantages of the various methods are summarized in Table 1.

**1.3. Normal Reference Values for 2DE.** Data were extracted from seven databases, including Asklepios (year 0 and year 10),<sup>7</sup> Flemengho,<sup>8</sup> CARDIA5 and CARDIA25,<sup>9</sup> Padua 3D Echo Normal,<sup>10</sup> and the Normal Reference Ranges for Echocardiography study,<sup>11,12</sup> to obtain reference values in normal subjects for the left ventricle and the left atrium (see section 10). All data were obtained without the use of contrast agents. Data sets for all patients included age, gender, ethnicity, height, and weight. To ensure a normal population, subjects in these studies were excluded if any of the following criteria were met: systolic blood pressure > 140 mm Hg, diastolic blood pressure > 80 mm Hg, history of drug-treated hypertension, diagnosis of diabetes, impaired fasting glucose > 100 mg/dL, body mass index > 30 kg/m<sup>2</sup>, creatinine > 1.3 mg/dL, estimated glomerular filtration rate < 60 mL/min/1.73 m<sup>2</sup>, total cholesterol > 240 mg/dL, low-density lipoprotein cholesterol > 130 mg/dL, and total triglycerides > 150 mg/dL. Details of the statistical analysis are described in the Appendix. Because of varied study aims, not all echocardiographic measurements were available for each database. Supplemental Table 1 summarizes the sources of the data for each measurement group and their baseline characteristics.

Table 2 shows the normal values for 2D echocardiographic parameters of LV size and function according to gender, while Supplemental Table 2 provides expanded data for the same parameters, obtained from different echocardiographic views, and also includes the corresponding number of subjects used to obtain these data. Supplemental Table 3 lists normal ranges and consensus-based partition cutoffs for LV dimensions, volumes, EF, and mass. On multivariate analysis, age, gender, and BSA were found to have a significant independent influence on LV end-diastolic volume (EDV) and LV end-systolic volume (ESV). The results across genders and age deciles subdivided into absolute and BSA-normalized values are shown in Supplemental Table 4 (see Appendix).

Because ethnicity is an important factor, results of analysis by race and gender are presented in Supplemental Table 5. From the regression analysis, nomograms are provided for plotting observed LV dimensions versus BSA or BSA-indexed LV volumes versus age

(Figures 1 and 2). Nomograms for absolute LV measurements against age (Supplemental Figures 1 and 2) and BSA (Supplemental Figures 3 and 4) are also provided (see Appendix).

**1.4. Normal Reference Values for 3DE.** Several studies have published 3D echocardiographic reference values for healthy normotensive subjects, which are summarized in Table 3.<sup>13</sup> The reported variations in the normal ranges from study to study are likely due to differences in populations, echocardiographic equipment, and analysis software, as well as variability in measurement techniques. In patients with good image quality, the accuracy of 3DE is comparable with that of CMR, although volumes tend to be lower on echocardiography.<sup>6</sup>

The effects of ethnicity on 3D echocardiographic LV volumes were investigated in one study, which reported that LV volumes were smaller among Asian Indians than white Europeans, but EF did not differ among ethnic groups.<sup>14</sup> In most 3D echocardiographic studies, the relationship between age and 3D echocardiographic LV volumes was examined, and weak to moderate negative correlations were seen between age and LV volumes, while EF did not change significantly with age.<sup>10,15,16</sup> This finding is similar to those described in the CMR literature.<sup>17,18</sup> On the basis of weighted averages of three studies,<sup>16,19,20</sup> 3D echocardiographic LV volumes were larger than 2D echocardiographic values, and corresponding upper limits of the normal range were EDVs of 79 mL/m<sup>2</sup> for men and 71 mL/m<sup>2</sup> for women and ESVs of 32 mL/m<sup>2</sup> for men and 28 mL/m<sup>2</sup> for women. Ultimately, a large study in a diverse population will be needed to establish normal reference ranges for 3DE for different ethnic groups.

**Recommendation.** LV size should be routinely assessed on 2DE by calculating volumes using the biplane method of disks summation technique. In laboratories with experience in 3DE, 3D measurement and reporting of LV volumes is recommended when feasible depending on image quality. When reporting LV linear dimensions, the recommended method is 2D-guided measurements. LV size and volume measurements should be reported indexed to BSA. For general reference, 2D echocardiographic LV EDVs of 74 mL/m<sup>2</sup> for men and 61 mL/m<sup>2</sup> for women and LV ESVs of 31 mL/m<sup>2</sup> for men and 24 mL/m<sup>2</sup> for women should be used as the upper limits of the corresponding normal range.

## 2. LV Global Systolic Function

Global LV function is usually assessed by measuring the difference between the end-diastolic and end-systolic value of a one-dimensional, 2D, or 3D parameter divided by its end-diastolic value. For this, end-diastole is preferably defined as the first frame after mitral valve closure or the frame in the cardiac cycle in which the respective LV dimension or volume measurement is the largest. End-systole is best defined as the frame after aortic valve closure or the frame in which the cardiac dimension or volume is smallest. In patients with regular heart rhythm, measurements of the timing of valve openings and closures derived from M-mode echocardiography, pulsed-wave (PW) or continuous-wave Doppler may be used for accurate definitions of ventricular time intervals.

**2.1. Fractional Shortening.** Fractional shortening can be derived from 2D-guided M-mode imaging or preferably from linear measurements obtained from 2D images. Deriving global LV function parameters from linear measurements is problematic when there are regional wall motion abnormalities due to coronary disease or

**Table 2** Normal values for 2D echocardiographic parameters of LV size and function according to gender

Parameter	Male		Female	
	Mean $\pm$ SD	2-SD range	Mean $\pm$ SD	2-SD range
LV internal dimension				
Diastolic dimension (mm)	50.2 $\pm$ 4.1	42.0–58.4	45.0 $\pm$ 3.6	37.8–52.2
Systolic dimension (mm)	32.4 $\pm$ 3.7	25.0–39.8	28.2 $\pm$ 3.3	21.6–34.8
LV volumes (biplane)				
LV EDV (mL)	106 $\pm$ 22	62–150	76 $\pm$ 15	46–106
LV ESV (mL)	41 $\pm$ 10	21–61	28 $\pm$ 7	14–42
LV volumes normalized by BSA				
LV EDV (mL/m <sup>2</sup> )	54 $\pm$ 10	34–74	45 $\pm$ 8	29–61
LV ESV (mL/m <sup>2</sup> )	21 $\pm$ 5	11–31	16 $\pm$ 4	8–24
LV EF (biplane)	62 $\pm$ 5	52–72	64 $\pm$ 5	54–74

BSA, body surface area; EDV, end-diastolic volume; EF, ejection fraction; ESV, end-systolic volume; LV, left ventricular; SD, standard deviation.

conduction abnormalities. In patients with uncomplicated hypertension, obesity or valvular diseases, such regional differences are rare in the absence of clinically recognized myocardial infarction, and accordingly, this parameter may provide useful information in clinical studies.<sup>21</sup> In patients with normal size of the LV base but enlarged midventricular and distal portions, LV volume would be a better marker of LV size than linear dimension measured at the LV base.

**2.2. EF.** EF is calculated from EDV and ESV estimates, using the following formula:

$$EF = (EDV - ESV) / EDV.$$

LV volume estimates may be derived from 2DE or 3DE, as described above (section 1.2). The biplane method of disks (modified Simpson's rule) is the currently recommended 2D method to assess LV EF by consensus of this committee. Table 4 lists 2DE-derived biplane LV EF, including normal ranges and consensus-based severity partition cutoffs according to gender. In patients with good image quality, 3DE-based EF measurements are accurate and reproducible and should be used when available and feasible.<sup>6,10,15,16,19,20</sup>

**2.3. Global Longitudinal Strain (GLS).** Lagrangian strain is defined as the change in length of an object within a certain direction relative to its baseline length:

$$\text{Strain}(\%) = (L_t - L_0) / L_0,$$

where  $L_t$  is the length at time  $t$ , and  $L_0$  is the initial length at time 0. The most commonly used strain-based measure of LV global systolic function is GLS. It is usually assessed by speckle-tracking echocardiography (STE)<sup>22–24</sup> (Table 1). On 2DE, peak GLS describes the relative length change of the LV myocardium between end-diastole and end-systole:

$$GLS(\%) = (MLs - MLd) / MLd,$$

where  $ML$  is myocardial length at end-systole ( $MLs$ ) and end-diastole ( $MLd$ ). Because  $MLs$  is smaller than  $MLd$ , peak GLS is a negative number. This negative nature of GLS can lead to confusion when

describing increases or decreases in strain. We recommend that all references to strain changes specifically mention an increase or decrease in the absolute value of strain, to avoid confusion.

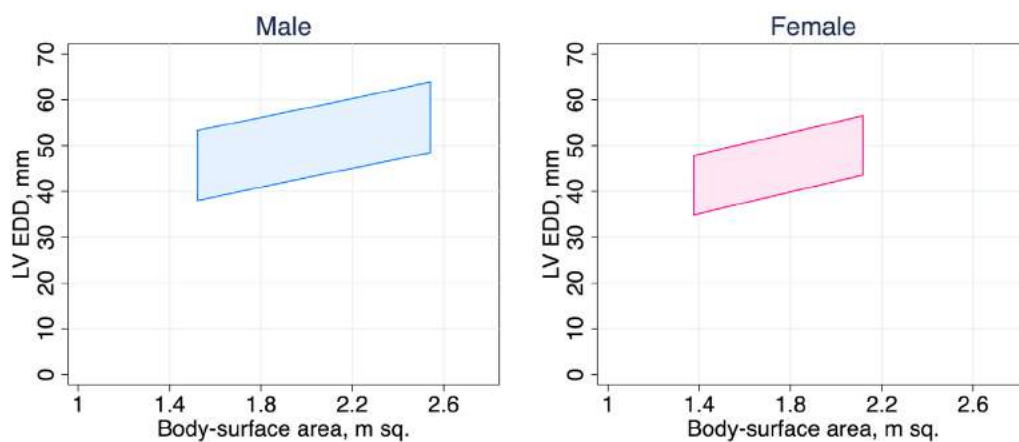
After optimizing image quality, maximizing frame rate, and minimizing foreshortening, which are all critical to reduce measurement variability, GLS measurements should be made in the three standard apical views and averaged.<sup>25</sup> Measurements should begin with the apical long-axis view to visualize aortic valve closure, using opening and closing clicks of the aortic valve or aortic valve opening and closing on M-mode imaging. When regional tracking is suboptimal in more than two myocardial segments in a single view, the calculation of GLS should be avoided. In such cases, alternative indices may be used to gain insight into longitudinal LV function, such as mitral annular plane systolic excursion or pulsed Doppler tissue imaging (DTI)-derived mitral annular peak systolic velocity ( $s'$ ).

There are concurrent definitions as a basis for GLS calculation using endocardial, midwall, or average deformation.<sup>24</sup> This committee refrains from recommendations in this regard and refers to the ongoing joint standardization initiative of the ASE, EACVI, and the ultrasound imaging industry.<sup>24,26</sup> Because of intervendor and intersoftware variability and age and load dependency, serial assessment of GLS in individual patients should be performed using the same vendor's equipment and the same software.

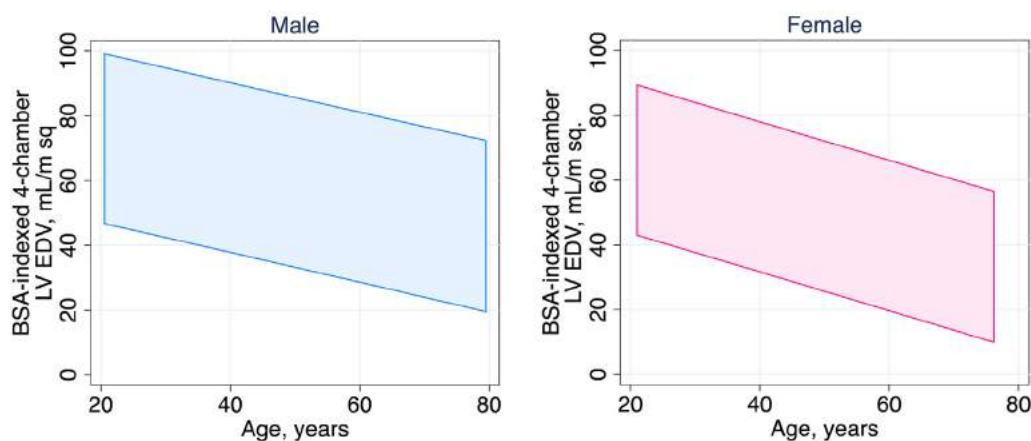
The preponderance of currently available data is for midwall GLS. Although the evidence base for its use in routine clinical echocardiography is far smaller than that for EF, measures of midwall GLS have been shown in several studies to be robust and reproducible<sup>27</sup> and to offer incremental predictive value in unselected patients undergoing echocardiography for the assessment of resting function,<sup>28,29</sup> as well as in predicting postoperative LV function in patients with valve disease.<sup>30,31</sup>

**2.4. Normal Reference Values.** Normal reference values for LV EF derived from 2DE have been updated using the population-based studies described in section 1.3 above. Details can be found in Tables 2 and 4 and Supplemental Tables 2–5 (see Appendix). EF is not significantly related to gender, age, or body size, as measured by BSA. Normal EF was  $63 \pm 5\%$  using the biplane method of disks. Therefore, in individuals aged  $> 20$  years, EF in the range of 53% to 73% should be classified as normal. Three-dimensional

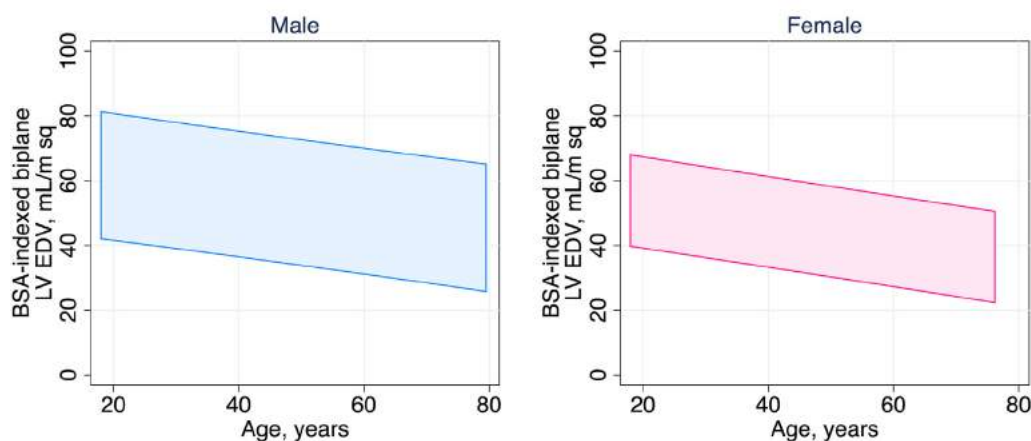
## Parasternal LV End-Diastolic Dimension



## Apical 4-chamber LV End-Diastolic Volume

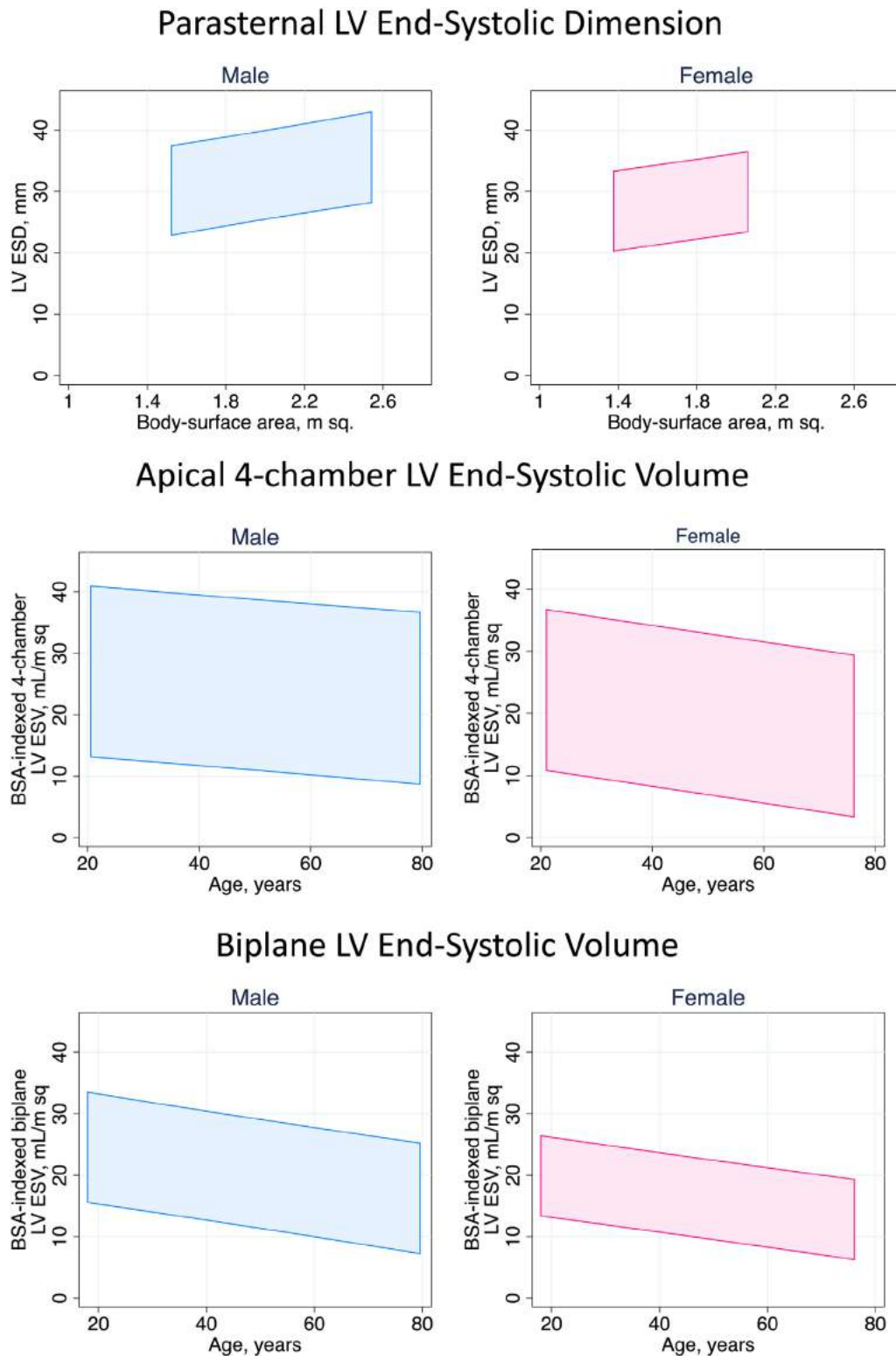


## Biplane LV End-Diastolic Volume



**Figure 1** For men (*left*) and women (*right*), the 95% confidence intervals for the following measurements are presented: LV end-diastolic dimension measured from a parasternal long-axis window on the basis of BSA (*top*), BSA-indexed LV EDV measured from an apical 4-chamber view on the basis of age (*middle*), and BSA-indexed biplane LV EDV on the basis of age (*bottom*). For example, a normal BSA-indexed LV EDV measured from the four-chamber view in a 40-year-old woman would fall between approximately 30 and 78 mL/m<sup>2</sup>.





**Figure 2** For men (*left*) and women (*right*), the 95% confidence intervals for the following measurements are presented: LV end-systolic dimensions measured from a parasternal long-axis window on the basis of BSA (*top*), BSA-indexed LV ESVs measured from an apical four-chamber view on the basis of age (*middle*), and BSA-indexed biplane LV ESVs based on age (*bottom*).

echocardiographic normal values have been recently reported in different ethnic populations (Table 3).

Normal values for GLS depend on the definition of the measurement position in the myocardium, the vendor, and the version of

the analysis software, resulting in considerable heterogeneity in the published literature.<sup>27,32,33</sup> It is the consensus of this writing committee that differences among vendors and software packages are still too large to recommend universal normal values and lower

**Table 3** Normal values for LV parameters obtained with 3DE

	Aune <i>et al.</i> (2010)	Fukuda <i>et al.</i> (2012)	Chahal <i>et al.</i> (2012)	Muraru <i>et al.</i> (2013)
Number of subjects	166	410	978	226
Ethnic makeup of population	Scandinavian	Japanese	51% European white, 49% Asian Indian	White European
EDVi (mL/m <sup>2</sup> )				
Men, mean (LLN, ULN)	66 (46, 86)	50 (26, 74)	White: 49 (31, 67); Indian: 41 (23, 59)	63 (41, 85)
Women, mean (LLN, ULN)	58 (42, 74)	46 (28, 64)	White: 42 (26, 58); Indian: 39 (23, 55)	56 (40, 78)
ESVi (mL/m <sup>2</sup> )				
Men, mean (LLN, ULN)	29 (17, 41)	19 (9, 29)	White: 19 (9, 29); Indian: 16 (6, 26)	24 (14, 34)
Women, mean (LLN, ULN)	23 (13, 33)	17 (9, 25)	White: 16 (8, 24); Indian: 15 (7, 23)	20 (12, 28)
EF (%)				
Men, mean (LLN, ULN)	57 (49, 65)	61 (53, 69)	White: 61 (49, 73); Indian: 62 (52, 72)	62 (54, 70)
Women, mean (LLN, ULN)	61 (49, 73)	63 (55, 71)	White: 62 (52, 72); Indian: 62 (52, 72)	65 (57, 73)

EDVi, LV EDV index; ESVi, LV ESV index; LLN, lower limit of normal; NR, not reported; RT3DTTE, real-time 3D TTE; SVi, LV stroke volume index; ULN, upper limit of normal.

Modified with permission from Bhawe *et al.*<sup>13</sup> LLN and ULN are defined as mean  $\pm$  2 SDs.

**Table 4** Normal ranges and severity partition cutoff values for 2DE-derived LV EF and LA volume

	Male				Female			
	Normal range	Mildly abnormal	Moderately abnormal	Severely abnormal	Normal range	Mildly abnormal	Moderately abnormal	Severely abnormal
LV EF (%)	52–72	41–51	30–40	<30	54–74	41–53	30–40	<30
Maximum LA volume/BSA (mL/m <sup>2</sup> )	16–34	35–41	42–48	>48	16–34	35–41	42–48	>48

limits of normal. To provide some guidance, a peak GLS in the range of  $-20\%$  can be expected in a healthy person. A selection of recently published data is provided in the [Appendix](#) together with the lower normal limits ([Supplemental Table 6](#)). There is evidence that women have slightly higher absolute values of GLS than men and that strain values decrease with age.<sup>32,34</sup> GLS is a valuable and sensitive tool for follow-up examinations, provided the same equipment, tracing methodology, and software are used.

**Recommendations.** LV systolic function should be routinely assessed using 2DE or 3DE by calculating EF from EDV and ESV. LV EFs of  $<52\%$  for men and  $<54\%$  for women are suggestive of abnormal LV systolic function. Two-dimensional STE-derived GLS appears to be reproducible and feasible for clinical use and offers incremental prognostic data over LV EF in a variety of cardiac conditions, although measurements vary among vendors and software versions. To provide some guidance, a peak GLS in the range of  $-20\%$  can be expected in a healthy person, and the lower the absolute value of strain is below this value, the more likely it is to be abnormal.

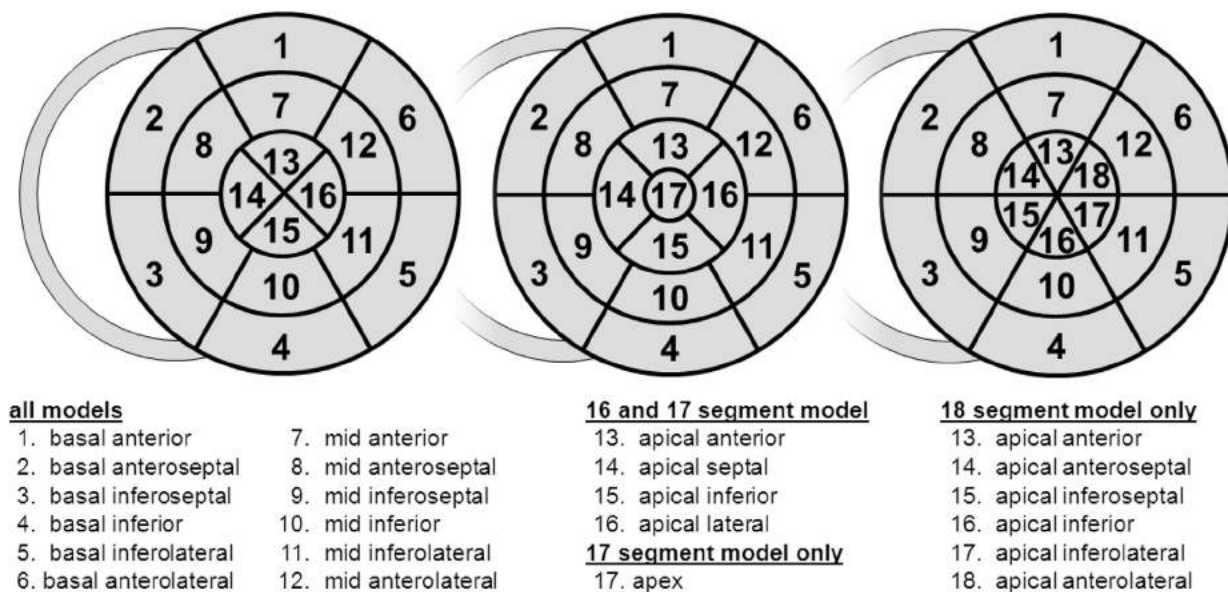
### 3. LV Regional Function

**3.1. Segmentation of the Left Ventricle.** For the assessment of regional LV function, the ventricle is divided into segments. Segmentation schemes should reflect coronary perfusion territories, result in segments with comparable myocardial mass, and allow standardized communication within echocardiography and with

other imaging modalities ([Figure 3](#)). Accordingly, a 17-segment model is commonly used. Beginning at the anterior junction of the interventricular septum and the RV free wall and continuing counterclockwise, basal and midventricular segments should be labeled as anteroseptal, inferoseptal, inferior, inferolateral, anterolateral, and anterior. In this 17-segment model, the apex is divided into five segments, including septal, inferior, lateral, and anterior segments, as well as the “apical cap,” which is defined as the myocardium beyond the end of the LV cavity ([Figures 3 and 4](#)).<sup>35</sup> The 17-segment model may be used for myocardial perfusion studies or when comparing between different imaging modalities, specifically single photon-emission computed tomography, positron emission tomography, and CMR. [Figure 5](#) shows a schematic representation of the perfusion territories of the three major coronary arteries. When using this 17-segment model to assess wall motion or regional strain, the 17th segment (the apical cap) should not be included.

Alternative segmentation models treat the apex differently: the 16-segment model<sup>36</sup> divides the entire apex into the same four segments (septal, inferior, lateral, and anterior; [Figure 3](#), left). Also, some segmentation schemes divide the apex into six segments, similar to the basal and midventricular levels, resulting in an 18-segment model ([Figure 3](#), right) that is simple but results in a slight overrepresentation of the distal myocardium when scoring.

All segments can be visualized by 2DE. On average, the two-chamber view and the apical long-axis view intersect with the four-chamber view at angles of approximately  $53^\circ$  and  $129^\circ$ ,



**Figure 3** Schematic diagram of the different LV segmentation models: 16-segment model (left),<sup>36</sup> 17-segment model (center),<sup>35</sup> and 18-segment model (right). In all diagrams, the outer ring represents the basal segments, the middle ring represents the segments at mid-papillary muscle level, and the inner ring represents the distal level. The anterior insertion of the right ventricular wall into the left ventricle defines the border between the anteroseptal and anterior segments. Starting from this point, the myocardium is subdivided into six equal segments of 60°. The apical myocardium in the 16- and 17-segment models is divided instead into four equal segments of 90°. In the 17-segment model an additional segment (*apical cap*) is added in the center of the bull's-eye. (modified from Voigt et al.<sup>24</sup>).

respectively,<sup>37</sup> allowing the assessment of the central region of all segments from an apical window, independent of the model used. Although certain variability exists in the coronary artery blood supply to myocardial segments, segments are usually attributed to the three major coronary arteries (Figure 5).<sup>35</sup>

**3.2. Visual Assessment.** In echocardiography, regional myocardial function is assessed on the basis of the observed wall thickening and endocardial motion of the myocardial segment. Because myocardial motion may be caused by adjacent segment tethering or overall LV displacement, regional deformation (thickening, shortening) should be the focus of the analysis. However, it must be recognized that deformation can also be passive and therefore may not always accurately reflect myocardial contraction.

It is recommended that each segment be analyzed individually in multiple views. A semiquantitative wall motion score can be assigned to each segment to calculate the LV wall motion score index as the average of the scores of all segments visualized. The following scoring system is recommended: (1) normal or hyperkinetic, (2) hypokinetic (reduced thickening), (3) akinetic (absent or negligible thickening, e.g., scar), and (4) dyskinetic (systolic thinning or stretching, e.g., aneurysm).

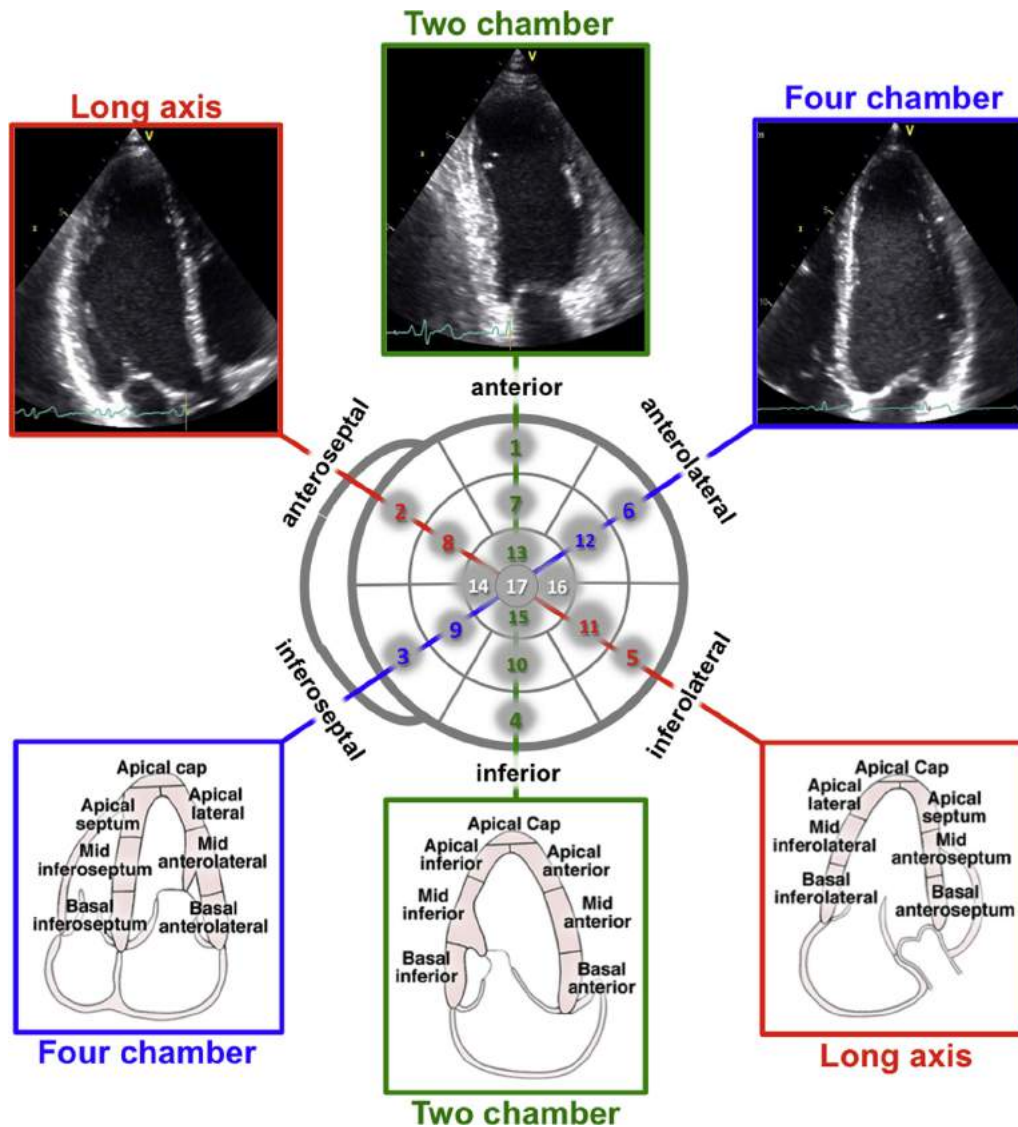
An aneurysm is a morphologic entity that demonstrates focal dilatation and thinning (remodeling) with either akinetic or dyskinetic systolic deformation.<sup>38</sup> In contrast to the recommendation of previous guidelines,<sup>1,2</sup> this committee refrains from assigning a separate wall motion score for aneurysm.

**3.3. Regional Wall Motion during Infarction and Ischemia.** Depending on the regional coronary flow reserve, stress echocardiography may reveal significant coronary artery stenoses by means of inducing a wall motion abnormality. Myocardial scar may also result in regional dysfunction of variable severity.

Echocardiography can over- or underestimate the amount of ischemic or infarcted myocardium, depending on the function of adjacent regions, regional loading conditions, and stunning.<sup>39</sup> In stress echocardiography, visual recognition of regional dysfunction can be improved with a synchronized side-by-side comparison of baseline and stress images using digital technology.<sup>40</sup>

**3.4. Regional Abnormalities in the Absence of Coronary Artery Disease.** Regional wall motion abnormalities may also occur in the absence of coronary artery disease, in a variety of conditions, such as myocarditis, sarcoidosis, and stress-induced (takotsubo) cardiomyopathy. Abnormal motion patterns of the interventricular septum may be found postoperatively or in the presence of a left bundle branch block or RV epicardial pacing, as well as RV dysfunction caused by RV pressure or volume overload. Furthermore, some conduction delays can cause regional wall motion abnormalities in the absence of primary myocardial dysfunction. This regional dysfunction is due to the abnormal sequence of myocardial activation, which causes heterogeneous loading conditions and remodeling.<sup>41</sup> Ideally, the temporal sequence of activation and motion should be described. Characteristic motion patterns, which result from abnormal activation sequences, such as septal bounce ("beaking," "flash") or lateral apical motion during systole ("apical rocking") should be reported.<sup>42-45</sup>

**3.5. Quantification of Regional Wall Motion Using Doppler and STE.** Echocardiographic quantification of regional myocardial function is currently based on DTI or speckle-tracking echocardiographic techniques.<sup>46-48</sup> Both techniques provide comparable data quality, although DTI is known to be angle dependent and prone to underestimating motion that is not parallel to the ultrasound beam. Commonly used parameters include velocity, motion, deformation, and deformation rate. Because velocity and motion are measured relative to the transducer, measurements may be influenced by



**Figure 4** Orientation of apical four-chamber (A4C), apical two-chamber (A2C), and apical long-axis (ALX) views in relation to the bull's-eye display of the LV segments (*center*). Top panels show actual images, and bottom panels schematically depict the LV wall segments in each view.

tethering or overall heart motion. Accordingly, the use of deformation parameters, such as strain and strain rate, is preferable.

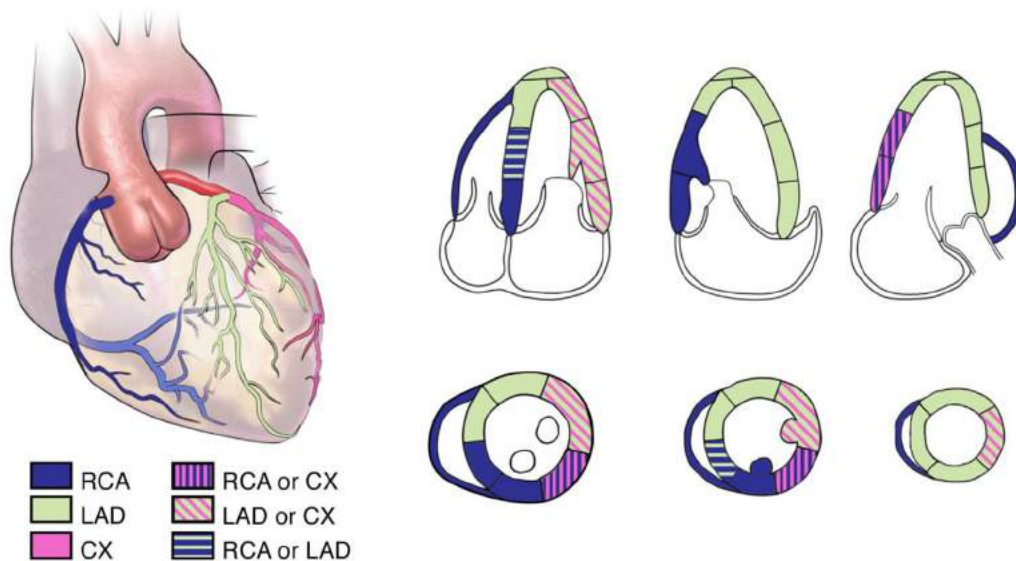
The most commonly used deformation parameter is longitudinal strain during LV systole. Similar to global strain, with current technology, regional deformation measurements may vary in amplitude, depending on the myocardial region being investigated, the measurement methodology, the vendor, and sample volume definition. Therefore, no specific normal ranges are provided in this document. These values await the upcoming consensus document of the joint task force of the ASE, EACVI, and the industry for the standardization of quantitative function imaging.<sup>23,25</sup>

Independent of strain magnitude, characteristic changes in temporal pattern of myocardial deformation can be assessed as well. Longitudinal shortening or radial thickening of the myocardium after aortic valve closure (postsystolic shortening or thickening, sometimes referred to as tardokinesis) of >20% of the total deformation during the cardiac cycle is a consistent sign of regional functional inhomogeneity (e.g., ischemia, scar).<sup>44</sup> The development of postsystolic

shortening during a stress test has been proposed as an indicator of regional ischemia.<sup>49</sup> The value of regional deformation parameters and temporal patterns of strain derived by speckle-tracking from either 2D or 3D echocardiographic data sets is the subject of ongoing research and remains to be determined.<sup>50,51</sup>

**Recommendations.** Different LV segmentation models are used in clinical practice. The 17-segment model is recommended to assess myocardial perfusion with echocardiography and other imaging techniques. The 16-segment model is recommended for routine studies assessing wall motion, because endocardial excursion and thickening of the tip of the apex are imperceptible. To assess wall motion, each segment should be evaluated in multiple views and a four-grade scoring should be applied: (1) normal or hyperkinetic, (2) hypokinetic (reduced thickening), (3) akinetic (absent or negligible thickening), and (4) dyskinetic (systolic thinning or stretching). Despite promising data, quantitative assessment of the magnitude of regional LV deformation cannot be recommended at this stage because of lack of





**Figure 5** Typical distributions of the right coronary artery (RCA), the left anterior descending coronary artery (LAD), and the circumflex coronary artery (CX). The arterial distribution varies among patients. Some segments have variable coronary perfusion.

reference values, suboptimal reproducibility, and considerable inter-vendor measurement variability.

#### 4. LV Mass

LV mass is an important risk factor for, and a strong predictor of, cardiovascular events.<sup>52-55</sup> There are several methods that effectively calculate LV mass from M-mode echocardiography, 2DE, and 3DE (Table 5). All measurements should be performed at the end of diastole (the frame before mitral valve closure or the frame in the cardiac cycle in which the ventricular dimension or volume is largest). Those that use M-mode (either blinded or 2D-guided) and 2D echocardiographic linear measurements of LV diastolic diameter and wall thickness rely on geometric formulas to calculate the volume of LV myocardium, while 3DE can measure it directly. All methods then convert the volume to mass by multiplying the volume of myocardium by the myocardial density (approximately 1.05 g/mL).

When the entire ventricle is measured from 2D echocardiographic images, either the area-length or truncated ellipsoid technique is used.<sup>1</sup> Each method for LV mass measurement has advantages, disadvantages, and value in specific situations (Table 5).

To measure LV mass in an individual patient over time, especially those with cardiac disease, the 2D echocardiographic methods have advantages compared with the linear dimension technique.<sup>1</sup> There are, however, fewer studies of the prognostic value of LV mass calculated by these methods compared with the linear dimension method described below. Unlike the linear dimension or M-mode method, the 2D echocardiographic methods can accommodate for the shape of the ventricle and account for changes in LV size that might occur along the long axis of the chamber. This is an important consideration, because changes in LV geometry are common in various cardiac diseases.

However, when there is a need to screen or study large populations, the M-mode method has advantages, because it is simple, quick, and subject to less measurement variability. There is a large body of evidence to support the accuracy of this method. Most studies that relate LV mass to prognosis are based on this method.<sup>56</sup> However,

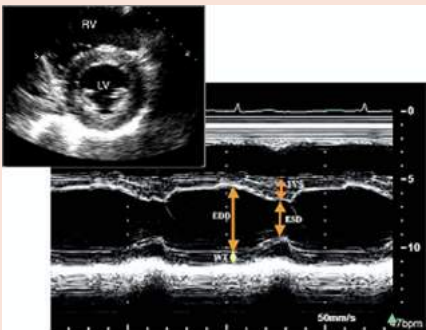

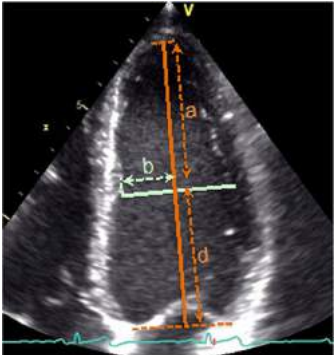
several caveats need to be mentioned. First, it is critical that the wall thickness and LV dimensions measured be truly perpendicular to the long axis of the left ventricle. Therefore, 2D-guided M-mode imaging or measurements from 2D echocardiographic images are preferred over blind M-mode imaging. Second, the formula includes a correction for the 20% overestimation that was found during the original validation studies of the M-mode technique. Because direct 2D measures of wall thickness may yield smaller values than the M-mode technique, LV mass calculated using this formula may not be directly interchangeable (Table 5). This may be a less important consideration if the method is being used to identify cutoff values for prognosis. It is also important to note that the formula raises the linear dimensions to the power of 3, and thus even small errors in dimensions can have significant effects on the calculated LV mass.

Most studies that have compared 2D-guided M-mode measurements of LV mass with the 2D echocardiographic area-length or truncated ellipsoid methods in normally shaped ventricles have shown subtle differences but no clear advantage of one technique over the other.<sup>57</sup> However, comparison studies have not been performed in the current era, when tremendous gains in 2D echocardiographic image quality have been made. In fact, large population studies confirming or reestablishing normal values for LV mass with harmonic imaging are limited.<sup>58,59</sup>

Because 3DE is the only echocardiographic method that directly measures myocardial volume, it is an appropriate approach. Numerous validation studies have been performed.<sup>60</sup> However, to date, there have been few studies assessing its practical use, feasibility, variability, or prognostic value in large-scale clinical environments.<sup>61</sup> Accordingly, it is the consensus of this committee that the 3D echocardiographic LV mass data available in normal subjects are not sufficient to recommend normal reference values. It must also be noted that continuous improvements in the spatial and temporal resolution of 3D echocardiographic imaging will also influence normal values and measurement variability.


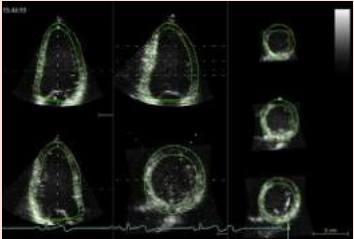
In patients with upper septal hypertrophy, the linear dimension methods, which use basal ventricular measurements, result in overestimation of the true mass, because the thickest region of the

**Table 5** Recommendations for the echocardiographic assessment of LV mass

Parameter and method	Echocardiographic imaging	Advantages	Limitations
<b>Linear method:</b> Cube formula $\text{LV mass} = 0.8 \cdot 1.04 \cdot [(\text{IVS} + \text{LVID} + \text{PWT})^3 - \text{LVID}^3] + 0.6\text{g}$ <p>Where IVS is interventricular septum; LVID is LV internal diameter, and PWT is inferolateral wall thickness. Linear internal measurements of the LV should be acquired from the parasternal approach and carefully obtained perpendicular to the LV long axis, and measured at the level of the mitral valve leaflet tips. M-mode measurements should be obtained from a targeted SAX or a parasternal LAX view. All measurements should be performed at end-diastole.</p>	<p><b>M-mode tracing</b></p>  <p><b>2D</b></p> 	<ul style="list-style-type: none"> <li>• Fast and widely used</li> <li>• Wealth of published data</li> <li>• Demonstrated prognostic value</li> <li>• Fairly accurate in normally shaped ventricles (i.e., systemic hypertension, aortic stenosis)</li> <li>• Simple for screening large populations</li> </ul>	<ul style="list-style-type: none"> <li>• Based on the assumption that the left ventricle is a prolate ellipsoid with a 2:1 long/short axis ratio and symmetric distribution of hypertrophy</li> <li>• Beam orientation frequently off axis</li> <li>• Since linear measurements are cubed, even small measurement errors in dimensions or thickness have an impact on accuracy</li> <li>• Overestimates LV mass</li> <li>• Inaccurate in the presence of asymmetric hypertrophy, dilated ventricles and other diseases with regional variations in wall thickness</li> </ul>
<b>2D based formulas.</b> Truncated ellipsoid: $\text{LV mass} = 1.05\pi \left\{ (b+t)^2 \left[ \frac{2}{3}(a+t) + d - \frac{d^3}{3(a+t)^2} \right] - b^2 \left[ \frac{2}{3}a + d - \frac{d^3}{3a^2} \right] \right\}$		<ul style="list-style-type: none"> <li>• Partial correction for shape distortions</li> <li>• Less dependent on geometrical assumptions than the linear measurements</li> </ul>	<ul style="list-style-type: none"> <li>• Good image quality and properly oriented parasternal short-axis views (no oblique planes) are required</li> <li>• Good epicardial definition is required</li> <li>• Cumbersome methodology</li> <li>• Higher measurement variability</li> <li>• Few published normative data</li> <li>• Limited prognostic data</li> </ul>

(Continued)

Table 5 (Continued)

Parameter and method	Echocardiographic imaging	Advantages	Limitations
<p>Area-length: LV mass = 1.05</p> $\left\{ \left[ \frac{5}{6} A_1 (a + d + t) \right] - \left[ \frac{5}{6} A_2 (a + d) \right] \right\}$ <p>Mean wall thickness is calculated from epicardial (<math>A_1</math>) and endocardial (<math>A_2</math>) cross-sectional areas in short-axis view at the papillary muscle level (top panel, green line) with the papillary muscles considered part of the LV cavity. The short axis radius is calculated as:</p> $b \sqrt{\frac{A_2}{\pi}}$ <p>Then, mean wall thickness <math>t</math> is calculated as:</p> $t = \left( \sqrt{\frac{A_1}{\pi}} \right) - b$ <p>and the cross sectional area of the myocardium (<math>A_m</math>) in short-axis view is:</p> $A_m = A_1 - A_2$ <p>LV mass is calculated from these measurements plus the LV length measured from the level of the short axis plane to the base (d) and to the apex (a).</p> <p>Key: a - distance from the minor axis to the endocardium at the LV apex; b = LV minor radius; d - distance from the minor axis to the mitral valve plane; t - mean wall thickness.</p> <p>LV mass = (LV epicardial volume – LV endocardial volume). 1.05 = LV myocardial volume. 1.05</p> <p>LV mass = (LV epicardial volume – LV endocardial volume). 1.05 = LV myocardial volume. 1.05</p>			
<p><b>3D based formula.</b></p>	<p>3D data set</p> 	<ul style="list-style-type: none"><li>• Direct measurement without geometrical assumptions about cavity shape and hypertrophy distribution</li><li>• More accurate than the linear or the 2D measurements</li><li>• Higher inter-measurement and test/re-test reproducibility</li><li>• Better discriminates small changes within a patient</li></ul>	<ul style="list-style-type: none"><li>• Normal values less well established</li><li>• Dependent on image quality</li><li>• Patient's cooperation required</li></ul>

interventricular septum is incorporated in the measurement. In contrast, the area-length method, which uses mid-ventricular measurements, underestimates LV mass, because the thickest part of the interventricular septum is not included in the measurement. In the setting of discrete upper septal or asymmetric hypertrophy, if these methods are used to serially assess LV mass in a patient, it is critical to use the same methodology over time and to measure the walls at the same level of the ventricle. The 3D method has the advantage of accommodating regional differences in wall thickness and therefore can provide the most accurate measurements of LV mass in this setting.

The values for LV mass vary according to gender, age, body size, obesity, and region of the world. Therefore, uniform reference values are difficult to define. LV mass is higher in men independent of body size and increases with body size. Since the publication of the 2005 recommendations, several studies, mostly using linear measurements, have reported normal values of LV mass in normal populations.<sup>59,62-66</sup> The larger studies reported values close to those recommended in the previous guidelines.<sup>62,65,66</sup> Therefore, the same reference values and abnormality partition cutoffs as reported in the previous guidelines continue to be recommended (Table 6). However, characterization of the population being studied, and differences in mass between different ethnic populations should be taken into account when determining normal values.<sup>10,16,67-69</sup>

The indexing of LV mass allows comparisons in subjects with different body sizes. However, whether to use height, weight, or BSA as the indexing term remains controversial. Studies suggest that indexing to height raised to allometric powers such as 1.7, 2.13, and 2.7 has advantages over indexing to BSA, especially when attempting to predict events in obese patients.<sup>65,70</sup> However most large population studies reporting LV mass have indexed to BSA.

Finally, calculation of relative wall thickness (RWT) with the formula  $(2 \times \text{posterior wall thickness})/(\text{LV internal diameter at end-diastole})$  permits categorization of an increase in LV mass as either concentric ( $\text{RWT} > 0.42$ ) or eccentric ( $\text{RWT} \leq 0.42$ ) hypertrophy and allows the identification of concentric remodeling (normal LV mass with increased RWT) (Figure 6).

**Recommendations.** In the normally shaped left ventricle, both M-mode and 2D echocardiographic formulas to calculate LV mass can be used. Normal values for these techniques remain unchanged from the previous guidelines and should be reported indexed to BSA. Reference upper limits of normal LV mass by linear measurements are 95 g/m<sup>2</sup> in women and 115 g/m<sup>2</sup> in men. Reference upper limits of normal LV mass by 2D measurements are 88 g/m<sup>2</sup> in women and 102 g/m<sup>2</sup> in men with 2D methods. Because 3DE is the only echocardiographic technique that measures myocardial volume directly, without geometric assumptions regarding LV shape and distribution of wall thickening, this technique is promising and may be used in abnormally shaped ventricles or in patients with asymmetric or localized hypertrophy. Limited upper normal limits of 3D echocardiographic LV mass data are currently available in the literature but are insufficient to substantiate recommendations for reference values.

## II. THE RIGHT VENTRICLE

The right ventricle has a unique crescent shape, which adds complexity to the quantification of its size and function. This chamber plays an important role in the morbidity and mortality of patients pre-

sented with signs and symptoms of cardiopulmonary disease. Until recently, little uniformity in echocardiographic imaging of the right heart existed because of a lack of familiarity with various techniques, and the enormous attention directed toward left heart quantification. The ASE has recently published a guidelines document, endorsed by the EACVI and the Canadian Society of Echocardiography, standardizing the approach for the evaluation of right heart dimensions and function during echocardiographic assessment of the right heart in adults.<sup>71</sup> Compared with that document, this section provides updated reference values for RV dimensions and most parameters of systolic and diastolic function, which should replace the previously published guideline.

### 5. General Recommendations for RV Quantification

In all clinical studies, a comprehensive examination of the right ventricle should be performed, taking into account the study indication and available clinical information. The operator should examine the right ventricle using multiple acoustic windows, and the report should present an assessment based on both qualitative and quantitative parameters. Parameters that can be measured include RV and right atrial (RA) size, a measure of RV systolic function, as assessed by at least one or a combination of the following: fractional area change (FAC), DTI-derived tricuspid lateral annular systolic velocity wave ( $S'$ ), tricuspid annular plane systolic excursion (TAPSE), and RV index of myocardial performance (RIMP). RV systolic pressure, typically calculated using the tricuspid regurgitation jet and an estimation of RA pressure based on inferior vena cava (IVC) size and collapsibility, should be reported when a complete TR Doppler velocity envelope is present.<sup>71</sup> When feasible, additional parameters such as RV volumes and EF using 3DE should complement the basic 2D echocardiographic measurements listed above. The recommended methods, as well as the advantages and limitations of each parameter, are summarized in Tables 7 and 9, whereas the new reference values are displayed in Tables 8 and 10. These reference values are based on published mean and SD data obtained from normal adult individuals without any histories of heart or pulmonary disease (Supplemental Table 7). This document uses the same methodology as in the previous RV guidelines, whereby a meta-analysis was performed for each parameter.

Not all of the recommended values are identical to those published in the previous guidelines.<sup>71</sup> On the basis of the inclusion of new data published in recent reports, minor changes were made in the cutoff values for RV dimension,  $S'$ , TAPSE, and RIMP. New publications since the last guidelines have resulted in changes in the reference values for 3DE-derived RV EF and volumes (Tables 8 and 10). It is important for the reader to recognize that most of the values proposed are not indexed to gender, BSA, or height, despite data suggesting the advantages of indexing.<sup>72-75</sup> As a result, it is possible that patients at either extreme of height or BSA may be misclassified as having values outside the reference ranges, and it is recommended that the interpreting physician consider these parameters when generating the report. This potential misclassification also applies to other groups, such as patients with congenital heart disease and endurance athletes, for whom specific reference values are nonexistent.<sup>76</sup>

### 6. Essential Imaging Windows and Views

Apical four-chamber, RV-focused apical four-chamber and modified apical four-chamber (Figure 7A), left parasternal long- and



Table 6 Normal ranges for LV mass indices		
	Women	Men
Linear method		
LV mass (g)	67–162	88–224
<b>LV mass/BSA (g/m<sup>2</sup>)</b>	<b>43–95</b>	<b>49–115</b>
Relative wall thickness (cm)	0.22–0.42	0.24–0.42
<b>Septal thickness (cm)</b>	<b>0.6–0.9</b>	<b>0.6–1.0</b>
<b>Posterior wall thickness (cm)</b>	<b>0.6–0.9</b>	<b>0.6–1.0</b>
2D method		
LV mass (g)	66–150	96–200
<b>LV mass/BSA (g/m<sup>2</sup>)</b>	<b>44–88</b>	<b>50–102</b>

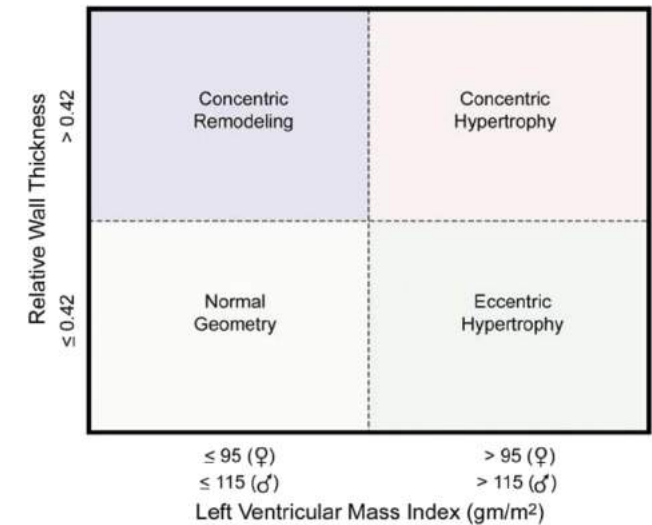
Bold italic values: recommended and best validated.

short-axis, left parasternal RV inflow, and subcostal views provide the images required for a comprehensive assessment of RV size, systolic and diastolic function, and RV systolic pressures.<sup>71</sup> In most cases, in the RV-focused view, visualization of the entire RV free wall is better than in a standard four-chamber view, which is centered on the left ventricle. It is therefore recommended that to measure the right ventricle, a dedicated view focused on the right ventricle be used. Figure 7A and Table 7 show the different RV views and recommendations for measurements.

7. RV Measurements

**7.1. Linear Measurements.** Quantitation of RV dimensions is critical and reduces interreader variability compared with visual assessment alone.<sup>77</sup> Measurements by 2DE are challenging because of the complex geometry of the right ventricle and the lack of specific right-sided anatomic landmarks to be used as reference points. The conventional apical four-chamber view (i.e., focused on the left ventricle) results in considerable variability in how the right heart is sectioned, and consequently, RV linear dimensions and areas may vary widely in the same patient with relatively minor rotations in transducer position (Figure 7B). RV dimensions are best estimated from a RV-focused apical four-chamber view obtained with either lateral or medial transducer orientation (Figure 7A and Table 7). Care should be taken to obtain the image with the LV apex at the center of the scanning sector, while displaying the largest basal RV diameter and thus avoiding foreshortening. Of note, the accuracy of RV measurements may be limited when the RV free wall is not well defined because of the dimension of the ventricle itself or its position behind the sternum. Recent data have suggested that indexing RV “size” to BSA may be relevant in some circumstances, but the measurements used in those studies lacked the reference points of the RV-focused view and frequently used RV areas, rather than linear dimensions.<sup>73,74</sup> Reference values for RV dimensions are listed in Table 8. In general, a diameter >41 mm at the base and >35 mm at the midlevel in the RV-focused view indicates RV dilatation.

**7.2. Volumetric Measurements.** Three-dimensional echocardiography allows measurements of RV volumes (Figure 8), thereby overcoming the limitations of conventional 2DE RV views with respect to orientation and reference points. Although technically challenging, particularly in patients with imperfect image quality or



**Figure 6** Comparison of RWT. Patients with normal LV mass can have either concentric remodeling (normal LV mass with increased RWT ≥ 0.42) or normal geometry (RWT ≤ 0.42) and normal LV mass. Patients with increased LV mass can have either concentric (RWT ≥ 0.42) or eccentric (RWT ≤ 0.42) hypertrophy. These LV mass measurements are based on linear measurements.

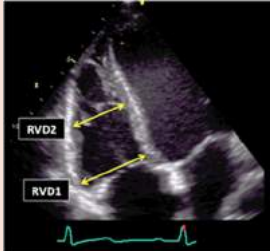


severely enlarged right ventricles, a reasonably accurate estimate of RV EDV and ESV can be obtained, and RV EF can be calculated.

Practical recommendations regarding RV 3D imaging and analysis have been recently published by the European Association of Echocardiography and the ASE.<sup>61</sup> During analysis of RV volume, it is critically important to manually define end-diastolic and end-systolic frames using maximal and minimal RV volumes, respectively, rather than LV chamber changes (Table 7). Myocardial trabeculae and the moderator band should be included in the cavity, and RV contours on dynamic images should closely follow endocardial displacement and excursion of the tricuspid annulus throughout the cardiac cycle.

Even though 3DE tends to underestimate RV volumes compared CMR,<sup>78</sup> 3DE has identified relationships between RV volumes and EF to age and gender, which are very similar to those described by CMR.<sup>72</sup> Overall, women have smaller 3D echocardiographic RV volumes, despite indexing to BSA, and higher EFs.<sup>75</sup> Also, older age is associated with smaller volumes (expected decrements of 5 mL/decade for EDV and 3 mL/decade for ESV) and higher EF (an expected increment of 1% per decade).<sup>75</sup> Reference values of 3DE-derived RV volumes (indexed to BSA) and EF obtained from the meta-analyses of all studies are summarized in Tables 8 and 10. Details of the above-described study factoring in age, gender, and BSA are listed in Supplemental Table 8.<sup>75</sup> Although RV volumes by CMR appear to be significantly influenced by race,<sup>72</sup> no 3D echocardiographic data are yet available.

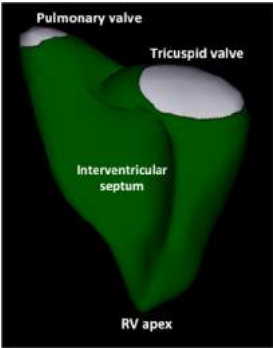
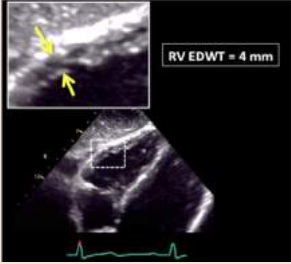
**Recommendations.** RV size should be routinely assessed by conventional 2DE using multiple acoustic windows, and the report should include both qualitative and quantitative parameters. In laboratories with experience in 3DE, when knowledge of RV volumes may be clinically important, 3D measurement of RV volumes is recommended. Although normal 3D echocardiographic values of RV volumes need to be established in larger groups of subjects, current published data suggest RV EDVs of 87 mL/m<sup>2</sup> in men and 74 mL/m<sup>2</sup>

**Table 7** Recommendations for the echocardiographic assessment of RV size

Echocardiographic imaging	Recommended methods	Advantages	Limitations
<b>RV linear dimensions (inflow)*</b> 	<ul style="list-style-type: none"> <li>• Basal RV linear dimension (RVD1) = maximal transversal dimension in the basal one third of RV inflow at end-diastole in the <i>RV-focused view</i></li> <li>• Mid-cavity RV linear dimension (RVD2) = transversal RV diameter in the middle third of RV inflow, approximately halfway between the maximal basal diameter and the apex, at the level of papillary muscles at end-diastole.</li> </ul>	<ul style="list-style-type: none"> <li>• Easily obtainable</li> <li>• Simple</li> <li>• Fast</li> <li>• Wealth of published data</li> </ul>	<ul style="list-style-type: none"> <li>• RV size may be underestimated due to the crescent RV shape</li> <li>• RV linear dimensions are dependent on probe rotation and different RV views; in order to permit inter-study comparison, the echocardiography report should state the window from which the measurement was performed.</li> </ul>
<b>RV linear dimensions (outflow)*</b> 	<ul style="list-style-type: none"> <li>• Proximal RV outflow diameter (RVOT prox) = linear dimension measured from the anterior RV wall to the inter-ventricular septal-aortic junction (in parasternal long-axis view) or to the aortic valve (in parasternal short-axis) at end-diastole</li> <li>• Distal RV outflow diameter (RVOT distal) = linear transversal dimension measured just proximal to the pulmonary valve at end-diastole</li> </ul>	<ul style="list-style-type: none"> <li>• Easily obtainable</li> <li>• Simple</li> <li>• Fast</li> </ul>	<ul style="list-style-type: none"> <li>• RVOT prox is dependent on imaging plane position and less reproducible than RVOT distal</li> <li>• Risk of underestimation or overestimation if the RV view is obliquely oriented with respect to RV outflow tract</li> <li>• RV outflow dimensions can be inaccurate in case of chest and spine deformities</li> <li>• Endocardial definition of the RV anterior wall is often sub-optimal</li> <li>• Limited normative data is available</li> <li>• Regional measure; may not reflect global RV size (underestimation or overestimation)</li> </ul>
<b>RV areas (inflow)</b> 	<ul style="list-style-type: none"> <li>• Manual tracing of RV endocardial border from the lateral tricuspid annulus along the free wall to the apex and back to medial tricuspid annulus, along the interventricular septum at end-diastole and at end-systole</li> <li>• Trabeculations, papillary muscles and moderator band are included in the cavity area</li> </ul>	<ul style="list-style-type: none"> <li>• Relatively easy to measure</li> </ul>	<ul style="list-style-type: none"> <li>• Challenging in case of sub-optimal image quality of RV free wall</li> <li>• Challenging in the presence of trabeculation</li> <li>• RV size underestimation if RV cavity is foreshortened</li> <li>• Due to the LV twisting motion and the crescent RV shape, the end-diastolic RV image may not be in the same tomographic plane as the end-systolic one</li> <li>• May not accurately reflect global RV size (underestimation or overestimation)</li> </ul>

(Continued)

Table 7 (Continued)

Echocardiographic imaging	Recommended methods	Advantages	Limitations
<b>3DE RV volumes</b> 	<ul style="list-style-type: none"><li>• Dedicated multibeam 3D acquisition, with minimal depth and sector angle (for a temporal resolution &gt; 20–25 volumes/sec) that encompasses entire RV cavity</li><li>• Automatically identified timing of end-diastole and end-systole should be verified</li><li>• Myocardial trabeculae and moderator band should be included in the cavity</li></ul>	<ul style="list-style-type: none"><li>• Unique measures of RV global size that includes inflow, outflow and apical regions</li><li>• Independent of geometric assumptions</li><li>• Validated against cardiac magnetic resonance</li></ul>	<ul style="list-style-type: none"><li>• Dependent on image quality, regular rhythm, patient cooperation</li><li>• Needs specific 3D echocardiographic equipment and training</li><li>• Reference values established in few publications</li></ul>
<b>RV wall thickness</b> 	<ul style="list-style-type: none"><li>• Linear measurement of RV free wall thickness (either by M-mode or 2DE) performed at end-diastole, below the tricuspid annulus at a distance approximating the length of anterior tricuspid leaflet, when it is fully open and parallel to the RV free wall.</li><li>• Trabeculae, papillary muscles and epicardial fat should be excluded</li><li>• Zoomed imaging with focus on the RV mid-wall and respiratory maneuvers may improve endocardial border definition</li></ul>	<ul style="list-style-type: none"><li>• Easy to perform</li></ul>	<ul style="list-style-type: none"><li>• Single-site measurement</li><li>• Harmonic imaging and oblique M-mode sampling may overestimate RV wall thickness</li><li>• Challenging in case of thickening of visceral pericardium</li><li>• There is no criterion for defining an abnormally thin RV wall</li></ul>

\*All linear dimensions should be obtained using inner-edge-to-inner-edge method.

in women, and RV ESVs of 44 mL/m<sup>2</sup> for men and 36 mL/m<sup>2</sup> for women as the upper limits of the corresponding normal ranges.

8. RV Systolic Function

RV systolic function has been evaluated using multiple parameters (Table 9), including RIMP, TAPSE, 2D FAC, 3DE EF, S', and longitudinal strain and strain rate by DTI and 2D STE.<sup>25</sup> Multiple studies have demonstrated the clinical utility and value of RIMP, TAPSE, 2D FAC, and S' of the tricuspid annulus, as well as longitudinal speckle-tracking echocardiographic strain. RV EF by 3DE seems to be more reliable and have better reproducibility when properly performed, and a growing body of data are currently available to provide normal reference values (Table 10 and Supplemental Table 8).

**8.1. RIMP.** RIMP is an index of global RV performance. The isovolumic contraction time, the isovolumic relaxation time, and ejection time intervals should be measured from the same heartbeat using either PW spectral Doppler or DTI velocity of the lateral tricuspid annulus (Table 9). When using PW spectral Doppler to calculate RIMP, it important to ensure that the nonconsecutive beats have similar RR intervals. This limitation does not apply to the DTI-based RIMP measurements. RIMP can be falsely low in conditions

associated with elevated RA pressures, which will shorten the IVRT. RIMP > 0.43 by PW Doppler and > 0.54 by DTI indicate RV dysfunction.

**8.2. TAPSE.** TAPSE is easily obtainable and represents a measure of RV longitudinal function. It is measured by M-mode echocardiography with the cursor optimally aligned along the direction of the tricuspid lateral annulus in the apical four-chamber view (Table 9). Although this index predominantly reflects RV longitudinal function, it has shown good correlations with parameters estimating RV global systolic function, such as radionuclide-derived RV EF, 2D echocardiographic RV FAC, and 2D echocardiographic EF. As a one-dimensional measurement relative to the transducer position, TAPSE may over- or underestimate RV function because of cardiac translation.<sup>79</sup> Although there may be minor variations in TAPSE values according to gender and BSA, generally, TAPSE < 17 mm is highly suggestive of RV systolic dysfunction.

**8.3. RV 2D FAC.** FAC provides an estimate of global RV systolic function. It is important to ensure that the entire right ventricle be contained in the imaging sector, including the apex and the free wall, during both systole and diastole. While tracing the RV area, care must be taken to include the trabeculae in the RV cavity (Table 9). RV FAC < 35% indicates RV systolic dysfunction.

**Table 8** Normal values for RV chamber size

Parameter	Mean $\pm$ SD	Normal range
RV basal diameter (mm)	33 $\pm$ 4	25-41
RV mid diameter (mm)	27 $\pm$ 4	19-35
RV longitudinal diameter (mm)	71 $\pm$ 6	59-83
RVOT PLAX diameter (mm)	25 $\pm$ 2.5	20-30
RVOT proximal diameter (mm)	28 $\pm$ 3.5	21-35
RVOT distal diameter (mm)	22 $\pm$ 2.5	17-27
RV wall thickness (mm)	3 $\pm$ 1	1-5
RVOT EDA (cm <sup>2</sup> )		
Men	17 $\pm$ 3.5	10-24
Women	14 $\pm$ 3	8-20
RV EDA indexed to BSA (cm <sup>2</sup> /m <sup>2</sup> )		
Men	8.8 $\pm$ 1.9	5-12.6
Women	8.0 $\pm$ 1.75	4.5-11.5
RV ESA (cm <sup>2</sup> )		
Men	9 $\pm$ 3	3-15
Women	7 $\pm$ 2	3-11
RV ESA indexed to BSA (cm <sup>2</sup> /m <sup>2</sup> )		
Men	4.7 $\pm$ 1.35	2.0-7.4
Women	4.0 $\pm$ 1.2	1.6-6.4
RV EDV indexed to BSA (mL/m <sup>2</sup> )		
Men	61 $\pm$ 13	35-87
Women	53 $\pm$ 10.5	32-74
RV ESV indexed to BSA (mL/m <sup>2</sup> )		
Men	27 $\pm$ 8.5	10-44
Women	22 $\pm$ 7	8-36

EDA, end-diastolic area; ESA, end-systolic area; PLAX, parasternal long-axis view; RVOT, RV outflow tract.

**8.4. DTI-Derived Tricuspid Lateral Annular Systolic Velocity.** DTI-derived  $S'$ -wave velocity is easy to measure, reliable, and reproducible, and it has been shown to correlate well with other measures of global RV systolic function. Specific age-related cutoff values have been reported in a large sample of healthy subjects.<sup>80</sup> It is important to keep the basal segment and the annulus aligned with the Doppler cursor to avoid velocity underestimation (Table 9). Similar to TAPSE,  $S'$  is measured relative to the transducer and may therefore be influenced by overall heart motion. An  $S'$  velocity  $< 9.5$  cm/sec measured on the free-wall side indicates RV systolic dysfunction.

**8.5. RV Strain and Strain Rate.** Strain and strain rate are useful parameters for estimating RV global and regional systolic function. Longitudinal strain is calculated as the percentage of systolic shortening of the RV free wall from base to apex, while longitudinal strain rate is the rate of this shortening. RV longitudinal strain is less confounded by overall heart motion<sup>79,81</sup> but depends on RV loading conditions as well as RV size and shape. RV longitudinal strain should be measured in the RV-focused four-chamber view. Compared with STE-derived strain, the angle dependency of DTI strain is a disadvantage. RV speckle-tracking echocardiographic strain is influenced by image quality, reverberation and other artifacts, as well as attenuation. Placing the basal reference points too low (i.e., on the atrial side of the tricuspid annulus) might result in

artificially low basal strain values. The width of the region of interest should be limited to the myocardium, excluding the pericardium, which may be difficult given the usually thin RV free wall (Table 9).

In the context of the right ventricle, GLS is a parameter borrowed from LV measurements, and software currently used to measure RV GLS from most manufacturers has been designed for LV measurements and later adapted for the right ventricle. The term *RV GLS* usually refers to either the average of the RV free wall and the septal segments or the RV free wall segments alone (Figure 9). Peak global longitudinal RV strain excluding the interventricular septum has been recently reported to have prognostic value in various disease states, such as heart failure,<sup>82,83</sup> acute myocardial infarction,<sup>84</sup> pulmonary hypertension,<sup>85,86</sup> and amyloidosis,<sup>87</sup> and to predict RV failure after LV assist device implantation.<sup>88</sup>

The largest body of evidence comes from the single-center studies cited above, which involved predominantly imaging equipment and software from two vendors, where pooled data were derived from limited number of subjects. Current reference values for global RV free wall speckle-tracking echocardiographic strain are reported in Table 10. Pooled data (though heavily weighted by a single vendor) suggest that global longitudinal RV free wall strain  $> -20\%$  (i.e.,  $<20\%$  in absolute value) is likely abnormal.

**Recommendations.** Two-dimensional STE-derived strain, particularly of the RV free wall, appears to be reproducible and feasible for clinical use. Because of the need for additional normative data from large studies involving multivendor equipment, no definite reference ranges are currently recommended for either global or regional RV strain or strain rate.

**8.6. RV 3D EF.** Three-dimensional echocardiographic RV EF is a global measure of RV systolic performance. Although RV EF does not directly reflect RV contractile function per se, it provides an integrated view of the interaction between RV contractility and load. RV EF can be of particular clinical value in patients after cardiac surgery (in the absence of marked septal shift), when conventional indices of longitudinal RV function (i.e., TAPSE,  $S'$  wave) are generally reduced and no longer representative of overall RV performance.<sup>81,89,90</sup> Three-dimensional echocardiography has been extensively validated against CMR,<sup>78,91</sup> and the volumetric semiautomated border detection approach is the recommended method for the assessment of RV EF.

The limitations of 3D assessment of RV EF are load dependency, interventricular changes affecting septal motion, poor acoustic windows, and irregular rhythms. As described above in the section on RV volume, the RV EF is slightly higher in women than in men, because of smaller volumes, and it is recommended to refer to gender-specific values (Supplemental Table 8).

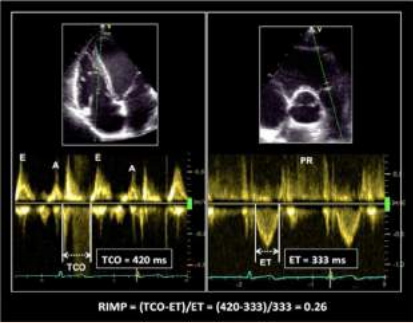
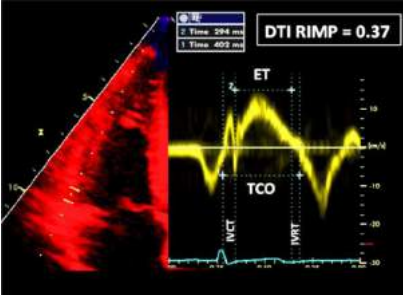
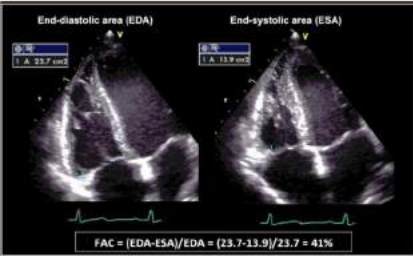
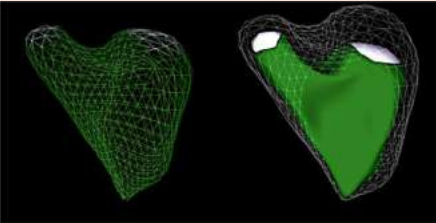
**Recommendation.** In laboratories with appropriate 3D platforms and experience, 3DE-derived RV EF should be considered as a method of quantifying RV systolic function, with the limitations mentioned above. Roughly, an RV EF of  $<45\%$  usually reflects abnormal RV systolic function, though laboratories may choose to refer to age- and gender-specific values.

### III. THE LEFT AND RIGHT ATRIA

The left atrium fulfills three major physiologic roles that influence LV filling and performance. The left atrium acts as a (1) contractile pump

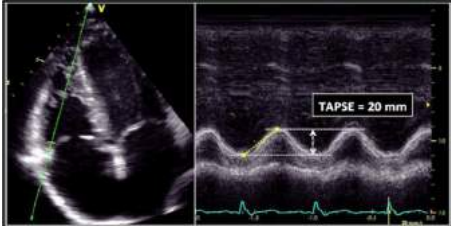
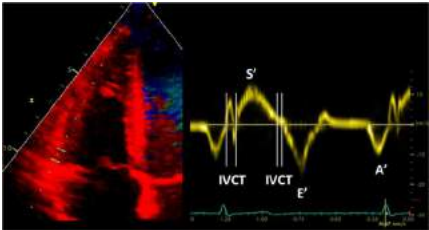
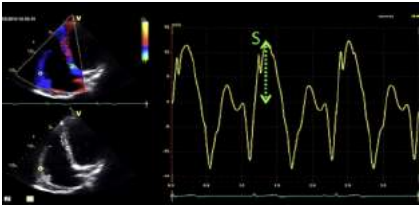
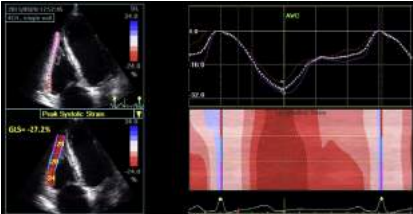


**Table 9** Recommendations for the echocardiographic assessment of RV function

Echocardiographic imaging	Recommended methods	Advantages	Limitations
<b>RV global function</b> Pulsed Doppler RIMP 	RIMP (Tei index) by pulsed Doppler: $RIMP = (TCO - ET)/ET$	<ul style="list-style-type: none"><li>• Prognostic value</li><li>• Less affected by heart rate</li></ul>	<ul style="list-style-type: none"><li>• Requires matching for R-R intervals when measurements are performed on separate recordings</li><li>• Unreliable when RA pressure is elevated</li></ul>
Tissue Doppler RIMP 	RIMP by tissue Doppler: $RIMP = (IVRT + IVCT)/ET = (TCO - ET)/ET$	<ul style="list-style-type: none"><li>• Less affected by heart rate</li><li>• Single-beat recording with no need for R-R interval matching</li></ul>	<ul style="list-style-type: none"><li>• Unreliable when RA pressure is elevated</li></ul>
<b>RV global systolic function</b> FAC 	RV FAC in RV-focused apical four-chamber view: $RV\ FAC\ (\%) = 100 \times (EDA - ESA)/EDA$	<ul style="list-style-type: none"><li>• Established prognostic value</li><li>• Reflects both longitudinal and radial components of RV contraction</li><li>• Correlates with RV EF by CMR</li></ul>	<ul style="list-style-type: none"><li>• Neglects the contribution of RV outflow tract to overall systolic function</li><li>• Only fair inter-observer reproducibility</li></ul>
EF 	Fractional RV volume change by 3D TTE: $RV\ EF\ (\%) = 100 \times (EDV - ESV)/EDV$	<ul style="list-style-type: none"><li>• Includes RV outflow tract contribution to overall function</li><li>• Correlates with RV EF by CMR</li></ul>	<ul style="list-style-type: none"><li>• Dependent on adequate image quality</li><li>• Load dependency</li><li>• Requires offline analysis and experience</li><li>• Prognostic value not established</li></ul>

(Continued)

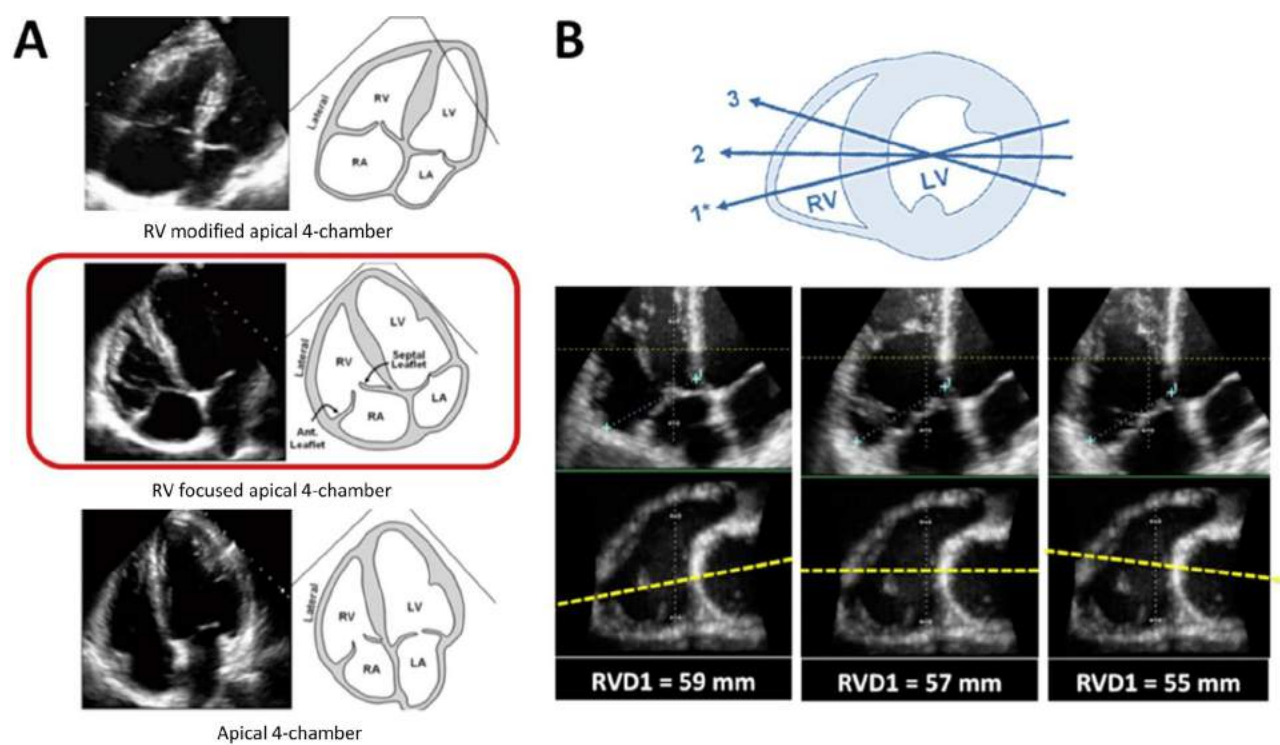
**Table 9** (Continued)

Echocardiographic imaging	Recommended methods	Advantages	Limitations
<b>RV longitudinal systolic function</b> <b>TAPSE</b> 	<ul style="list-style-type: none"> <li>Tricuspid annular longitudinal excursion by M-mode (mm), measured between end-diastole and peak systole</li> <li>Proper alignment of M-mode cursor with the direction of RV longitudinal excursion should be achieved from the apical approach.</li> </ul>	<ul style="list-style-type: none"> <li>Established prognostic value</li> <li>Validated against radionuclide EF</li> </ul>	<ul style="list-style-type: none"> <li>Angle dependency</li> <li>Partially representative of RV global function*</li> </ul>
<b>Pulsed tissue Doppler S wave</b> 	<ul style="list-style-type: none"> <li>Peak systolic velocity of tricuspid annulus by pulsed-wave DTI (cm/sec), obtained from the apical approach, in the view that achieves parallel alignment of Doppler beam with RV free wall longitudinal excursion</li> </ul>	<ul style="list-style-type: none"> <li>Easy to perform</li> <li>Reproducible</li> <li>Validated against radionuclide EF</li> <li>Established prognostic value</li> </ul>	<ul style="list-style-type: none"> <li>Angle dependent</li> <li>Not fully representative of RV global function, particularly after thoracotomy, pulmonary thromboendarterectomy or heart transplantation</li> </ul>
<b>Color tissue Doppler S wave</b> 	<ul style="list-style-type: none"> <li>Peak systolic velocity of tricuspid annulus by color DTI (cm/sec)</li> </ul>	<ul style="list-style-type: none"> <li>Sampling is performed after image acquisition</li> <li>Allows multisite sampling on the same beat</li> </ul>	<ul style="list-style-type: none"> <li>Angle dependent</li> <li>Not fully representative of RV global function, particularly after thoracotomy, pulmonary thromboendarterectomy or heart transplantation</li> <li>Lower absolute values and reference ranges than pulsed DTI S' wave</li> <li>Requires offline analysis</li> </ul>
<b>GLS</b> 	<ul style="list-style-type: none"> <li>Peak value of 2D longitudinal speckle tracking derived strain, averaged over the three segments of the RV free wall in RV-focused apical four-chamber view (%)</li> </ul>	<ul style="list-style-type: none"> <li>Angle independent</li> <li>Established prognostic value</li> </ul>	<ul style="list-style-type: none"> <li>Vendor dependent</li> </ul>

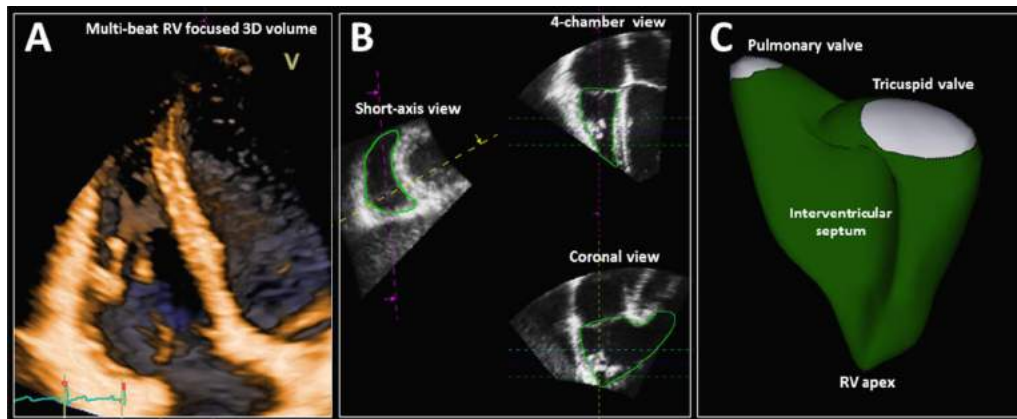
EDA, End-diastolic area; ESA, end-systolic area; ET, ejection time; GLS, global longitudinal strain; IVCT, isovolumic contraction time; TCO, tricuspid valve closure-to-opening time.

Table 10 Normal values for parameters of RV function		
Parameter	Mean ± SD	Abnormality threshold
TAPSE (mm)	24 ± 3.5	<17
Pulsed Doppler S wave (cm/sec)	14.1 ± 2.3	<9.5
Color Doppler S wave (cm/sec)	9.7 ± 1.85	<6.0
RV fractional area change (%)	49 ± 7	<35
RV free wall 2D strain* (%)	−29 ± 4.5	>−20 (<20 in magnitude with the negative sign)
RV 3D EF (%)	58 ± 6.5	<45
Pulsed Doppler MPI	0.26 ± 0.085	>0.43
Tissue Doppler MPI	0.38 ± 0.08	>0.54
E wave deceleration time (msec)	180 ± 31	<119 or >242
E/A	1.4 ± 0.3	<0.8 or >2.0
e′/a′	1.18 ± 0.33	<0.52
e′	14.0 ± 3.1	<7.8
E/e′	4.0 ± 1.0	>6.0

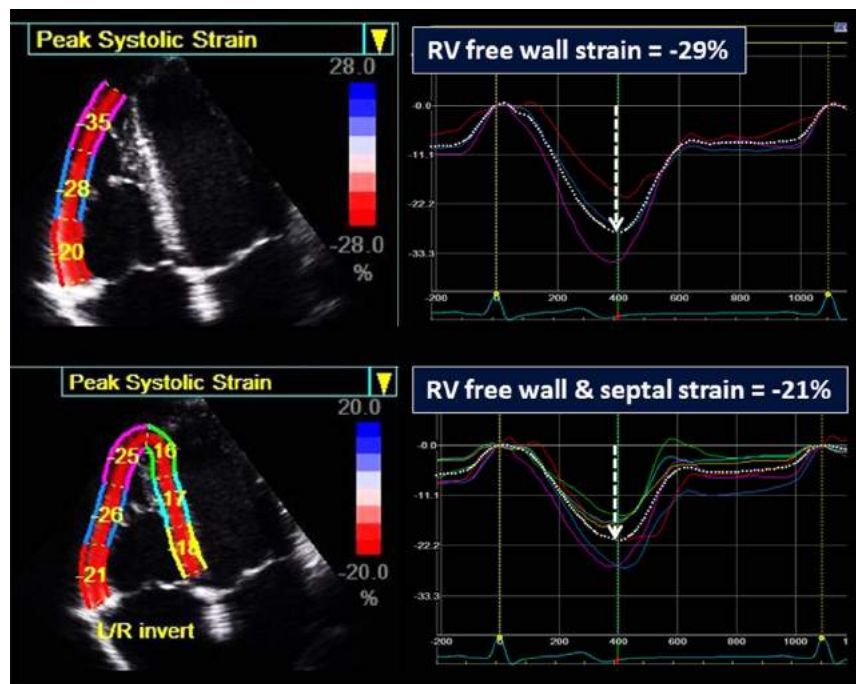
MPI, Myocardial performance index.  
\*Limited data; values may vary depending on vendor and software version.



**Figure 7** (A) Three apical images demonstrating different views of the right ventricle (RV). The middle image shows the right ventricular–focused view. (B) The rationale for maximizing the right ventricular basal dimension in the right ventricular–focused view. Below the cartoon, by manipulating offline the same 3D right ventricular data set, it is apparent that minor variations in the four-chamber plane position (*dashed line*) with respect to the right ventricular crescent shape may result in variability of right ventricular size when performed by linear measurements.



**Figure 8** Three-dimensional analysis of the right ventricle (RV). **(A)** A 3D data set is acquired from a right ventricular–focused apical four-chamber view by stitching together the subvolumes generated from several (four to six) consecutive beats. **(B)** The right ventricular endocardial surface is semiautomatically identified after manual initialization in the right ventricular short-axis, four-chamber, and coronal views in both end-systole and end-diastole. **(C)** The generated 3D surface model of the RV enables the quantitation of right ventricular ESV and ESV, stroke volume, and EF.



**Figure 9** Measurement of RV systolic strain by 2D STE. The upper panel demonstrates RV “global” free wall strain whereby the three segments of the free wall are averaged, and the lower panel demonstrates “global” longitudinal strain of the six segments of the apical four-chamber view: three free wall and three septal segments. Note that RV longitudinal strain is significantly higher (as an absolute value) than the strain averaged from both septal and free wall segments. Until a universal standard is established, the interpretation of RV longitudinal strain values should take into account the methodology and vendor- and method-specific reference values.

that delivers 15% to 30% of the entire LV filling, (2) reservoir that collects pulmonary venous return during ventricular systole, and (3) conduit for the passage of stored blood from the left atrium to the left ventricle during early ventricular diastole.<sup>92,93</sup> An enlarged left atrium is associated with adverse cardiovascular outcomes.<sup>94-99</sup> In the absence of mitral valve disease, an increase in LA size most commonly reflects increased wall tension as a result of increased LA pressure,<sup>100-103</sup> as well as impairment in LA function secondary to an atrial myopathy.<sup>104,105</sup> A clear relationship exists between an enlarged left atrium and the incidence of atrial fibrillation and stroke,<sup>92,106-115</sup> risk for overall mortality after myocardial

infarction,<sup>104,105,116,117</sup> risk for death and hospitalization in patients with dilated cardiomyopathy,<sup>118-122</sup> and major cardiac events or death in patients with diabetes mellitus.<sup>123</sup> LA enlargement is a marker of both the severity and chronicity of diastolic dysfunction and magnitude of LA pressure elevation.<sup>98,100-103</sup>

## 9. LA Measurements

**9.1. General Considerations for LA Size.** TTE is the recommended approach for assessing LA size. Recommendations for LA



quantification are summarized in Table 11. With TEE, the entire left atrium frequently cannot be fit in the image sector. Accordingly, TEE should not be used to assess LA size. LA size should be measured at the end of LV systole, when the LA chamber is at its greatest dimension. While acquiring images to measure LA size and volumes, care should be taken to avoid foreshortening of the left atrium. Because the longitudinal axes of the left ventricle and left atrium frequently lie in different planes, dedicated acquisitions of the left atrium from the apical approach should be obtained for optimal LA volume measurements. The base of the left atrium should be at its largest size, indicating that the imaging plane passes through the maximal short-axis area. LA length should also be maximized to ensure alignment along the true long axis of the left atrium. When using the biplane disk summation method to calculate LA volumes, the lengths of the long axes measured in the two- and four-chamber views should be similar. When tracing the borders of the left atrium, the confluences of the pulmonary veins and the LA appendage should be excluded. The atrioventricular interface should be represented by the mitral annulus plane, not by the tip of the mitral leaflets.

**9.2. Linear Dimensions and Area Measurements.** The most widely used linear dimension is the LA anteroposterior (AP) measurement in the parasternal long-axis view using M-mode echocardiography or, preferably, 2DE.<sup>92,107,109,110,114,118,120,121,124,125</sup> Although this measurement has been used extensively in clinical practice and research, it has become clear that frequently it may not represent an accurate picture of LA size.<sup>126,127</sup> Traditionally, the AP dimension was widely used because it was known to be the most reproducible measurement. However, assessment of LA size using only the AP diameter assumes that when the left atrium enlarges, all its dimensions change similarly, which is often not the case during LA remodeling.<sup>128-130</sup> Therefore, AP linear dimension should not be used as the sole measure of LA size. LA area can be planimetered in the apical four- and two-chamber views and normal values for these parameters have been reported.<sup>12</sup> Optimal contours should be obtained orthogonally around the long axis of the left atrium from good quality images while avoiding foreshortening.<sup>1</sup> The ease with which LA volumes can be obtained in clinical practice in conjunction with the existing robust literature on normal values and the prognostic value of LA volumes renders reporting of LA area unnecessary.

**9.3. Volume Measurements.** When assessing the LA size and remodeling, the measurement of LA volume is recommended. Evaluation of volume takes into account alterations in LA chamber size in all directions. LA volume has been shown to be a powerful prognostic variable in a variety of cardiac disease states.<sup>99,106,112,113,115-117,122,131-136</sup> Compared with AP diameter, LA volume has a stronger association with outcomes in cardiac patients.<sup>113,137</sup> Two-dimensional echocardiographic LA volumes are typically smaller than those reported from computed tomography or CMR.<sup>138-142</sup> Measurements of LA volumes are important, because they reflect the burden and chronicity of elevated LV filling pressures and are a strong predictor of outcomes.

Different methods exist for measuring LA volumes. Although the three linear measurements have been used to calculate LA volume using an ellipsoid model,<sup>131,137,143</sup> the relative inaccuracy of these linear measurements limits this method. LA volume should be measured using the disk summation algorithm, similar to that used to measure LV volume (Table 11).<sup>144,145</sup>

The LA endocardial borders should be traced in both the apical four- and two-chamber views. A single-plane approach can also be

used, but this method is based on the geometric assumption that the left atrium is circular in the short-axis cut plane, which may not be always accurate.<sup>146</sup> Although not recommended for routine use, this approach could be used in cases when planimetry in both views is difficult. Single-plane apical four-chamber indexed LA volumes are typically 1 to 2 mL/m<sup>2</sup> smaller than apical two-chamber volumes.<sup>12,146</sup>

Alternatively, a biplane calculation could also be performed using the LA areas and lengths measured from both the apical four- and two-chamber views (Table 11). Although the area-length method still assumes an ellipsoidal LA shape, it has the advantage of reducing linear dimensions to only two measurements of atrial length, of which the shorter one is selected.<sup>98,147</sup>

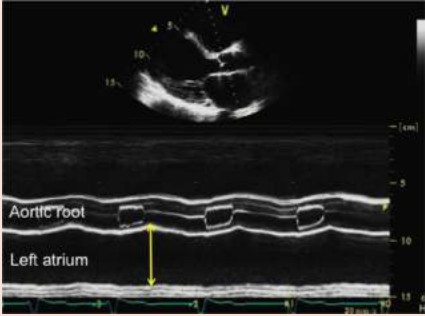
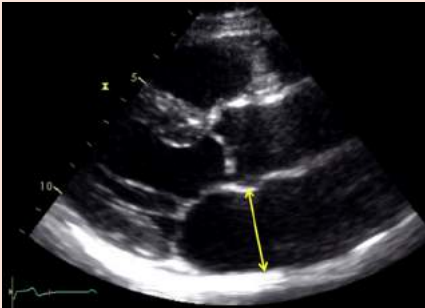

**9.4. Normal Values of LA Measurements.** Since the publication of the 2005 chamber quantification guidelines, two articles have reported normal values for LA linear measurements.<sup>12,143</sup> These values were in keeping with prior recommendations, and accordingly, no modifications have been made to the normal values of LA AP diameters (Supplemental Table 9). Although not recommended for routine clinical use, normal values for apical four- and two-chamber linear measurements and nonindexed LA area and volume measurements have been reported.<sup>12</sup>

LA size is dependent on gender. However the gender differences in LA size are generally accounted for when adjusting for body size.<sup>12</sup> Several indexing methods have been proposed,<sup>137,148</sup> but indexing to BSA has yielded the most available data and is recommended by the writing group. Indexing by BSA accounts for the gender differences in LA size, such that only the indexed value should be reported.<sup>93,137,149,150</sup>

In the prior chamber quantification guideline document, the reported BSA-indexed LA volume normal values were based on two studies performed in a small number of subjects.<sup>98,144</sup> Since the publication of that document, eight additional studies (1,234 patients) describing normal values of LA volumes using the area-length ellipsoid or the disk summation techniques have been reported.<sup>11,12,145,147,151-155</sup> This has resulted in a change in the recommended upper normal indexed LA volume to 34 mL/m<sup>2</sup> (previously 28 mL/m<sup>2</sup>). In addition, LA volume data became available in 1,331 patients from the five databases described earlier in this document, wherein the mean calculated LA volume was 25 mL/m<sup>2</sup>. This upper normal revised value of 34 mL/m<sup>2</sup> also seems to fit in well with a risk-based approach for determination of cut-offs between a normal and an enlarged left atrium.<sup>106,123,134,136</sup> This cutoff value is also consistent with the ASE and European Association of Echocardiography guideline document on evaluation of diastolic function.<sup>156</sup> The 2DE-derived biplane LA volumes are listed in Table 4, including normal ranges and severity partition cutoffs. Of note, LA volume can be increased in elite athletes, which needs to be taken into account to avoid misinterpretation as abnormal.<sup>146</sup>

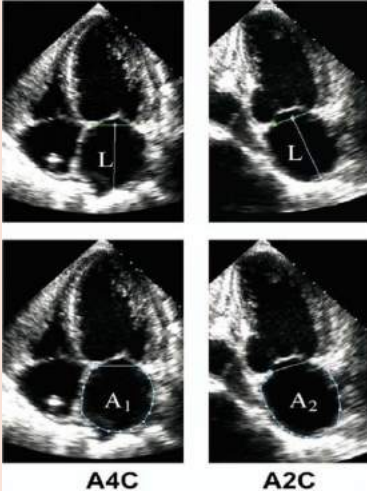
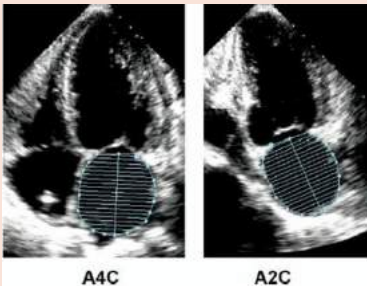
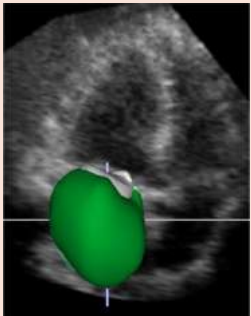
Three-dimensional echocardiography holds promise for assessing LA volume and correlates with cardiac computed tomography<sup>157,158</sup> and magnetic resonance imaging.<sup>159,160</sup> Compared with 2D assessment of LA volume, 3DE is more accurate compared with CMR<sup>159,160</sup> and has superior prognostic ability.<sup>161,162</sup> Three-dimensional echocardiographic LA volumes are typically larger than 2D echocardiographic volumes in most studies.<sup>160,163</sup> Despite these advantages, the lack of a standardized methodology and limited normative data<sup>164</sup> prevent this committee from recommending the use of 3D echocardiographic normal values at this time.

**Table 11** Recommendations for the echocardiographic assessment of LA size

Parameter and method	Echocardiographic imaging	Advantages	Limitations
<b>Internal linear dimensions.</b> The anteroposterior diameter of the left atrium can be measured in the parasternal long-axis view perpendicular to the aortic root long axis, and measured at the level of the aortic sinuses by using the leading-edge to leading-edge convention.	M-mode tracing 	<ul style="list-style-type: none"><li>• Reproducible</li><li>• High temporal resolution</li><li>• Wealth of published data</li></ul>	Single dimension not representative of actual LA size (particularly in dilated atria)
	2D-guided linear measurements 	<ul style="list-style-type: none"><li>• Facilitates orientation perpendicular to LA posterior wall</li></ul>	<ul style="list-style-type: none"><li>• Lower frame rates than in M-mode</li><li>• Single dimension only</li></ul>
<b>Area.</b> Measured in four-chamber apical view, at end-systole, on the frame just prior to mitral valve opening by tracing the LA inner border, excluding the area under the mitral valve annulus and the inlet of the pulmonary veins.	2D images 	<ul style="list-style-type: none"><li>• More representative of actual LA size than anteroposterior diameter only</li></ul>	<ul style="list-style-type: none"><li>• Need for a dedicated view to avoid LA foreshortening</li><li>• Assumes a symmetric shape of the atrium</li></ul>

(Continued)

Table 11 (Continued)

Parameter and method	Echocardiographic imaging	Advantages	Limitations
<p><b>Volume.</b></p> <p>2D volumetric measurements are based on tracings of the blood-tissue interface on apical four- and two-chamber views. At the mitral valve level, the contour is closed by connecting the two opposite sections of the mitral annulus with a straight line. Endocardial tracing should exclude atrial appendage and pulmonary veins. LA length L is defined as the shortest of the two long axes measured in the apical two- and four-chamber views (to provide reliable calculations the two lengths should not differ more than 5 mm). Volumes can be computed by using the area-length approximation:</p> $\frac{8}{3\pi} \left[ \frac{(A_1 \cdot A_2)}{L} \right]$ <p>where A1 and A2 are the corresponding LA areas. Alternatively LA volume can be calculated using the disk summation technique by adding the volume of a stack of cylinders of height h and area calculated by orthogonal minor and major transverse axes (D1 and D2) assuming an oval shape:</p> $\pi/4(h) \sum (D1)(D2)$ <p>3D data sets are usually obtained from the apical approach using a multibeam full-volume acquisition</p>	<p>2DE</p> <p>Area-length technique</p>  <p>A4C A2C</p> <p>Biplane method of disks</p>  <p>A4C A2C</p> <p>3D data sets</p> 	<ul style="list-style-type: none"> <li>Enables accurate assessment of the asymmetric remodeling of the left atrium</li> <li>More robust predictor of cardiovascular events than linear or area measurements</li> </ul>	<ul style="list-style-type: none"> <li>Geometric assumptions about LA shape</li> <li>Few accumulated data on normal population</li> <li>Single plane volume calculations are inaccurate since they are based on the assumption that <math>A1 = A2</math></li> </ul>
		<ul style="list-style-type: none"> <li>No geometrical assumption about LA shape</li> <li>More accurate when compared to 2D measurements</li> </ul>	<ul style="list-style-type: none"> <li>Dependent on adequate image quality</li> <li>Lower temporal resolution</li> <li>Limited data on normal values</li> <li>Patient's cooperation required</li> </ul>

**Recommendations.** Because it is theoretically more accurate than the area-length method, the biplane disk summation technique, which incorporates fewer geometric assumptions, should be the preferred method to measure LA volume in clinical practice. The upper normal limit for 2D echocardiographic LA volume is 34 mL/m<sup>2</sup> for both genders.

## 10. Right Atrial measurements

Less research and fewer clinical outcomes data are available on the quantification of RA size. Although the right atrium can be assessed from different views, quantification of RA size is most commonly performed from the apical four-chamber view (Table 12). The minor-axis dimension should be taken from a plane perpendicular to the long axis of the right atrium, extending from the lateral border of the right atrium to the interatrial septum. In contrast to the left atrium, RA size appears to be gender dependent, but prior ASE guidelines did not have sufficient data to provide normative data by gender.<sup>1,71</sup> Recent data obtained from three cohorts of >2,400 patients now provide normal values of RA dimensions for men and women.<sup>12,73,165</sup>

As with the left atrium, RA volumes are likely to be more robust and accurate for determination of RA size compared with linear dimensions. At the time of the prior guideline document, limited data were available for the determination of normative RA volumes. Because there are no standard orthogonal RA views to use for an apical biplane calculation, a single-view area-length and/or disk summation techniques has been proposed for RA volume determination.<sup>150,153,165-167</sup> Of note, normal RA volumes for men are slightly larger than those for women, with indexing to BSA failing to equalize values between genders for reasons that are not fully understood.<sup>150,165</sup> Recommendations for RA volume normative data are made from the two largest most contemporary data sets<sup>12,165</sup> (Table 13). RA volumes are underestimated with 2D echocardiographic techniques compared with 3DE.<sup>164,165,168</sup> RA volumes in adult subjects appear to be smaller than LA volumes.<sup>12,150,153,165</sup> This is because the RA volumes were obtained using a single-plane method of disks, in contrast to the LA volumes, which were established using the biplane technique.

**Recommendations.** The recommended parameter to assess RA size is RA volume, calculated using single-plane area-length or disk summation techniques in a dedicated apical four-chamber view. The normal ranges for 2D echocardiographic RA volume are 25 ± 7 mL/m<sup>2</sup> in men and 21 ± 6 mL/m<sup>2</sup> in women.

## IV. THE AORTIC ANNULUS AND AORTIC ROOT

Detailed knowledge and quantification of the aortic root and aortic valve morphology has become even more crucial with the increasing use of transcatheter aortic valve implantation (TAVI) and transcatheter aortic valve replacement (TAVR) procedures. This knowledge is critically important for preprocedural planning, intraprocedural guidance, and postprocedural assessment.

The aortic root extends from the basal attachments of the aortic valve leaflets within the LV outflow tract to their distal attachment at the tubular portion of the aorta (the sinotubular junction).<sup>169</sup> The aortic root is a geometrically complex structure that includes (1) the aortic valve annulus, (2) the interleaflet triangles, (3) the semilunar

aortic leaflets and their attachments, (4) the aortic sinuses of Valsalva, and (5) the sinotubular junction.<sup>170-172</sup> Aortic measurements should be made at the following sites: (1) the aortic valve annulus, (2) the maximal diameter of the sinuses of Valsalva, (3) the sinotubular junction (usually a demarcated transition between the sinuses of Valsalva and the tubular portion of the ascending aorta), and (4) the maximal diameter of the proximal ascending aorta, including a notation of the distance between the measurement site and the sinotubular junction (Figure 10A).

## 11. The Aortic Annulus

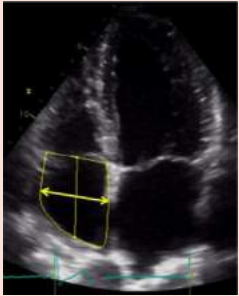


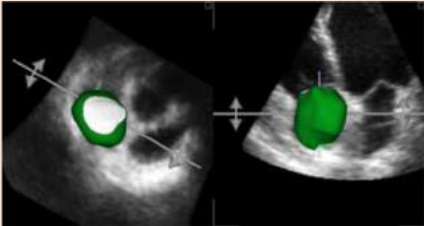
The “aortic annulus” is not a true or distinct anatomic structure but is a virtual ring that may be defined by joining the basal attachments, or nadirs, of the three aortic leaflets. The distal (uppermost) attachments of the leaflets, in the shape of a crown, form a true anatomic ring.<sup>169,173</sup> (Figure 10B). Approximately two-thirds of the circumference of the lower part of the aortic root is attached to the muscular interventricular septum, while the remaining one-third is in fibrous continuity with the anterior mitral valve leaflet.<sup>174</sup> Measurement of the aortic valve annulus before TAVI or TAVR is a challenge, and the ideal modality for its measurement has yet to be established. During the initial TAVI and TAVR experience, aortic annular measurements were routinely performed using 2DE.<sup>174,175</sup> Although the standard approach during the early years of TAVI and TAVR was echocardiography using a one-dimensional measurement, this method has clear limitations for TAVI and TAVR valve sizing. At present, the two most commonly used imaging techniques used for measuring the aortic annulus before TAVI or TAVR are echocardiography and multidetector computed tomography (MDCT).

With echocardiography, measurements of the aortic annulus should be made in the zoom mode using standard electronic calipers in midsystole, when the annulus is slightly larger and rounder than in diastole, between the hinge points of the aortic valve leaflets (usually between the hinge point of the right coronary cusp and the edge of the sinus at the side of the commissures between the left coronary cusp and the noncoronary cusp) from inner edge to inner edge. All other aortic measurements should be made at end-diastole, in a strictly perpendicular plane to that of the long axis of the aorta. Aortic annular measurements may be difficult in patients with acoustic blooming caused by a calcified aortic annulus.<sup>176-179</sup> As a general rule, calcium protuberances should be considered as part of the lumen, not of the aortic wall, and therefore excluded from the diameter measurement.

The anteroposterior diameter is commonly measured by both 2D TTE (from the parasternal long-axis view) and 3D TEE (from the longitudinal view of the proximal aortic root, usually 110°–130°) and approximates the minor dimension of the annulus measured by MDCT.<sup>3,176,180</sup> However, because the annulus is often elliptical, with variable diameters, it is preferable to measure the annulus in a cross-sectional view, using 3D imaging, as recommended by the European Association of Echocardiography and ASE guidelines<sup>181</sup>; the American College of Cardiology Foundation, American Association for Thoracic Surgery, Society for Cardiac Angiography and Interventions, and Society of Thoracic Surgeons consensus document on TAVR<sup>182</sup>; the Society of Cardiovascular Computed Tomography expert consensus document on MDCT<sup>183</sup>; and others.<sup>184-187</sup> Using 3D TEE, both the smaller (anteroposterior, sagittal) and larger (medial-lateral, coronal) diameters, as well as the perimeter and annular area, should be measured in a cross-sectional



**Table 12** Recommendations for the echocardiographic assessment of RA size

Parameter and method	Echocardiographic imaging	Advantages	Limitations
<b>Linear dimensions.</b> The minor axis of the right atrium should be measured in the apical four-chamber view as the distance between the lateral RA wall and interatrial septum, at the midatrial level defined by half of RA long axis	2D-guided linear measurements 	<ul style="list-style-type: none"><li>• Easy to obtain</li><li>• Established normal values</li></ul>	<ul style="list-style-type: none"><li>• Single dimension only</li><li>• Assumes that RA enlargement is symmetrical</li><li>• View dependent</li></ul>
<b>Area.</b> Measured in the apical four-chamber view at end-systole, on the frame just prior to tricuspid valve opening, by tracing the RA blood-tissue interface, excluding the area under the tricuspid valve annulus.	2D view 	<ul style="list-style-type: none"><li>• More representative of actual RA size than linear dimensions</li><li>• Established normal values</li></ul>	<ul style="list-style-type: none"><li>• Need of a dedicated view to avoid RA foreshortening</li><li>• Assumes a symmetrical shape of the cavity</li><li>• View dependent</li></ul>
<b>Volume.</b> 2D volumetric measurements are usually based on tracings of the blood-tissue interface on the apical four-chamber view. At the tricuspid valve level, the contour is closed by connecting the two opposite sections of the tricuspid ring with a straight line. Volumes can be computed by using either the single plane area-length: $\frac{8}{3\pi} \left[ \frac{(A)^2}{L} \right]$ or the disks summation technique. 3D data sets are usually obtained from the apical approach using a full-volume acquisition	2D view   3D data sets 	<ul style="list-style-type: none"><li>• More representative of actual RA size than linear dimensions</li><li>• No geometrical assumption</li><li>• Established normal values</li></ul>	<ul style="list-style-type: none"><li>• Assumes a symmetrical shape of the cavity</li><li>• Single plane volume calculation may be inaccurate since it assumes that RA enlargement is symmetrical</li><li>• Normal values not well established</li><li>• Dependent on image quality</li><li>• Lower temporal resolution</li><li>• Patient's cooperation required</li></ul>

view in midsystole (Figure 11). It should be noted that the difference between major and minor diameters may be up to 6 mm.<sup>173,188-193</sup> For a detailed, step-by-step approach to making these measurements using 3D TEE, which is beyond the scope of this document, the reader is referred to four recent publications.<sup>184-187</sup> By using these techniques, close agreement with MDCT can be achieved.<sup>184,185</sup>

It should be noted that proponents of each of the two modalities (3D TEE and MDCT) tout advantages. In fact, each of these methods has certain strengths and limitations. Limitations of MDCT include the need for contrast media, radiation exposure, inability to obtain real-time measurements during the procedure, and the need to control the heart rate for suitable gating. Three-dimensional TEE also has limitations. First, the software required to use the methodology described by Kasel *et al.*<sup>184</sup> and Pershad *et al.*<sup>185</sup> is not currently available on all echocardiographic platforms. Second, visualization of the anterior portion of the annulus can be obscured by echo “dropout” due to annular calcification. In addition, calcification at the level of the annulus may hinder the ability to determine boundary definition and may make its shape irregular. Third, the plane formed by the nadirs of the three cusps is often not orthogonal to the LV outflow tract or aortic root; frequently the insertion of the right coronary cusp is inferior to that of the left and noncoronary cusps.<sup>183</sup> Fourth, both the spatial and temporal resolution of 3D echocardiography is currently limited. Last, this technique is operator dependent and may be difficult at times, even in experienced hands.<sup>173,174</sup> Because of these potential limitations, it is desirable to use a multimodality approach for aortic annular measurement.

12. The Aortic Root

With 2D TTE, the diameter of the aortic root (at the maximal diameter of the sinuses of Valsalva) should be obtained from the parasternal long-axis view, which depicts the aortic root and the proximal ascending aorta. This plane is slightly different from that of the long axis of the left ventricle (Figure 10A). Acquisition of this LV long-axis view may be performed from different intercostal spaces and at various distances from the left sternal border. Use of simultaneous biplane orthogonal images provided by matrix transducers may be helpful. The tubular ascending aorta is often not adequately visualized from a standard parasternal window. In these instances, moving the transducer closer to the sternum may allow visualization of a longer portion of the ascending aorta. In addition, the ascending aorta may sometimes be well visualized from right parasternal windows in the second or third intercostal space, especially when the aorta is dilated.

Measurements should be made in the view that depicts the maximum aortic diameter perpendicular to the long axis of the aorta. In patients with tricuspid aortic valves, the closure line of the leaflets (typically the right coronary cusp and the noncoronary cusp) is in the center of the aortic root lumen, and the closed leaflets are seen on the aortic side of a line connecting the hinge points of the two visualized leaflets. An asymmetric closure line, in which the tips of the closed leaflets are closer to one of the hinge points, is an indication that the cross-section is not encompassing the largest root diameter (Figure 12).

Unfortunately, there is no uniform method of measurement of the aortic root and aorta. Echocardiography uses the leading edge–to–leading edge (L-L) convention, but other techniques, such as MDCT and CMR, use the inner edge–to–inner edge (I-I) or outer edge–to–outer edge convention. In the consensus document,<sup>194</sup> the ASE and EACVI writing committee took the initiative to provide

Table 13 Normal RA size obtained from 2D echocardiographic studies

	Women	Men
RA minor axis dimension (cm/m <sup>2</sup> )	1.9 ± 0.3	1.9 ± 0.3
RA major axis dimension (cm/m <sup>2</sup> )	2.5 ± 0.3	2.4 ± 0.3
2D echocardiographic RA volume (mL/m <sup>2</sup> )	21 ± 6	25 ± 7

Data are expressed as mean ± SD.

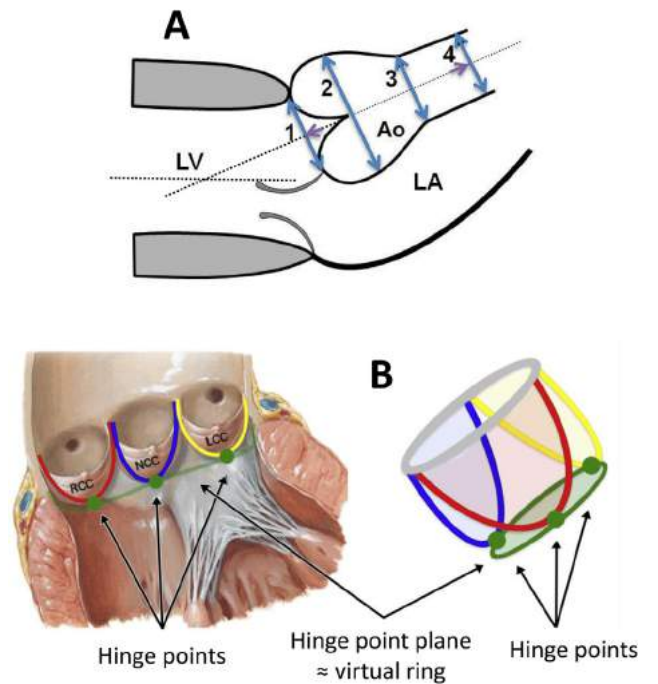
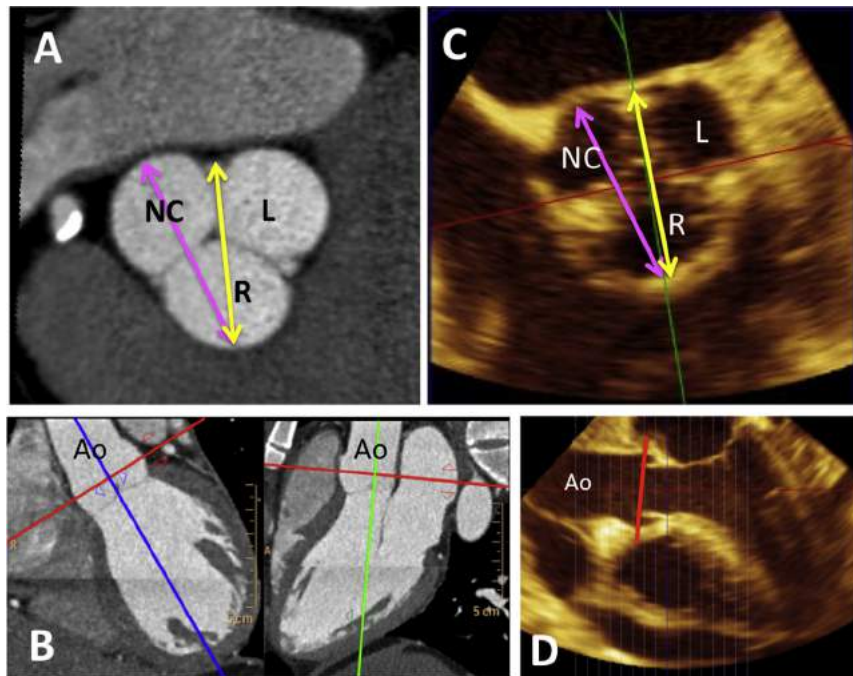
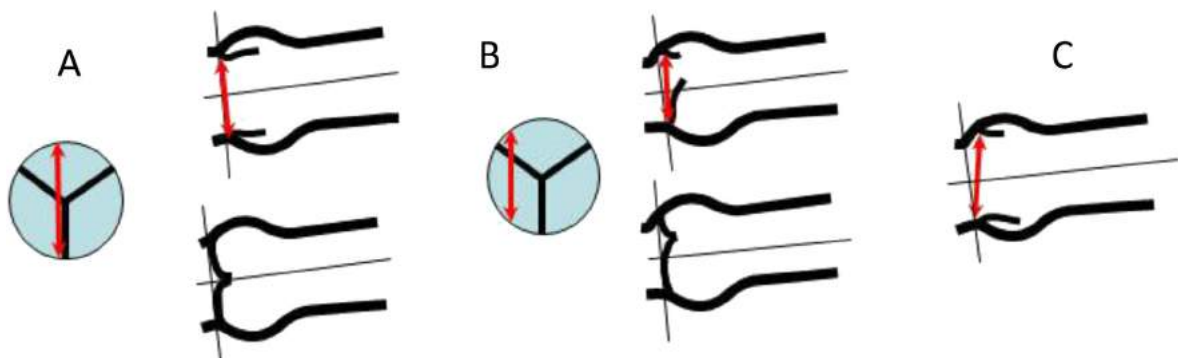


Figure 10 (A) Sites for measurements of the aortic root and ascending aorta. This diagram illustrates the four sites at which measurements are recommended (light blue arrows): (1) the aortic valve annulus (hinge point of aortic leaflets), (2) the sinuses of Valsalva (maximal diameter, usually the midpoint), (3) the sinotubular junction, and (4) the proximal ascending aorta (the distance between the measurement site and the annular plane [purple arrowheads] should always be reported). The aortic annulus should be measured at peak systole, in contrast to the other dimensions, which are measured at end-diastole. The dashed lines, depicting the longitudinal axis of the left ventricle (LV) and that of the aortic root and proximal ascending aorta, are different. Note that the angle between these two axes varies from individual to individual and with age and pathology. (B) Normal anatomy of the aortic annulus. The aortic annulus accounts for the tightest part of the aortic root and is defined as a virtual ring (shaded) with three anatomic anchor points at the nadir of each of the attachments of the three aortic leaflets. Reproduced with permission from Kasel *et al.*<sup>184</sup> Ao, Aorta; LA, left atrium.

a common standard for measurement of the aortic root and aorta by recommending a switch to the I-I convention for echocardiography. However, this goal of achieving uniformity among modalities was ultimately abandoned for several reasons. First, currently used long-standing reference values for the aorta were obtained using the L-L convention.<sup>195,196</sup> Second, the L-L convention provides statistically



**Figure 11** The smaller (antero-posterior, sagittal) aortic root diameter is measured using CT (**A**) or 3D TEE (**C**, zoomed cross sectional view) between the inner edges of the left (L) and non-coronary (NC) commissure to the opposite right (R) coronary sinus (**A** and **C**, yellow double arrows). The larger diameter (medial-lateral) is measured from the middle of the right sinus to the most distal point of the NC sinus (**A** and **C**, purple double arrows). Panel **B** shows zoomed cross-sectional CT views of aortic root at the sinus of Valsalva level using a double oblique image for orientation. Panel **D** shows a long-axis view of the aorta in obtained by multiplanar reconstruction. The red lines in (**B**) and (**D**) represent the planes from which the diameter of the aortic root should be measured at the level of the sinuses of Valsalva.

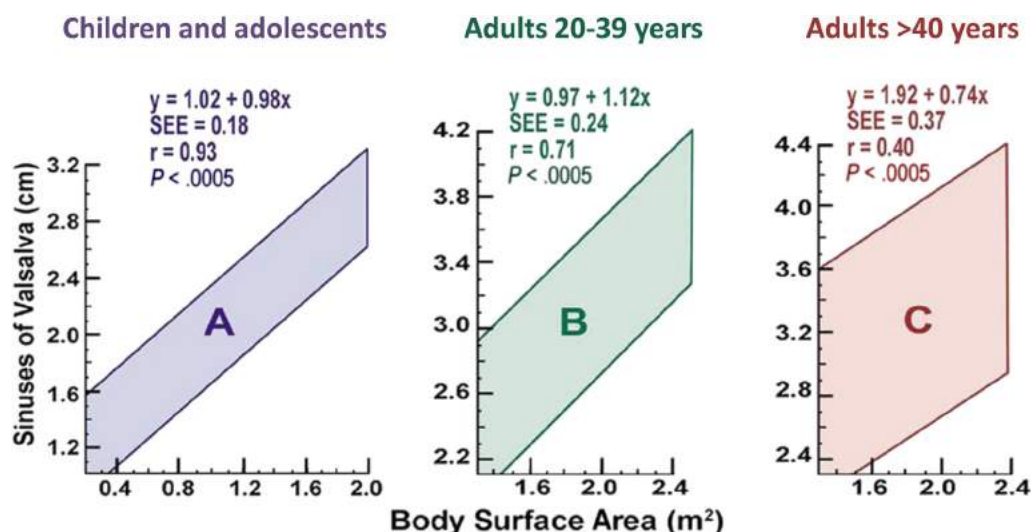


**Figure 12** Correct (**A**) and incorrect (**B**, **C**) measurements of the aortic annulus (double arrows). (**A**) Centrally positioned diameter and central closure of leaflets. Thin lines correspond to the long axis of the ascending aorta and, orthogonally, to correct orientation of the annular diameter. (**B**) Incorrect, eccentric annular measurement. The hinge points are slightly displaced upward and do not correspond to the nadir of the cusp attachments, with incomplete opening and closing of leaflets. (**C**) Incorrect, oblique annular measurement. The annulus is “virtual” and only defined by the hinge-points of the three aortic valve leaflets. As such, much of the ring is without a visible anatomic structure. However, its location on any long-axis two-dimensional view can be approximated since the plane of the virtual annulus is approximately perpendicular to the long-axis of the aorta. When bisecting the maximum dimension of the annulus in the sagittal plane, one will image the right coronary cusp anteriorly and the fibrous trigone between the left and noncoronary cusps posteriorly. Because only one anatomic marker (the RCC hinge-point) is seen, the opposing annulus must be approximated with a measurement that is perpendicular to the long axis of the aorta. Attempting to measure what you believe to be 2 hinge-points (**B** and **C**) typically will measure within the sinuses of Valsalva and overestimate the annulus.

larger diameters than the I-I convention (by 2–4 mm), and switching to the I-I convention raised a concern that patients at potential risk for developing life-threatening complications such as aortic dissection and/or rupture would fall below a threshold for intervention recommendation by current guidelines. Accordingly, the aortic annulus should be measured using the I-I convention, but we continue to

recommend the L-L convention for measurements of the aortic root and aorta.

Two-dimensional echocardiographic aortic diameter measurements are preferable to M-mode measurements, because cardiac motion may result in changes in the position of the M-mode cursor relative to the maximum diameter of the sinuses of Valsalva. This



**Figure 13** The 95% confidence intervals for aortic root diameter at sinuses of Valsalva on the basis of BSA in children and adolescents (A), adults aged 20 to 39 years (B), and adults aged  $\geq 40$  years (C). Reprinted with permission from Roman *et al.*<sup>195</sup>

**Table 14** Aortic root dimensions in normal adults

Aortic Root	Absolute values (cm)		Indexed values (cm/m <sup>2</sup> )	
	Men	Women	Men	Women
Annulus	2.6 $\pm$ 0.3	2.3 $\pm$ 0.2	1.3 $\pm$ 0.1	1.3 $\pm$ 0.1
Sinuses of Valsalva	3.4 $\pm$ 0.3	3.0 $\pm$ 0.3	1.7 $\pm$ 0.2	1.8 $\pm$ 0.2
Sinotubular junction	2.9 $\pm$ 0.3	2.6 $\pm$ 0.3	1.5 $\pm$ 0.2	1.5 $\pm$ 0.2
Proximal ascending aorta	3.0 $\pm$ 0.4	2.7 $\pm$ 0.4	1.5 $\pm$ 0.2	1.6 $\pm$ 0.3

Adapted from Roman *et al.*<sup>195</sup> and Hiratzka *et al.*<sup>204</sup>

translational motion may result in systematic underestimation (by approximately 2 mm) of the aortic diameter by M-mode imaging in comparison with 2D echocardiographic measurements.<sup>195</sup> The thoracic aorta can be better imaged using TEE compared with the TTE approach, because that aortic segment is in the near field of the transesophageal echocardiographic transducer. The aortic root and ascending aorta can be best seen in the midesophageal aortic valve long-axis view (three-chamber view at about 120°–140°).<sup>3</sup> The short-axis view of the ascending aorta is best obtained using the midesophageal views at about 45°. For measurements of the descending aorta, short-axis views at about 0° and long-axis views at about 90° should be obtained from the level of the diaphragm up to the aortic arch. The biplane imaging function on current 3D echocardiographic imaging systems allows simultaneous visualization of both short- and long-axis views.

### 13. Identification of Aortic Root Dilatation

Aortic root dilatation is associated with the presence and progression of aortic regurgitation<sup>197</sup> and with the occurrence of aortic dissection. The presence of hypertension appears to have minimal impact on aortic root diameter at the level of the sinuses of Valsalva level<sup>197</sup> but is associated with enlargement of more distal aortic segments. Aortic root diameter measurements at the level of the sinuses of Valsalva is closely related to BSA and age. Therefore, BSA may be used to predict aortic root diameter in three age strata, <20, 20 to 40, and >40 years, by using published equations.<sup>195</sup> Aortic root dilatation at the sinuses of Valsalva is defined as an aortic root diameter above the upper limit of the 95% confidence interval of the distribu-

tion in a large reference population. Aortic dilatation can be easily detected by plotting observed aortic root diameter versus BSA on previously published nomograms (Figure 13).<sup>195</sup> Equations to determine the expected aortic diameter at the sinuses of Valsalva in relation to BSA for each of the three age strata are also shown in Table 14 and Figure 13. The aortic root index or ratio of observed to expected aortic root diameters can be calculated by dividing the observed by the expected diameter.

**Recommendations.** The aortic annulus should be measured at midsystole from inner edge to inner edge. All other aortic root measurements (i.e., maximal diameter of the sinuses of Valsalva, the sinotubular junction, and the proximal ascending aorta) should be made at end-diastole, in a strictly perpendicular plane to that of the long axis of the aorta using the L-L convention. Measurements of maximal diameter of the aortic root at the sinuses of Valsalva should be compared with age- and BSA-related nomograms or to values calculated from specific allometric equations. Accurate measurement of the aortic annulus before TAVI or TAVR is crucial. To date, there is no established gold-standard technique for measuring the aortic annulus before TAVI or TAVR. Three-dimensional TEE and MDCT are emerging as reliable and possibly preferred methods for aortic annulus measurements.

### V. THE INFERIOR VENA CAVA

Examination of the IVC from the subcostal view should be included as part of the routine transthoracic echocardiographic examination. It



is generally agreed that the diameter of the IVC should be measured in the subcostal view with the patient in the supine position at 1.0 to 2.0 cm from the junction with the right atrium, using the long-axis view. For accuracy, this measurement should be made perpendicular to the IVC long axis. The diameter of the IVC decreases in response to inspiration when the negative intrathoracic pressure leads to an increase in RV filling from the systemic veins. The diameter of the IVC and the percentage decrease in the diameter during inspiration correlate with RA pressure. The relationship may be quantified as the collapsibility index.<sup>198</sup> Evaluation of the inspiratory response often requires a brief sniff, as normal inspiration may not elicit this response.

For simplicity and uniformity of reporting, specific values of RA pressure, rather than ranges, should be used in the determination of systolic pulmonary artery pressure. IVC diameter < 2.1 cm that collapses >50% with a sniff suggests normal RA pressure of 3 mm Hg (range, 0–5 mm Hg), whereas IVC diameter > 2.1 cm that collapses < 50% with a sniff suggests high RA pressure of 15 mm Hg (range, 10–20 mm Hg).<sup>199</sup> In scenarios in which IVC diameter and collapse do not fit this paradigm, an intermediate value of 8 mm Hg (range, 5–10 mm Hg) may be used, or, preferably, other indices of RA pressure should be integrated to downgrade or upgrade to the normal or high values of RA pressure. It should be noted that in normal young athletes, the IVC may be dilated in the presence of normal pressure.<sup>200,201</sup> In addition, the IVC is commonly dilated and may not collapse in patients on ventilators, so it should not be routinely used in such cases to estimate RA pressure.<sup>202</sup> However, IVC diameter measured on TEE at the cavoatrial junction has been successfully used to derive central venous pressure in anesthetized mechanically ventilated patients.<sup>203</sup> The use of the IVC size and dynamics is encouraged for estimation of RA pressure. This estimate should be used in estimation of the pulmonary artery pressure on the basis of the tricuspid regurgitant jet velocity, rather than assuming a constant RA pressure for all patients.

## NOTICE AND DISCLAIMER

This report is made available by the ASE and EACVI as a courtesy reference source for members. This report contains recommendations only and should not be used as the sole basis to make medical practice decisions or for disciplinary action against any employee. The statements and recommendations contained in this report are based primarily on the opinions of experts, rather than on scientifically verified data. The ASE and EACVI make no express or implied warranties regarding the completeness or accuracy of the information in this report, including the warranty of merchantability or fitness for a particular purpose. In no event shall the ASE and EACVI be liable to you, your patients, or any other third parties for any decision made or action taken by you or such other parties in reliance on this information. Nor does your use of this information constitute the offering of medical advice by the ASE and EACVI or create any physician-patient relationship between the ASE and EACVI and your patients or anyone else.

## REFERENCES

1. Lang RM, Bierig M, Devereux RB, Flachskampf FA, Foster E, Pellikka PA, et al. Recommendations for chamber quantification: a report from the American Society of Echocardiography's Guidelines and Standards Committee and the Chamber Quantification Writing Group, developed in conjunction with the European Association of Echocardiography, a branch of the European Society of Cardiology. *J Am Soc Echocardiogr* 2005;18:1440-63.
2. Lang RM, Bierig M, Devereux RB, Flachskampf FA, Foster E, Pellikka PA, et al. Recommendations for chamber quantification. *Eur J Echocardiogr* 2006;7:79-108.
3. Hahn RT, Abraham T, Adams MS, Bruce CJ, Glas KE, Lang RM, et al. Guidelines for performing a comprehensive transesophageal echocardiographic examination: recommendations from the American Society of Echocardiography and the Society of Cardiovascular Anesthesiologists. *J Am Soc Echocardiogr* 2013;26:921-64.
4. Mulvagh SL, Rakowski H, Vannan MA, Abdelmoneim SS, Becher H, Bierig SM, et al. American Society of Echocardiography Consensus Statement on the Clinical Applications of Ultrasonic Contrast Agents in Echocardiography. *J Am Soc Echocardiogr* 2008;21:1179-201. quiz 281.
5. Hoffmann R, von Bardeleben S, Kasprzak JD, Borges AC, ten Cate F, Firschke C, et al. Analysis of regional left ventricular function by cineventriculography, cardiac magnetic resonance imaging, and unenhanced and contrast-enhanced echocardiography: a multicenter comparison of methods. *J Am Coll Cardiol* 2006;47:121-8.
6. Dorosz JL, Lezotte DC, Weizenkamp DA, Allen LA, Salcedo EE. Performance of 3-dimensional echocardiography in measuring left ventricular volumes and ejection fraction: a systematic review and meta-analysis. *J Am Coll Cardiol* 2012;59:1799-808.
7. Rietzschel ER, De Buyzere ML, Bekaert S, Segers P, De Bacquer D, Cooman L, et al. Rationale, design, methods and baseline characteristics of the Asklepios Study. *Eur J Cardiovasc Prev Rehabil* 2007;14:179-91.
8. Kuznetsova T, Herbots L, Lopez B, Jin Y, Richart T, Thijs L, et al. Prevalence of left ventricular diastolic dysfunction in a general population. *Circ Heart Fail* 2009;2:105-12.
9. Friedman GD, Cutter GR, Donahue RP, Hughes GH, Hulley SB, Jacobs DR Jr, et al. CARDIA: study design, recruitment, and some characteristics of the examined subjects. *J Clin Epidemiol* 1988;41:1105-16.
10. Muraru D, Badano LP, Peluso D, Dal Bianco L, Casablanca S, Kocabay G, et al. Comprehensive analysis of left ventricular geometry and function by three-dimensional echocardiography in healthy adults. *J Am Soc Echocardiogr* 2013;26:618-28.
11. Lancellotti P, Badano LP, Lang RM, Akhaladze N, Athanassopoulos GD, Barone D, et al. Normal Reference Ranges for Echocardiography: rationale, study design, and methodology (NORRE Study). *Eur Heart J Cardiovasc Imaging* 2013;14:303-8.
12. Kou S, Caballero L, Dulgheru R, Voilliot D, De Sousa C, Kacharava G, et al. Echocardiographic reference ranges for normal cardiac chamber size: results from the NORRE study. *Eur Heart J Cardiovasc Imaging* 2014;15:680-90.
13. Bhawe NM, Lang RM. Evaluation of left ventricular structure and function by three-dimensional echocardiography. *Curr Opin Crit Care* 2013;19:387-96.
14. Chahal NS, Lim TK, Jain P, Chambers JC, Kooner JS, Senior R. Population-based reference values for 3D echocardiographic LV volumes and ejection fraction. *JACC Cardiovasc Imaging* 2012;5:1191-7.
15. Kaku K, Takeuchi M, Otani K, Sugeng L, Nakai H, Haruki N, et al. Age- and gender-dependency of left ventricular geometry assessed with real-time three-dimensional transthoracic echocardiography. *J Am Soc Echocardiogr* 2011;24:541-7.
16. Fukuda S, Watanabe H, Daimon M, Abe Y, Hirashiki A, Hirata K, et al. Normal values of real-time 3-dimensional echocardiographic parameters in a healthy Japanese population: the JAMP-3D Study. *Circ J* 2012;76:1177-81.
17. Germans T, Gotte MJ, Nijveldt R, Spreeuwenberg MD, Beek AM, Bronzwaer JG, et al. Effects of aging on left atrioventricular coupling and left ventricular filling assessed using cardiac magnetic resonance imaging in healthy subjects. *Am J Cardiol* 2007;100:122-7.
18. Sandstede J, Lipke C, Beer M, Hofmann S, Pabst T, Kenn W, et al. Age- and gender-specific differences in left and right ventricular cardiac

- function and mass determined by cine magnetic resonance imaging. *Eur Radiol* 2000;10:438-42.
19. Muraru D, Badano LP, Piccoli G, Gianfagna P, Del Mestre L, Ermacora D, et al. Validation of a novel automated border-detection algorithm for rapid and accurate quantitation of left ventricular volumes based on three-dimensional echocardiography. *Eur J Echocardiogr* 2010;11:359-68.
  20. Aune E, Baekkevar M, Rodevand O, Otterstad JE. Reference values for left ventricular volumes with real-time 3-dimensional echocardiography. *Scand Cardiovasc J* 2010;44:24-30.
  21. Lang RM, Borow KM, Neumann A, Janzen D. Systemic vascular resistance: an unreliable index of left ventricular afterload. *Circulation* 1986;74:1114-23.
  22. Reisner SA, Lysyansky P, Agmon Y, Mutlak D, Lessick J, Friedman Z. Global longitudinal strain: a novel index of left ventricular systolic function. *J Am Soc Echocardiogr* 2004;17:630-3.
  23. Dalen H, Thorstensen A, Aase SA, Ingul CB, Torp H, Vatten LJ, et al. Segmental and global longitudinal strain and strain rate based on echocardiography of 1266 healthy individuals: the HUNT study in Norway. *Eur J Echocardiogr* 2010;11:176-83.
  24. Voigt JU, Pedrizzetti G, Lysyansky P, Marwick TH, Houle HC, Baumann R, et al. Definitions for a Common Standard for 2D Speckle Tracking Echocardiography. Consensus document of the EACVI/ASE/Industry Task Force to Standardize Deformation Imaging. *Eur Heart J Cardiovasc Imaging* 2014 (in press).
  25. Mor-Avi V, Lang RM, Badano LP, Belohlavek M, Cardim NM, Derumeaux G, et al. Current and evolving echocardiographic techniques for the quantitative evaluation of cardiac mechanics: ASE/EAE consensus statement on methodology and indications endorsed by the Japanese Society of Echocardiography. *J Am Soc Echocardiogr* 2011;24:277-313.
  26. Thomas JD, Badano LP. EACVI-ASE-industry initiative to standardize deformation imaging: a brief update from the co-chairs. *Eur Heart J Cardiovasc Imaging* 2013;14:1039-40.
  27. Yingchoncharoen T, Agarwal S, Popovic ZB, Marwick TH. Normal ranges of left ventricular strain: a meta-analysis. *J Am Soc Echocardiogr* 2013;26:185-91.
  28. Mignot A, Donal E, Zaroui A, Reant P, Salem A, Hamon C, et al. Global longitudinal strain as a major predictor of cardiac events in patients with depressed left ventricular function: a multicenter study. *J Am Soc Echocardiogr* 2010;23:1019-24.
  29. Stanton T, Leano R, Marwick TH. Prediction of all-cause mortality from global longitudinal speckle strain: comparison with ejection fraction and wall motion scoring. *Circ Cardiovasc Imaging* 2009;2:356-64.
  30. Di Salvo G, Rea A, Mormile A, Limongelli G, D'Andrea A, Pergola V, et al. Usefulness of bidimensional strain imaging for predicting outcome in asymptomatic patients aged  $\leq 16$  years with isolated moderate to severe aortic regurgitation. *Am J Cardiol* 2012;110:1051-5.
  31. Witkowski TG, Thomas JD, Debonnaire PJ, Delgado V, Hoke U, Ewe SH, et al. Global longitudinal strain predicts left ventricular dysfunction after mitral valve repair. *Eur Heart J Cardiovasc Imaging* 2013;14:69-76.
  32. Kocabay G, Muraru D, Peluso D, Cucchini U, Mihaila S, Padayattil-Jose S, et al. Normal left ventricular mechanics by two-dimensional speckle tracking echocardiography. *Rev Esp Cardiol* 2014;67:651-8.
  33. Takigiku K, Takeuchi M, Izumi C, Yuda S, Sakata K, Ohte N, et al. Normal range of left ventricular 2-dimensional strain: Japanese Ultrasound Speckle Tracking of the Left Ventricle (JUSTICE) study. *Circ J* 2012;76:2623-32.
  34. Kuznetsova T, Herbots L, Richart T, D'Hooge J, Thijs L, Fagard RH, et al. Left ventricular strain and strain rate in a general population. *Eur Heart J* 2008;29:2014-23.
  35. Cerqueira MD, Weissman NJ, Dilsizian V, Jacobs AK, Kaul S, Laskey WK, et al. Standardized myocardial segmentation and nomenclature for tomographic imaging of the heart. A statement for healthcare professionals from the Cardiac Imaging Committee of the Council on Clinical Cardiology of the American Heart Association. *Circulation* 2002;105:539-42.
  36. Schiller NB, Shah PM, Crawford M, DeMaria A, Devereux R, Feigenbaum H, et al. Recommendations for quantitation of the left ventricle by two-dimensional echocardiography. American Society of Echocardiography Committee on Standards, Subcommittee on Quantitation of Two-Dimensional Echocardiograms. *J Am Soc Echocardiogr* 1989;2:358-67.
  37. Amzulescu MS, Slavich M, Florian A, Goetschalckx K, Voigt JU. Does two-dimensional image reconstruction from three-dimensional full volume echocardiography improve the assessment of left ventricular morphology and function? *Echocardiography* 2013;30:55-63.
  38. Voigt JU, Lindenmeier G, Exner B, Regenfus M, Werner D, Reulbach U, et al. Incidence and characteristics of segmental postsystolic longitudinal shortening in normal, acutely ischemic, and scarred myocardium. *J Am Soc Echocardiogr* 2003;16:415-23.
  39. Lieberman AN, Weiss JL, Jugdutt BI, Becker LC, Bulkley BH, Garrison JC, et al. Two-dimensional echocardiography and infarct size: relationship of regional wall motion and thickening to the extent of myocardial infarction in the dog. *Circulation* 1981;63:739-46.
  40. Takeuchi M, Sonoda S, Miura Y, Kuroiwa A. Reproducibility of dobutamine digital stress echocardiography. *J Am Soc Echocardiogr* 1997;10:344-51.
  41. Lumens J, Leenders GE, Cramer MJ, De Boeck BW, Doevendans PA, Prinzen FW, et al. Mechanistic evaluation of echocardiographic dyssynchrony indices: patient data combined with multiscale computer simulations. *Circ Cardiovasc Imaging* 2012;5:491-9.
  42. Little WC, Reeves RC, Arciniegas J, Katholi RE, Rogers EW. Mechanism of abnormal interventricular septal motion during delayed left ventricular activation. *Circulation* 1982;65:1486-91.
  43. Parsai C, Bijnens B, Sutherland GR, Baltabaeva A, Claus P, Marciniak M, et al. Toward understanding response to cardiac resynchronization therapy: left ventricular dyssynchrony is only one of multiple mechanisms. *Eur Heart J* 2009;30:940-9.
  44. Voigt JU, Schneider TM, Korder S, Szulik M, Gurel E, Daniel WG, et al. Apical transverse motion as surrogate parameter to determine regional left ventricular function inhomogeneities: a new, integrative approach to left ventricular asynchrony assessment. *Eur Heart J* 2009;30:959-68.
  45. Stankovic I, Aaronson M, Smith HJ, Voros G, Kongsgaard E, Neskovic AN, et al. Dynamic relationship of left-ventricular dyssynchrony and contractile reserve in patients undergoing cardiac resynchronization therapy. *Eur Heart J* 2014;35:48-55.
  46. Heimdal A, Stoylen A, Torp H, Skjaerpe T. Real-time strain rate imaging of the left ventricle by ultrasound. *J Am Soc Echocardiogr* 1998;11:1013-9.
  47. Leitman M, Lysyansky P, Sidenko S, Shir V, Peleg E, Binenbaum M, et al. Two-dimensional strain—a novel software for real-time quantitative echocardiographic assessment of myocardial function. *J Am Soc Echocardiogr* 2004;17:1021-9.
  48. Stefani L, Toncelli L, Gianassi M, Manetti P, Di Tante V, Vono MR, et al. Two-dimensional tracking and TDI are consistent methods for evaluating myocardial longitudinal peak strain in left and right ventricle basal segments in athletes. *Cardiovasc Ultrasound* 2007;5:7.
  49. Voigt JU, Exner B, Schmiedehausen K, Huchzermeyer C, Reulbach U, Nixdorff U, et al. Strain-rate imaging during dobutamine stress echocardiography provides objective evidence of inducible ischemia. *Circulation* 2003;107:2120-6.
  50. Maffessanti F, Nesser HJ, Weinert L, Steringer-Mascherbauer R, Niel J, Gorissen W, et al. Quantitative evaluation of regional left ventricular function using three-dimensional speckle tracking echocardiography in patients with and without heart disease. *Am J Cardiol* 2009;104:1755-62.
  51. Badano LP, Cucchini U, Muraru D, Ai Nono O, Sarais C, Iliceto S. Use of three-dimensional speckle tracking to assess left ventricular myocardial mechanics: inter-vendor consistency and reproducibility of strain measurements. *Eur Heart J Cardiovasc Imaging* 2013;14:285-93.

52. Verdecchia P, Carini G, Circo A, Dovellini E, Giovannini E, Lombardo M, et al. Left ventricular mass and cardiovascular morbidity in essential hypertension: the MAVI study. *J Am Coll Cardiol* 2001;38:1829-35.
53. Schillaci G, Verdecchia P, Porcellati C, Cuccurullo O, Cosco C, Perticone F. Continuous relation between left ventricular mass and cardiovascular risk in essential hypertension. *Hypertension* 2000;35:580-6.
54. Ghali JK, Liao Y, Simmons B, Castaner A, Cao G, Cooper RS. The prognostic role of left ventricular hypertrophy in patients with or without coronary artery disease. *Ann Intern Med* 1992;117:831-6.
55. Verma A, Meris A, Skali H, Ghali JK, Arnold JM, Bourgoun M, et al. Prognostic implications of left ventricular mass and geometry following myocardial infarction: the VALIANT (VALsartan In Acute myocardial iNfarcTion) Echocardiographic Study. *JACC Cardiovasc Imaging* 2008;1:582-91.
56. Armstrong AC, Gidding S, Gjesdal O, Wu C, Bluemke DA, Lima JA. LV mass assessed by echocardiography and CMR, cardiovascular outcomes, and medical practice. *JACC Cardiovasc Imaging* 2012;5:837-48.
57. Park SH, Shub C, Nobrega TP, Bailey KR, Seward JB. Two-dimensional echocardiographic calculation of left ventricular mass as recommended by the American Society of Echocardiography: correlation with autopsy and M-mode echocardiography. *J Am Soc Echocardiogr* 1996;9:119-28.
58. McGavigan AD, Dunn FG, Goodfield NE. Secondary harmonic imaging overestimates left ventricular mass compared to fundamental echocardiography. *Eur J Echocardiogr* 2003;4:178-81.
59. de Las Fuentes L, Spence KE, Davila-Roman VG, Waggoner AD. Are normative values for LV geometry and mass based on fundamental imaging valid with use of harmonic imaging? *J Am Soc Echocardiogr* 2010;23:1317-22.
60. Mor-Avi V, Sugeng L, Weinert L, MacEneaney P, Caiani EG, Koch R, et al. Fast measurement of left ventricular mass with real-time three-dimensional echocardiography: comparison with magnetic resonance imaging. *Circulation* 2004;110:1814-8.
61. Lang RM, Badano LP, Tsang W, Adams DH, Agricola E, Buck T, et al. EAE/ASE recommendations for image acquisition and display using three-dimensional echocardiography. *J Am Soc Echocardiogr* 2012;25:3-46.
62. Lam CS, Roger VL, Rodeheffer RJ, Bursi F, Borlaug BA, Ommen SR, et al. Cardiac structure and ventricular-vascular function in persons with heart failure and preserved ejection fraction from Olmsted County, Minnesota. *Circulation* 2007;115:1982-90.
63. Ng AC, Tran da T, Newman M, Allman C, Vidaic J, Lo ST, et al. Left ventricular longitudinal and radial synchrony and their determinants in healthy subjects. *J Am Soc Echocardiogr* 2008;21:1042-8.
64. Chahal NS, Lim TK, Jain P, Chambers JC, Kooner JS, Senior R. Ethnicity-related differences in left ventricular function, structure and geometry: a population study of UK Indian Asian and European white subjects. *Heart* 2010;96:466-71.
65. Chirinos JA, Segers P, De Buyzere ML, Kronmal RA, Raja MW, De Bacquer D, et al. Left ventricular mass: allometric scaling, normative values, effect of obesity, and prognostic performance. *Hypertension* 2010;56:91-8.
66. Cuspidi C, Facchetti R, Sala C, Bombelli M, Negri F, Carugo S, et al. Normal values of left-ventricular mass: echocardiographic findings from the PAMELA study. *J Hypertens* 2012;30:997-1003.
67. Kizer JR, Arnett DK, Bella JN, Parancas M, Rao DC, Province MA, et al. Differences in left ventricular structure between black and white hypertensive adults: the Hypertension Genetic Epidemiology Network study. *Hypertension* 2004;43:1182-8.
68. Rodriguez CJ, Diez-Roux AV, Moran A, Jin Z, Kronmal RA, Lima J, et al. Left ventricular mass and ventricular remodeling among Hispanic subgroups compared with non-Hispanic blacks and whites: MESA (Multi-ethnic Study of Atherosclerosis). *J Am Coll Cardiol* 2010;55:234-42.
69. Park CM, March K, Ghosh AK, Jones S, Coady E, Tison C, et al. Left-ventricular structure in the Southall And Brent REvisited (SABRE) study: explaining ethnic differences. *Hypertension* 2013;61:1014-20.
70. de Simone G, Kizer JR, Chinali M, Roman MJ, Bella JN, Best LG, et al. Normalization for body size and population-attributable risk of left ventricular hypertrophy: the Strong Heart Study. *Am J Hypertens* 2005;18:191-6.
71. Rudski LG, Lai WW, Afilalo J, Hua L, Handschumacher MD, Chandrasekaran K, et al. Guidelines for the echocardiographic assessment of the right heart in adults: a report from the American Society of Echocardiography endorsed by the European Association of Echocardiography, a registered branch of the European Society of Cardiology, and the Canadian Society of Echocardiography. *J Am Soc Echocardiogr* 2010;23:685-713. quiz 86-8.
72. Kawut SM, Lima JA, Barr RG, Chahal H, Jain A, Tandri H, et al. Sex and race differences in right ventricular structure and function: the multi-ethnic study of atherosclerosis-right ventricle study. *Circulation* 2011;123:2542-51.
73. D'Oronzio U, Senn O, Biaggi P, Gruner C, Jenni R, Tanner FC, et al. Right heart assessment by echocardiography: gender and body size matters. *J Am Soc Echocardiogr* 2012;25:1251-8.
74. Willis J, Augustine D, Shah R, Stevens C, Easaw J. Right ventricular normal measurements: time to index? *J Am Soc Echocardiogr* 2012;25:1259-67.
75. Maffessanti F, Muraru D, Esposito R, Gripari P, Ermacora D, Santoro C, et al. Age-, body size-, and sex-specific reference values for right ventricular volumes and ejection fraction by three-dimensional echocardiography: a multicenter echocardiographic study in 507 healthy volunteers. *Circ Cardiovasc Imaging* 2013;6:700-10.
76. D'Andrea A, Cocchia R, Caso P, Riegler L, Scarafie R, Salerno G, et al. Global longitudinal speckle-tracking strain is predictive of left ventricular remodeling after coronary angioplasty in patients with recent non-ST elevation myocardial infarction. *Int J Cardiol* 2011;153:185-91.
77. Ling LF, Obuchowski NA, Rodriguez L, Popovic Z, Kwon D, Marwick TH. Accuracy and interobserver concordance of echocardiographic assessment of right ventricular size and systolic function: a quality control exercise. *J Am Soc Echocardiogr* 2012;25:709-13.
78. Shimada YJ, Shiota M, Siegel RJ, Shiota T. Accuracy of right ventricular volumes and function determined by three-dimensional echocardiography in comparison with magnetic resonance imaging: a meta-analysis study. *J Am Soc Echocardiogr* 2010;23:943-53.
79. Giusca S, Dambrauskaite V, Scheurwegs C, D'Hooge J, Claus P, Herbots L, et al. Deformation imaging describes right ventricular function better than longitudinal displacement of the tricuspid ring. *Heart* 2010;96:281-8.
80. Innelli P, Esposito R, Olibet M, Nistri S, Galderisi M. The impact of ageing on right ventricular longitudinal function in healthy subjects: a pulsed tissue Doppler study. *Eur J Echocardiogr* 2009;10:491-8.
81. Maffessanti F, Gripari P, Tamborini G, Muratori M, Fusini L, Alamanni F, et al. Evaluation of right ventricular systolic function after mitral valve repair: a two-dimensional Doppler, speckle-tracking, and three-dimensional echocardiographic study. *J Am Soc Echocardiogr* 2012;25:701-8.
82. Verhaert D, Mullens W, Borowski A, Popovic ZB, Curtin RJ, Thomas JD, et al. Right ventricular response to intensive medical therapy in advanced decompensated heart failure. *Circ Heart Fail* 2010;3:340-6.
83. Guendouz S, Rappeneau S, Nahum J, Dubois-Rande JL, Gueret P, Monin JL, et al. Prognostic significance and normal values of 2D strain to assess right ventricular systolic function in chronic heart failure. *Circ J* 2012;76:127-36.
84. Antoni ML, Scherptong RW, Atary JZ, Boersma E, Holman ER, van der Wall EE, et al. Prognostic value of right ventricular function in patients after acute myocardial infarction treated with primary percutaneous coronary intervention. *Circ Cardiovasc Imaging* 2010;3:264-71.
85. Hardegree EL, Sachdev A, Villarraga HR, Frantz RP, McGoon MD, Kushwaha SS, et al. Role of serial quantitative assessment of right ventricular function by strain in pulmonary arterial hypertension. *Am J Cardiol* 2013;111:143-8.
86. Haecck ML, Scherptong RW, Marsan NA, Holman ER, Schalij MJ, Bax JJ, et al. Prognostic value of right ventricular longitudinal peak systolic strain



- in patients with pulmonary hypertension. *Circ Cardiovasc Imaging* 2012; 5:628-36.
87. Cappelli F, Porciani MC, Bergesio F, Perlini S, Attana P, Moggi Pignone A, et al. Right ventricular function in AL amyloidosis: characteristics and prognostic implication. *Eur Heart J Cardiovasc Imaging* 2012;13:416-22.
  88. Grant AD, Smedira NG, Starling RC, Marwick TH. Independent and incremental role of quantitative right ventricular evaluation for the prediction of right ventricular failure after left ventricular assist device implantation. *J Am Coll Cardiol* 2012;60:521-8.
  89. Unsworth B, Casula RP, Kyriacou AA, Yadav H, Chukwuemeka A, Cherian A, et al. The right ventricular annular velocity reduction caused by coronary artery bypass graft surgery occurs at the moment of pericardial incision. *Am Heart J* 2010;159:314-22.
  90. Lindqvist P, Holmgren A, Zhao Y, Henein MY. Effect of pericardial repair after aortic valve replacement on septal and right ventricular function. *Int J Cardiol* 2012;155:388-93.
  91. Sugeng L, Mor-Avi V, Weinert L, Niel J, Ebner C, Steringer-Mascherbauer R, et al. Multimodality comparison of quantitative volumetric analysis of the right ventricle. *JACC Cardiovasc Imaging* 2010;3:10-8.
  92. Rosca M, Lancellotti P, Popescu BA, Pierard LA. Left atrial function: pathophysiology, echocardiographic assessment, and clinical applications. *Heart* 2011;97:1982-9.
  93. Spencer KT, Mor-Avi V, Gorcsan J, DeMaria AN, Kimball TR, Monaghan MJ, et al. Effects of aging on left atrial reservoir, conduit, and booster pump function: a multi-institution acoustic quantification study. *Heart* 2001;85:272-7.
  94. Bouzas-Mosquera A, Brouillon FJ, Alvarez-Garcia N, Mendez E, Peteiro J, Gandara-Sambade T, et al. Left atrial size and risk for all-cause mortality and ischemic stroke. *Can Med Assoc J* 2011;183:E657-64.
  95. Kizer JR, Bella JN, Palmieri V, Liu JE, Best LG, Lee ET, et al. Left atrial diameter as an independent predictor of first clinical cardiovascular events in middle-aged and elderly adults: The Strong Heart Study (SHS). *Am Heart J* 2006;151:412-8.
  96. Lancellotti P, Donal E, Magne J, Moonen M, O'Connor K, Daubert JC, et al. Risk stratification in asymptomatic moderate to severe aortic stenosis: the importance of the valvular, arterial and ventricular interplay. *Heart* 2010;96:1364-71.
  97. Le Tourneau T, Messika-Zeitoun D, Russo A, Detaint D, Topilsky Y, Mahoney DW, et al. Impact of Left Atrial Volume on Clinical Outcome in Organic Mitral Regurgitation. *J Am Coll Cardiol* 2010;56:570-8.
  98. Tsang TSM, Barnes ME, Gersh BJ, Bailey KR, Seward JB. Left atrial volume as a morphophysiologic expression of left ventricular diastolic dysfunction and relation to cardiovascular risk burden. *Am J Cardiol* 2002;90:1284-9.
  99. Tsang TSM, Barnes ME, Gersh BJ, Takemoto Y, Rosales AG, Bailey KR, et al. Prediction of risk for first age-related cardiovascular events in an elderly population: The incremental value of echocardiography. *J Am Coll Cardiol* 2003;42:1199-205.
  100. Appleton CP, Galloway JM, Gonzalez MS, Gaballa M, Basnight MA. Estimation of left ventricular filling pressures using two-dimensional and Doppler echocardiography in adult patients with cardiac disease. Additional value of analyzing left atrial size, left atrial ejection fraction and the difference in duration of pulmonary venous and mitral flow velocity at atrial contraction. *J Am Coll Cardiol* 1993;22:1972-82.
  101. Geske JB, Sorajja P, Nishimura RA, Ommen SR. The Relationship of Left Atrial Volume and Left Atrial Pressure in Patients With Hypertrophic Cardiomyopathy: An Echocardiographic and Cardiac Catheterization Study. *J Am Soc Echocardiogr* 2009;22:961-6.
  102. Guron CW, Hartford M, Rosengren A, Thelle D, Wallentin I, Caidahl K. Usefulness of atrial size inequality as an indicator of abnormal left ventricular filling. *Am J Cardiol* 2005;95:1448-52.
  103. Simek CL, Feldman MD, Haber HL, Wu CC, Jayaweera AR, Kaul S. Relationship between left ventricular wall thickness and left atrial size: comparison with other measures of diastolic function. *J Am Soc Echocardiogr* 1995;8:37-47.
  104. Ersboll M, Anderson MJ, Valeur N, Mogensen UM, Waziri H, Moller JE, et al. The prognostic value of left atrial peak reservoir strain in acute myocardial infarction is dependent on left ventricular longitudinal function and left atrial size. *Circ Cardiovasc Imaging* 2013;6:26-33.
  105. Lonborg JT, Engstrom T, Moller JE, Ahtarovski KA, Kelbaek H, Holmvang L, et al. Left atrial volume and function in patients following ST elevation myocardial infarction and the association with clinical outcome: a cardiovascular magnetic resonance study. *Eur Heart J Cardiovasc Imaging* 2013;14:118-26.
  106. Barnes ME, Miyasaka Y, Seward JB, Gersh BJ, Rosales AG, Bailey KR, et al. Left atrial volume in the prediction of first ischemic stroke in an elderly cohort without atrial fibrillation. *Mayo Clin Proc* 2004;79:1008-14.
  107. Benjamin EJ, D'Agostino RB, Belanger AJ, Wolf PA, Levy D. Left Atrial Size and the Risk of Stroke and Death - the Framingham Heart Study. *Circulation* 1995;92:835-41.
  108. Bolca O, Akdemir O, Eren M, Dagdeviren B, Yildirim A, Tezel T. Left atrial maximum volume is a recurrence predictor in lone-atrial fibrillation - An acoustic quantification study. *Jpn Heart J* 2002;43:241-8.
  109. Di Tullio MR, Sacco RL, Sciacca RR, Homma S. Left atrial size and the risk of ischemic stroke in an ethnically mixed population. *Stroke* 1999; 30:2019-24.
  110. Flaker GC, Fletcher KA, Rothbart RM, Halperin JL, Hart RG. Clinical and Echocardiographic Features of Intermittent Atrial-Fibrillation That Predict Recurrent Atrial-Fibrillation. *Am J Cardiol* 1995;76:355-8.
  111. Kottkamp H. Fibrotic Atrial Cardiomyopathy: A Specific Disease/Syndrome Supplying Substrates for Atrial Fibrillation, Atrial Tachycardia, Sinus Node Disease, AV Node Disease, and Thromboembolic Complications. *J Cardiovasc Electrophysiol* 2012;23:797-9.
  112. Tsang TS, Gersh BJ, Appleton CP, Tajik AJ, Barnes ME, Bailey KR, et al. Left ventricular diastolic dysfunction as a predictor of the first diagnosed nonvalvular atrial fibrillation in 840 elderly men and women. *J Am Coll Cardiol* 2002;40:1636-44.
  113. Tsang TS, Barnes ME, Bailey KR, Leibson CL, Montgomery SC, Takemoto Y, et al. Left atrial volume: Important risk marker of incident atrial fibrillation in 1655 older men and women. *Mayo Clin Proc* 2001; 76:467-75.
  114. Vaziri SM, Larson MG, Benjamin EJ, Levy D. Echocardiographic predictors of nonrheumatic atrial fibrillation. The Framingham Heart Study. *Circulation* 1994;89:724-30.
  115. Tsang TS, Barnes ME, Gersh BJ, Bailey KR, Seward JB. Risks for atrial fibrillation and congestive heart failure in patients  $\geq 65$  years of age with abnormal left ventricular diastolic relaxation. *Am J Cardiol* 2004;93: 54-8.
  116. Beinart R, Boyko V, Schwammenthal E, Kuperstein R, Sagie A, Hod H, et al. Long-term prognostic significance of left atrial volume in acute myocardial infarction. *J Am Coll Cardiol* 2004;44:327-34.
  117. Moller JE, Hillis GS, Oh JK, Seward JB, Reeder GS, Wright RS, et al. Left atrial volume - A powerful predictor of survival after acute myocardial infarction. *Circulation* 2003;107:2207-12.
  118. Dini FL, Cortigiani L, Baldini U, Boni A, Nuti R, Barsotti L, et al. Prognostic value of left atrial enlargement in patients with idiopathic dilated cardiomyopathy and ischemic cardiomyopathy. *Am J Cardiol* 2002;89:518-23.
  119. Kim H, Cho YK, Jun DH, Nam CW, Han SW, Hur SH, et al. Prognostic implications of the NT-ProBNP level and left atrial size in non-ischemic dilated cardiomyopathy. *Circ J* 2008;72:1658-65.
  120. Modena MG, Muia N, Sgura FA, Molinari R, Castelli A, Rossi R. Left atrial size is the major predictor of cardiac death and overall clinical outcome in patients with dilated cardiomyopathy: A long-term follow-up study. *Clin Cardiol* 1997;20:553-60.
  121. Quinones MA, Greenberg BH, Kopelen HA, Koipillai C, Limacher MC, Shindler DM, et al. Echocardiographic predictors of clinical outcome in patients with Left Ventricular Dysfunction enrolled in the SOLVD Registry and Trials: Significance of left ventricular hypertrophy. *J Am Coll Cardiol* 2000;35:1237-44.



122. Sabharwal N, Cemin R, Rajan K, Hickman M, Lahiri A, Senior R. Usefulness of left atrial volume as a predictor of mortality in patients with ischemic cardiomyopathy. *Am J Cardiol* 2004;94:760-3.
123. Poulsen MK, Dahl JS, Henriksen JE, Hey TM, Hoiland-Carsen PF, Beck-Nielsen H, et al. Left atrial volume index: relation to long-term clinical outcome in type 2 diabetes. *J Am Coll Cardiol* 2013;62:2416-21.
124. Olshansky B, Heller EN, Mitchell LB, Chandler M, Slater W, Green M, et al. Are transthoracic echocardiographic parameters associated with atrial fibrillation recurrence or stroke? - Results from the atrial fibrillation follow-up investigation of rhythm management (AFFIRM) study. *J Am Coll Cardiol* 2005;45:2026-33.
125. Rusinaru D, Tribouilloy C, Grigioni F, Avierinos JF, Suri RM, Barbieri A, et al. Left Atrial Size Is a Potent Predictor of Mortality in Mitral Regurgitation Due to Flail Leaflets Results From a Large International Multi-center Study. *Circ Cardiovasc Imaging* 2011;4:473-81.
126. Schabelman S, Schiller NB, Silverman NH, Ports TA. Left Atrial Volume Estimation by Two-Dimensional Echocardiography. *Cathet Cardiovasc Diagn* 1981;7:165-78.
127. Wade MR, Chandraratna PAN, Reid CL, Lin SL, Rahimtoola SH. Accuracy of Nondirected and Directed M-Mode Echocardiography as an Estimate of Left Atrial Size. *Am J Cardiol* 1987;60:1208-11.
128. Lester SJ, Ryan EW, Schiller NB, Foster E. Best method in clinical practice and in research studies to determine left atrial size. *Am J Cardiol* 1999;84:829-32.
129. Loperfido F, Pennestri F, Digaetano A, Scabbia E, Santarelli P, Mongiardo R, et al. Assessment of left atrial dimensions by cross sectional echocardiography in patients with mitral valve disease. *Br Heart J* 1983;50:570-8.
130. Vyas H, Jackson K, Chenzbraun A. Switching to volumetric left atrial measurements: impact on routine echocardiographic practice. *Eur J Echocardiogr* 2011;12.
131. Gottdiener JS, Kitzman DW, Aurigemma GP, Arnold AM, Manolio TA. Left atrial volume, geometry, and function in systolic and diastolic heart failure of persons  $\geq 65$  years of age (The Cardiovascular Health Study). *Am J Cardiol* 2006;97:83-9.
132. Losi Ma, Betocchi S, Aversa M, Lombardi R, Miranda M, Ciampi Q, et al. Determinants of the development of atrial fibrillation in hypertrophic cardiomyopathy. *Circulation* 2002;106:710.
133. Rossi A, Ciccoira M, Zanolli L, Sandrini R, Golia G, Zardini P, et al. Determinants and prognostic value of left atrial volume in patients with dilated cardiomyopathy. *J Am Coll Cardiol* 2002;40:1425-30.
134. Takemoto Y, Barnes ME, Seward JB, Lester SJ, Appleton CA, Gersh BJ, et al. Usefulness of left atrial volume in predicting first congestive heart failure in patients  $\geq 65$  years of age with well-preserved left ventricular systolic function. *Am J Cardiol* 2005;96:832-6.
135. Tani T, Tanabe K, Ono M, Yamaguchi K, Okada M, Sumida T, et al. Left atrial volume and the risk of paroxysmal atrial fibrillation in patients with hypertrophic cardiomyopathy. *J Am Soc Echocardiogr* 2004;17:644-8.
136. Tsang TS, Abhayaratna WP, Barnes ME, Miyasaka Y, Gersh BJ, Bailey KR, et al. Prediction of cardiovascular outcomes with left atrial size - Is volume superior to area or diameter? *J Am Coll Cardiol* 2006;47:1018-23.
137. Pritchett AM, Jacobsen SJ, Mahoney DW, Rodeheffer RJ, Bailey KR, Redfield MM. Left atrial volume as an index of left atrial size: a population-based study. *J Am Coll Cardiol* 2003;41:1036-43.
138. Jenkins C, Bricknell K, Marwick TH. Use of real-time three-dimensional echocardiography to measure left atrial volume: Comparison with other echocardiographic techniques. *J Am Soc Echocardiogr* 2005;18:991-7.
139. Maceira AM, Cosin-Sales J, Roughton M, Prasad SK, Pennell DJ. Reference left atrial dimensions and volumes by steady state free precession cardiovascular magnetic resonance. *J Cardiovasc Magn Reson* 2010;12:65.
140. Rodevand O, Bjornerheim R, Ljosland M, Maehle J, Smith HJ, Ihlen H. Left atrial volumes assessed by three- and two-dimensional echocardiography compared to MRI estimates. *Int J Cardiovasc Imaging* 1999;15:397-410.
141. Stojanovska J, Cronin P, Patel S, Gross BH, Oral H, Chughtai K, et al. Reference Normal Absolute and Indexed Values From ECG-Gated MDCT: Left Atrial Volume, Function, and Diameter. *Am J Roentgenol* 2011;197:631-7.
142. Ujino K, Barnes ME, Cha SS, Langins AP, Bailey KR, Seward JB, et al. Two-dimensional echocardiographic methods for assessment of left atrial volume. *Am J Cardiol* 2006;98:1185-8.
143. Aurigemma GP, Gottdiener JS, Arnold AM, Chinali M, Hill JC, Kitzman D. Left Atrial Volume and Geometry in Healthy Aging The Cardiovascular Health Study. *Circ Cardiovasc Imaging* 2009;2:282-9.
144. Thomas L, Levett K, Boyd A, Leung DYC, Schiller NB, Ross DL. Compensatory changes in atrial volumes with normal aging: Is atrial enlargement inevitable? *J Am Coll Cardiol* 2002;40:1630-5.
145. Yamaguchi K, Tanabe K, Tani T, Yagi T, Fujii Y, Konda T, et al. Left atrial volume in normal Japanese adults. *Circ J* 2006;70:285-8.
146. Russo C, Hahn RT, Jin ZZ, Homma S, Sacco RL, Di Tullio MR. Comparison of Echocardiographic Single-Plane versus Biplane Method in the Assessment of Left Atrial Volume and Validation by Real Time Three-Dimensional Echocardiography. *J Am Soc Echocardiogr* 2010;23:954-60.
147. Nistri S, Galderisi M, Ballo P, Olivetto I, D'Andrea A, Pagliani L, et al. Determinants of echocardiographic left atrial volume: implications for normalcy. *Eur J Echocardiogr* 2011;12:826-33.
148. Vasan RS, Levy D, Larson MG, Benjamin EJ. Interpretation of echocardiographic measurements: a call for standardization. *Am Heart J* 2000;139:412-22.
149. Knutsen KM, Stugaard M, Michelsen S, Otterstad JE. M-mode echocardiographic findings in apparently healthy, non-athletic Norwegians aged 20-70 years. Influence of age, sex and body surface area. *J Intern Med* 1989;225:111-5.
150. Wang Y, Gutman JM, Heilbron D, Wahr D, Schiller NB. Atrial volume in a normal adult population by two-dimensional echocardiography. *Chest* 1984;86:595-601.
151. Cacciapuoti F, Scognamiglio A, Paoli VD, Romano C, Cacciaputo F. Left Atrial Volume Index as Indicator of Left Ventricular Diastolic Dysfunction. *J Cardiovasc Ultrasound* 2012;20:25-9.
152. Orban M, Bruce CJ, Pressman GS, Leinveber P, Romero-Corral A, Korinek J, et al. Dynamic Changes of Left Ventricular Performance and Left Atrial Volume Induced by the Mueller Maneuver in Healthy Young Adults and Implications for Obstructive Sleep Apnea, Atrial Fibrillation, and Heart Failure. *Am J Cardiol* 2008;102:1557-61.
153. Whitlock M, Garg A, Gelow J, Jacobson T, Broberg C. Comparison of Left and Right Atrial Volume by Echocardiography Versus Cardiac Magnetic Resonance Imaging Using the Area-Length Method. *Am J Cardiol* 2010;106:1345-50.
154. Yoshida C, Nakao S, Goda A, Naito Y, Matsumoto M, Otsuka M, et al. Value of assessment of left atrial volume and diameter in patients with heart failure but with normal left ventricular ejection fraction and mitral flow velocity pattern. *Eur J Echocardiogr* 2009;10:278-81.
155. Iwataki M, Takeuchi M, Otani K, Kuwaki H, Haruki N, Yoshitani H, et al. Measurement of left atrial volume from transthoracic three-dimensional echocardiographic datasets using the biplane Simpson's technique. *J Am Soc Echocardiogr* 2012;25:1319-26.
156. Nagueh SF, Appleton CP, Gillebert TC, Marino PN, Oh JK, Smiseth OA, et al. Recommendations for the evaluation of left ventricular diastolic function by echocardiography. *J Am Soc Echocardiogr* 2009;22:107-33.
157. Miyasaka Y, Tsujimoto S, Maeba H, Yuasa F, Takehana K, Dote K, et al. Left atrial volume by real-time three-dimensional echocardiography: validation by 64-slice multidetector computed tomography. *J Am Soc Echocardiogr* 2011;24:680-6.
158. Rohner A, Brinkert M, Kawel N, Buechel RR, Leibundgut G, Grize L, et al. Functional assessment of the left atrium by real-time three-dimensional echocardiography using a novel dedicated analysis tool: initial validation studies in comparison with computed tomography. *Eur J Echocardiogr* 2011;12:497-505.

159. Artang R, Migrino RQ, Harmann L, Bowers M, Woods TD. Left atrial volume measurement with automated border detection by 3-dimensional echocardiography: comparison with Magnetic Resonance Imaging. *Cardiovasc Ultrasound* 2009;7:16.
160. Mor-Avi V, Yodwut C, Jenkins C, Kuhl H, Nesser HJ, Marwick TH, et al. Real-time 3D echocardiographic quantification of left atrial volume: multicenter study for validation with CMR. *JACC Cardiovasc Imaging* 2012;5:769-77.
161. Caselli S, Canali E, Foschi ML, Santini D, Di Angelantonio E, Pandian NG, et al. Long-term prognostic significance of three-dimensional echocardiographic parameters of the left ventricle and left atrium. *Eur J Echocardiogr* 2010;11:250-6.
162. Suh IW, Song JM, Lee EY, Kang SH, Kim MJ, Kim JJ, et al. Left atrial volume measured by real-time 3-dimensional echocardiography predicts clinical outcomes in patients with severe left ventricular dysfunction and in sinus rhythm. *J Am Soc Echocardiogr* 2008;21:439-45.
163. Maddukuri PV, Vieira ML, DeCastro S, Maron MS, Kuvlin JT, Patel AR, et al. What is the best approach for the assessment of left atrial size? Comparison of various unidimensional and two-dimensional parameters with three-dimensional echocardiographically determined left atrial volume. *J Am Soc Echocardiogr* 2006;19:1026-32.
164. Aune E, Baekkevar M, Roislien J, Rodevand O, Otterstad JE. Normal reference ranges for left and right atrial volume indexes and ejection fractions obtained with real-time three-dimensional echocardiography. *Eur J Echocardiogr* 2009;10:738-44.
165. Peluso D, Badano LP, Muraru D, Dianco LD, Cucchini U, Kocabay G, et al. Right Atrial Size and FUnction assessed with three-dimensional and speckle-tracking echocardiography in 200 healthy volunteers. *Eur Heart J Cardiovasc Imaging* 2013;14:1106-14.
166. DePace NL, Ren JF, Kotler MN, Mintz GS, Kimbiris D, Kalman P. Two-dimensional echocardiographic determination of right atrial emptying volume: a noninvasive index in quantifying the degree of tricuspid regurgitation. *Am J Cardiol* 1983;52:525-9.
167. Kaplan JD, Evans GT, Foster E, Lim D, Schiller NB. Evaluation of Electrocardiographic Criteria for Right Atrial Enlargement by Quantitative 2-Dimensional Echocardiography. *J Am Coll Cardiol* 1994;23:747-52.
168. Quraini D, Pandian NG, Patel AR. Three-Dimensional Echocardiographic Analysis of Right Atrial Volume in Normal and Abnormal Hearts: Comparison of Biplane and Multiplane Methods. *Echocardiogr J Cardiovasc Ultrasound Allied Tech* 2012;29:608-13.
169. Anderson RH. Clinical anatomy of the aortic root. *Heart* 2000;84:670-3.
170. Anderson RH. Further anatomical insights regarding the Ross procedure. *Ann Thorac Surg* 2006;81:411-2.
171. Piazza N, de Jaegere P, Schultz C, Becker AE, Serruys PW, Anderson RH. Anatomy of the aortic valvar complex and its implications for transcatheter implantation of the aortic valve. *Circ Cardiovasc Interv* 2008;1:74-81.
172. Ho SY. Structure and anatomy of the aortic root. *Eur J Echocardiogr* 2009;10:i3-10.
173. Messika-Zeitoun D, Serfaty JM, Brochet E, Ducrocq G, Lepage L, Detaint D, et al. Multimodal assessment of the aortic annulus diameter: implications for transcatheter aortic valve implantation. *J Am Coll Cardiol* 2010;55:186-94.
174. Moss RR, Ivens E, Pasupati S, Humphries K, Thompson CR, Munt B, et al. Role of echocardiography in percutaneous aortic valve implantation. *JACC Cardiovasc Imaging* 2008;1:15-24.
175. Walther T, Dewey T, Borger MA, Kempfert J, Linke A, Becht R, et al. Transapical aortic valve implantation: step by step. *Ann Thorac Surg* 2009;87:276-83.
176. Tops LF, Wood DA, Delgado V, Schuijff JD, Mayo JR, Pasupati S, et al. Noninvasive evaluation of the aortic root with multislice computed tomography implications for transcatheter aortic valve replacement. *JACC Cardiovasc Imaging* 2008;1:321-30.
177. Kazui T, Izumoto H, Yoshioka K, Kawazoe K. Dynamic morphologic changes in the normal aortic annulus during systole and diastole. *J Heart Valve Dis* 2006;15:617-21.
178. Shiran A, Adawi S, Gananeem M, Asmer E. Accuracy and reproducibility of left ventricular outflow tract diameter measurement using transthoracic when compared with transesophageal echocardiography in systole and diastole. *Eur J Echocardiogr* 2009;10:319-24.
179. Hamdan A, Guetta V, Konen E, Goitein O, Segev A, Raanani E, et al. Deformation dynamics and mechanical properties of the aortic annulus by 4-dimensional computed tomography: insights into the functional anatomy of the aortic valve complex and implications for transcatheter aortic valve therapy. *J Am Coll Cardiol* 2012;59:119-27.
180. Chin D. Echocardiography for transcatheter aortic valve implantation. *Eur J Echocardiogr* 2009;10:i21-9.
181. Zamorano JL, Badano LP, Bruce C, Chan KL, Goncalves A, Hahn RT, et al. EAE/ASE recommendations for the use of echocardiography in new transcatheter interventions for valvular heart disease. *J Am Soc Echocardiogr* 2011;24:937-65.
182. Holmes DR Jr., Mack MJ, Kaul S, Agnihotri A, Alexander KP, Bailey SR, et al. 2012 ACCF/AATS/SCAI/STS expert consensus document on transcatheter aortic valve replacement. *J Am Coll Cardiol* 2012;59:1200-54.
183. Achenbach S, Delgado V, Hausleiter J, Schoenhagen P, Min JK, Leipsic JA. SCCT expert consensus document on computed tomography imaging before transcatheter aortic valve implantation (TAVI)/transcatheter aortic valve replacement (TAVR). *J Cardiovasc Comput Tomogr* 2012;6:366-80.
184. Kasel AM, Cassese S, Bleiziffer S, Amaki M, Hahn RT, Kastrati A, et al. Standardized imaging for aortic annular sizing: implications for transcatheter valve selection. *JACC Cardiovasc Imaging* 2013;6:249-62.
185. Pershad A, Stone D, Morris MF, Fang K, Gellert G. Aortic annulus measurement and relevance to successful transcatheter aortic valve replacement: a new technique using 3D TEE. *J Interv Cardiol* 2013;26:302-9.
186. Hahn RT, Khalique O, Williams MR, Koss E, Paradis JM, Daneault B, et al. Predicting paravalvular regurgitation following transcatheter valve replacement: utility of a novel method for three-dimensional echocardiographic measurements of the aortic annulus. *J Am Soc Echocardiogr* 2013;26:1043-52.
187. Flachskampf FA, Wouters PF, Edvardsen T, Evangelista A, Habib G, Hoffman P, et al. Recommendations for transoesophageal echocardiography: EACVI update 2014. *Eur Heart J Cardiovasc Imaging* 2014;15:353-65.
188. Hutter A, Opitz A, Bleiziffer S, Ruge H, Hettich I, Mazzitelli D, et al. Aortic annulus evaluation in transcatheter aortic valve implantation. *Catheter Cardiovasc Interv* 2010;76:1009-19.
189. Leipsic J, Gurvitch R, Labounty TM, Min JK, Wood D, Johnson M, et al. Multidetector computed tomography in transcatheter aortic valve implantation. *JACC Cardiovasc Imaging* 2011;4:416-29.
190. Delgado V, Ng AC, van de Veire NR, van der Kley F, Schuijff JD, Tops LF, et al. Transcatheter aortic valve implantation: role of multidetector row computed tomography to evaluate prosthesis positioning and deployment in relation to valve function. *Eur Heart J* 2010;31:1114-23.
191. Willson AB, Webb JG, Freeman M, Wood DA, Gurvitch R, Thompson CR, et al. Computed tomography-based sizing recommendations for transcatheter aortic valve replacement with balloon-expandable valves: Comparison with transesophageal echocardiography and rationale for implementation in a prospective trial. *J Cardiovasc Comput Tomogr* 2012;6:406-14.
192. Utsunomiya H, Yamamoto H, Horiguchi J, Kunita E, Okada T, Yamazato R, et al. Underestimation of aortic valve area in calcified aortic valve disease: effects of left ventricular outflow tract ellipticity. *Int J Cardiol* 2012;157:347-53.
193. Gurvitch R, Webb JG, Yuan R, Johnson M, Hague C, Willson AB, et al. Aortic annulus diameter determination by multidetector computed tomography: reproducibility, applicability, and implications for transcatheter aortic valve implantation. *JACC Cardiovasc Interv* 2011;4:1235-45.

194. Goldstein SA, Evangelista A, Abbara S, Arai A, Acsh F, Badano LP, et al. ASE/EAE recommendations for multimodality imaging techniques for diseases of the aorta: Expert consensus statement. *J Am Soc Echocardiogr* 2014 (in press).
195. Roman MJ, Devereux RB, Kramer-Fox R, O'Loughlin J. Two-dimensional echocardiographic aortic root dimensions in normal children and adults. *Am J Cardiol* 1989;64:507-12.
196. Vasan RS, Larson MG, Benjamin EJ, Levy D. Echocardiographic reference values for aortic root size: the Framingham Heart Study. *J Am Soc Echocardiogr* 1995;8:793-800.
197. Roman MJ, Devereux RB, Niles NW, Hochreiter C, Kligfield P, Sato N, et al. Aortic root dilatation as a cause of isolated, severe aortic regurgitation. Prevalence, clinical and echocardiographic patterns, and relation to left ventricular hypertrophy and function. *Ann Intern Med* 1987;106:800-7.
198. Moreno FL, Hagan AD, Holmen JR, Pryor TA, Strickland RD, Castle CH. Evaluation of size and dynamics of the inferior vena cava as an index of right-sided cardiac function. *Am J Cardiol* 1984;53:579-85.
199. Brennan JM, Blair JE, Goonewardena S, Ronan A, Shah D, Vasaiwala S, et al. Reappraisal of the use of inferior vena cava for estimating right atrial pressure. *J Am Soc Echocardiogr* 2007;20:857-61.
200. Kircher BJ, Himelman RB, Schiller NB. Noninvasive estimation of right atrial pressure from the inspiratory collapse of the inferior vena cava. *Am J Cardiol* 1990;66:493-6.
201. Goldhammer E, Mesnick N, Abinader EG, Sagiv M. Dilated inferior vena cava: a common echocardiographic finding in highly trained elite athletes. *J Am Soc Echocardiogr* 1999;12:988-93.
202. Jue J, Chung W, Schiller NB. Does inferior vena cava size predict right atrial pressures in patients receiving mechanical ventilation? *J Am Soc Echocardiogr* 1992;5:613-9.
203. Arthur ME, Landolfo C, Wade M, Castresana MR. Inferior vena cava diameter (IVCD) measured with transesophageal echocardiography (TEE) can be used to derive the central venous pressure (CVP) in anesthetized mechanically ventilated patients. *Echocardiography* 2009;26:140-9.
204. Hiratzka LF, Bakris GL, Beckman JA, Bersin RM, Carr VF, Casey DE Jr, et al. 2010 ACCF/AHA/AATS/ACR/ASA/SCA/SCAI/SIR/STS/SVM guidelines for the diagnosis and management of patients with Thoracic Aortic Disease: a report of the American College of Cardiology Foundation/American Heart Association Task Force on Practice Guidelines, American Association for Thoracic Surgery, American College of Radiology, American Stroke Association, Society of Cardiovascular Anesthesiologists, Society for Cardiovascular Angiography and Interventions, Society of Interventional Radiology, Society of Thoracic Surgeons, and Society for Vascular Medicine. *Circulation* 2010;121:e266-369.
205. Mosteller RD. Simplified calculation of body-surface area. *N Engl J Med* 1987;317:1098.

## APPENDIX

---

### Methods

When possible, data on systolic blood pressure, diastolic blood pressure, diagnosis of hypertension, treatment of hypertension, diagnosis of diabetes, fasting glucose levels, creatinine levels, total cholesterol level, low-density lipoprotein cholesterol levels, and triglyceride levels were obtained. BSA was calculated using the Mosteller formula.<sup>205</sup> Body mass index was calculated by dividing the weight in kilograms by the height in meters squared.

### Echocardiographic Measurements

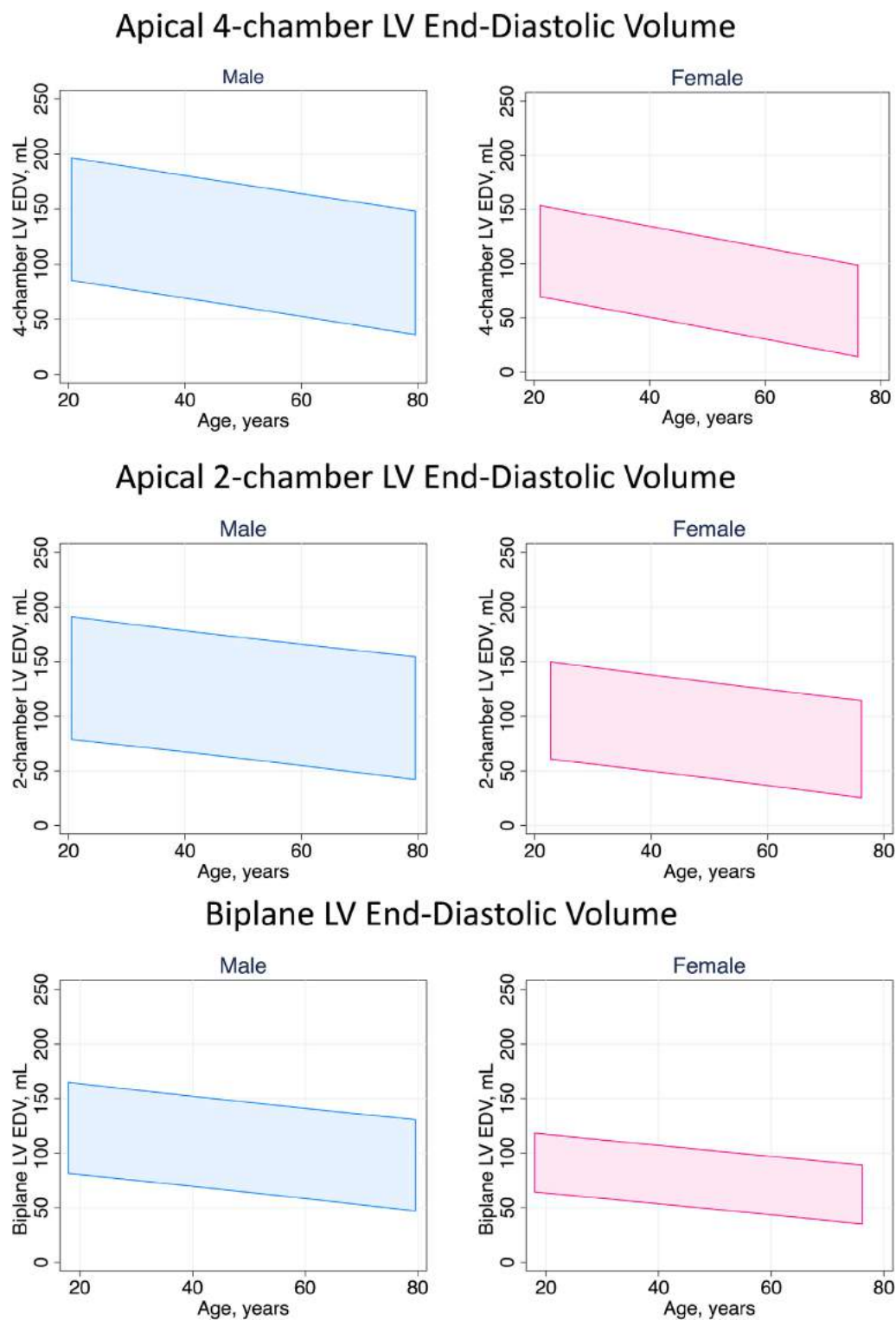
Transthoracic echocardiographic measurements were performed for each of the studies as per available published guidelines.<sup>1</sup> Values for the following measurements were provided from the following 2D

transthoracic echocardiographic views: LV end-diastolic diameter and LV end-systolic diameter from the parasternal long-axis view; LV EDV, LV ESV, and LV EF from the apical four- and two-chamber views; and LV EDV, LV ESV, LV stroke volume, and LV EF from the biplane view.

### Statistical Analysis

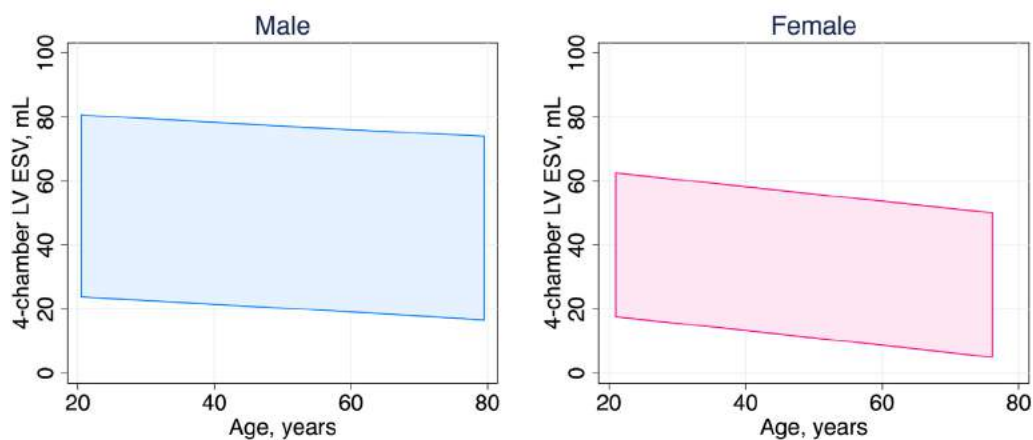
All studied parameters were found to satisfy a normal distribution using the Kolmogorov-Smirnov test, and summary data for these variables are expressed as mean  $\pm$  SD. Multivariate analysis was used to determine the dependence of the measured parameters on age, gender, and BSA. Simple univariate linear regression against age was then used to construct the presented nomograms normalized for BSA and divided by gender as mean and 95% confidence intervals. *P* values  $< .05$  were considered significant.



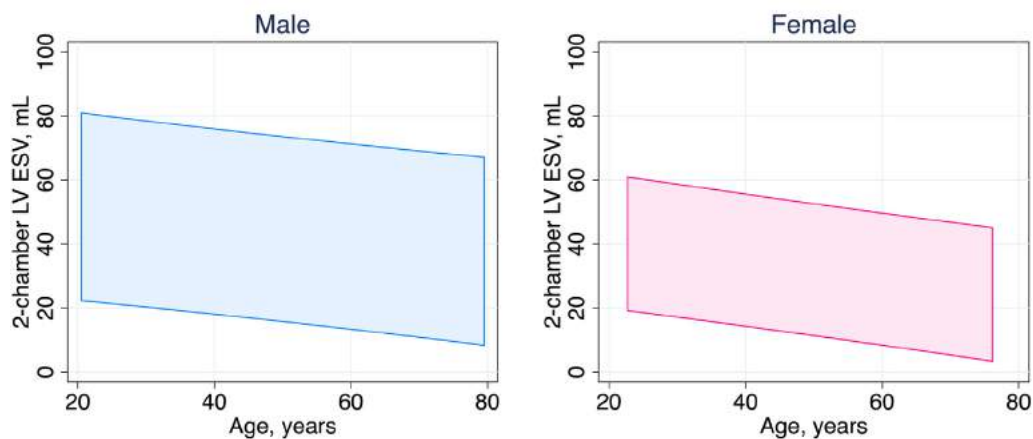


**Supplemental Figure 1** For men (*left column*) and women (*right column*), the 95% confidence intervals for apical four-chamber view (*top row*), apical two-chamber view (*middle row*) and the biplane (*bottom row*) LV EDV on the basis of age.

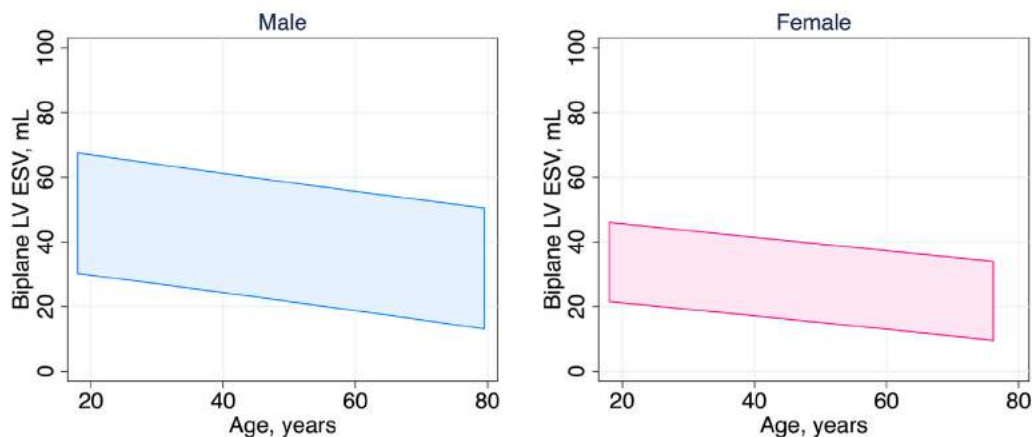
### Apical 4-chamber LV End-Systolic Volume



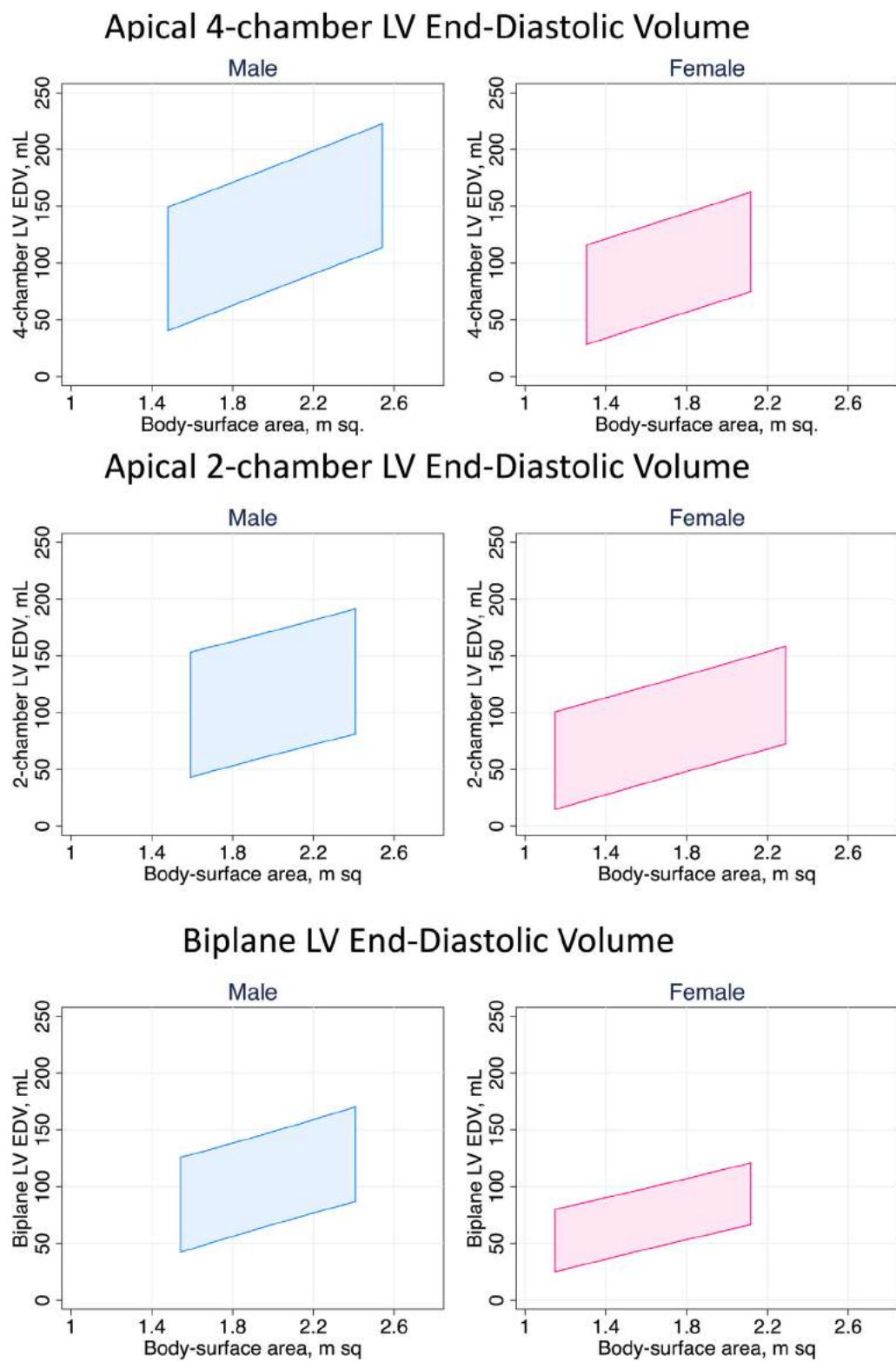
### Apical 2-chamber LV End-Systolic Volume



### Biplane LV End-Systolic Volume

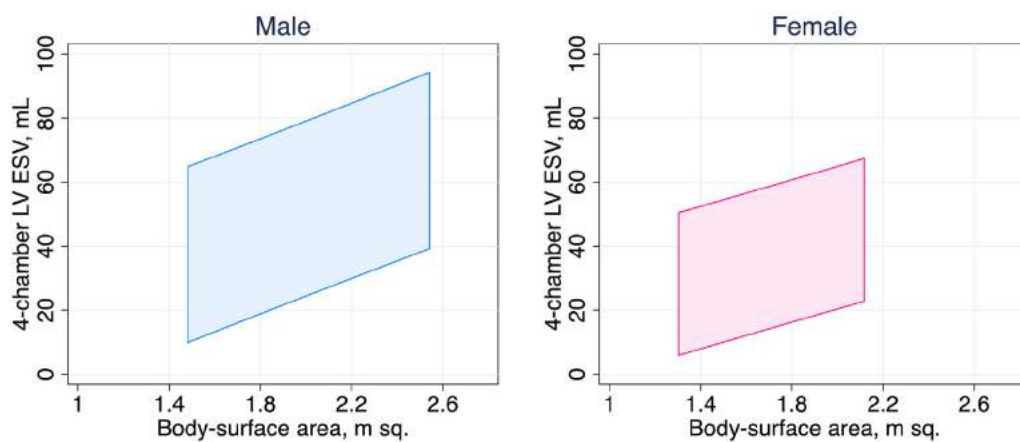


**Supplemental Figure 2** For men (*left column*) and women (*right column*), the 95% confidence intervals for apical four-chamber view (*top row*), apical two-chamber view (*middle row*), and the biplane (*bottom row*) LV ESVs on the basis of age.

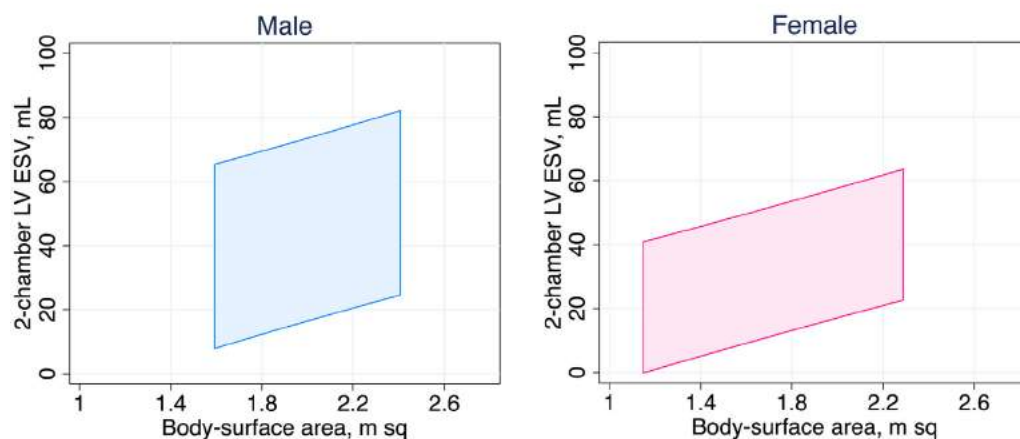


**Supplemental Figure 3** For men (*left column*) and women (*right column*), the 95% confidence intervals for apical four-chamber view (*top row*), apical two-chamber view (*middle row*), and the biplane (*bottom row*) LV EDVs on the basis of BSA.

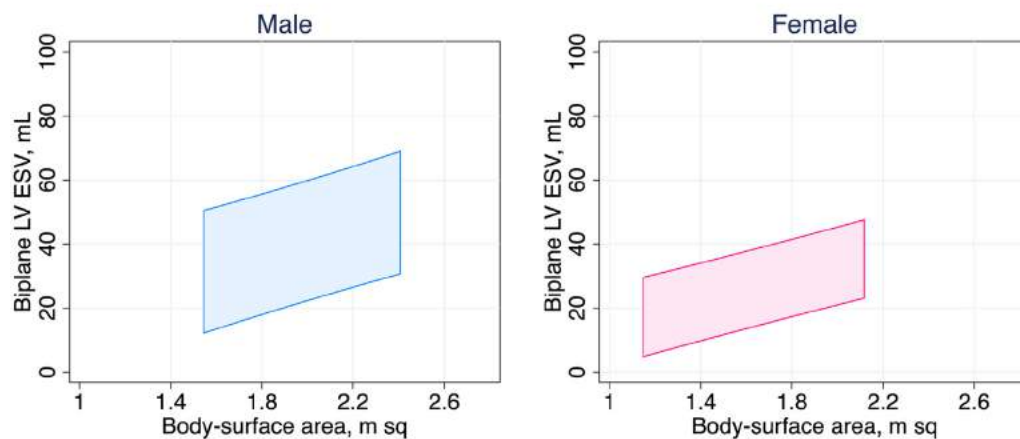
## Apical 4-chamber LV End-Systolic Volume



## Apical 2-chamber LV End-Systolic Volume



## Biplane LV End-Systolic Volume



**Supplemental Figure 4** For men (left column) and women (right column), the 95% confidence intervals for apical four-chamber view (top row), apical two-chamber view (middle row), and the biplane (bottom row) LV ESVs on the basis of BSA.



**Supplemental Table 1** Sources of the data from which LV measurements were obtained, grouped by echocardiographic view, gender, and baseline characteristics

	Parasternal long-axis view	Apical four-chamber view	Apical two-chamber view	Biplane view
Data Sources (n)	Asklepios (1,019) Flemengho (252)	CARDIA5 (1,027) Asklepios (1,006) Flemengho (245)	CARDIA25 (588) Asklepios10 (161) Flemengho (244)	Padua (111) Asklepios10 (161) Flemengho (248)
<b>Men</b>				
n	502	962	410	201
Race white (n)	502	770	345	201
Race black (n)	0	192	65	0
Age (y)	45 ± 8	37 ± 10	50 ± 8	47 ± 14
Height (cm)	177 ± 7	178 ± 7	178 ± 7	177 ± 8
Weight (kg)	78 ± 10	77 ± 10	80 ± 10	79 ± 11
BSA (m <sup>2</sup> )	1.96 ± 0.14	1.94 ± 0.15	1.99 ± 0.15	1.97 ± 0.17
BMI (kg/m <sup>2</sup> )	25 ± 3	24 ± 3	25 ± 3	25 ± 3
<b>Women</b>				
n	769	1,316	583	319
Race white (n)	769	244	509	319
Race black (n)	0	1,072	74	0
Age (y)	45 ± 7	37 ± 10	50 ± 7	48 ± 12
Height (cm)	164 ± 6	164 ± 6	165 ± 6	164 ± 7
Weight (kg)	63 ± 8	62 ± 9	66 ± 9	63 ± 9
BSA (m <sup>2</sup> )	1.69 ± 0.13	1.68 ± 0.13	1.73 ± 0.15	1.70 ± 0.14
BMI (kg/m <sup>2</sup> )	23 ± 3	23 ± 3	24 ± 3	24 ± 3

**Supplemental Table 2** Normal values for LV size and function parameters for men and women obtained from different echocardiographic views, listed with the number of subjects used to derive them

Parameter	Male			Female		
	n	Mean $\pm$ SD	2-SD range	n	Mean $\pm$ SD	2-SD range
Parasternal long-axis view*						
Diastolic LV internal dimension (mm)	502	50.2 $\pm$ 4.1	42.0–58.4	769	45.0 $\pm$ 3.6	37.8–52.2
Systolic LV internal dimension (mm)	389	32.4 $\pm$ 3.7	25.0–39.8	630	28.2 $\pm$ 3.3	21.6–34.8
Apical two-chamber view†						
LV EF (%)	410	62 $\pm$ 7	48–76	583	64 $\pm$ 6	52–76
LV EDV (mL)	410	117 $\pm$ 29	59–175	583	87 $\pm$ 23	41–133
LV ESV (mL)	410	45 $\pm$ 15	15–75	583	32 $\pm$ 11	10–54
Apical four-chamber view‡						
LV EF (%)	962	60 $\pm$ 7	46–74	1316	62 $\pm$ 8	46–78
LV EDV (mL)	962	127 $\pm$ 29	69–185	1316	94 $\pm$ 23	48–140
LV ESV (mL)	962	50 $\pm$ 14	22–78	1316	36 $\pm$ 12	12–60
Biplane§						
LV EF (%)	201	62 $\pm$ 5	52–72	319	64 $\pm$ 5	54–74
LV EDV (mL)	201	106 $\pm$ 22	62–150	319	76 $\pm$ 15	46–106
LV ESV (mL)	201	41 $\pm$ 10	21–61	319	28 $\pm$ 7	14–42
Normalized to BSA						
Apical two-chamber view†						
LV EDV (mL/m <sup>2</sup> )	410	59 $\pm$ 14	31–87	583	50 $\pm$ 12	26–74
LV ESV (mL/m <sup>2</sup> )	410	23 $\pm$ 7	9–37	583	18 $\pm$ 6	6–30
Apical four-chamber view‡						
LV EDV (mL/m <sup>2</sup> )	962	65 $\pm$ 14	37–93	1316	56 $\pm$ 13	30–82
LV ESV (mL/m <sup>2</sup> )	962	26 $\pm$ 7	12–40	1316	21 $\pm$ 7	7–35
Biplane§						
LV EDV (mL/m <sup>2</sup> )	201	54 $\pm$ 10	34–74	319	45 $\pm$ 8	29–61
LV ESV (mL/m <sup>2</sup> )	201	21 $\pm$ 5	11–31	319	16 $\pm$ 4	8–24

Data Sources.

\*Asklepios, Flemengho.

†Asklepios, CARDIA5, Flemengho.

‡Flemengho, CARDIA25; Asklepios10.

§Asklepios10, Flemengho, Padua.

**Supplemental Table 3** Normal ranges and severity partition cutoff values for 2DE-derived LV size, function and mass

	Male				Female			
	Normal range	Mildly abnormal	Moderately abnormal	Severely abnormal	Normal range	Mildly abnormal	Moderately abnormal	Severely abnormal
LV dimension								
LV diastolic diameter (cm)	4.2–5.8	5.9–6.3	6.4–6.8	>6.8	3.8–5.2	5.3–5.6	5.7–6.1	>6.1
LV diastolic diameter/BSA (cm/m <sup>2</sup> )	2.2–3.0	3.1–3.3	3.4–3.6	>3.6	2.3–3.1	3.2–3.4	3.5–3.7	>3.7
LV systolic diameter (cm)	2.5–4.0	4.1–4.3	4.4–4.5	>4.5	2.2–3.5	3.6–3.8	3.9–4.1	>4.1
LV systolic diameter/BSA (cm/m <sup>2</sup> )	1.3–2.1	2.2–2.3	2.4–2.5	>2.5	1.3–2.1	2.2–2.3	2.4–2.6	>2.6
LV volume								
LV diastolic volume (mL)	62–150	151–174	175–200	>200	46–106	107–120	121–130	>130
LV diastolic volume/BSA (mL/m <sup>2</sup> )	34–74	75–89	90–100	>100	29–61	62–70	71–80	>80
LV systolic volume (mL)	21–61	62–73	74–85	>85	14–42	43–55	56–67	>67
LV systolic volume/BSA (mL/m <sup>2</sup> )	11–31	32–38	39–45	>45	8–24	25–32	33–40	>40
LV function								
LV EF (%)	52–72	41–51	30–40	<30	54–74	41–53	30–40	<30
LV mass by linear method								
Septal wall thickness (cm)	0.6–1.0	1.1–1.3	1.4–1.6	>1.6	0.6–0.9	1.0–1.2	1.3–1.5	>1.5
Posterior wall thickness (cm)	0.6–1.0	1.1–1.3	1.4–1.6	>1.6	0.6–0.9	1.0–1.2	1.3–1.5	>1.5
LV mass (g)	88–224	225–258	259–292	>292	67–162	163–186	187–210	>210
LV mass/BSA (g/m <sup>2</sup> )	49–115	116–131	132–148	>148	43–95	96–108	109–121	>121
LV mass by 2D method								
LV mass (g)	96–200	201–227	228–254	>254	66–150	151–171	172–193	>193
LV mass/BSA (g/m <sup>2</sup> )	50–102	103–116	117–130	>130	44–88	89–100	101–112	>112

**Supplemental Table 4** LV function by age decile and gender (mean and 2 SDs)

Parameter	Age 20–29 y				Age 30–39 y				Age 40–49 y				Age 50–59				Age 60			
	Male		Female		Male		Female		Male		Female		Male		Female		Male		Female	
	n	Mean ± SD	n	Mean ± SD	n	Mean ± SD	n	Mean ± SD	n	Mean ± SD	n	Mean ± SD	n	Mean ± SD	n	Mean ± SD	n	Mean ± SD	n	Mean ± SD
Apical two-chamber view*																				
LV EF (%)	14	62 ± 4	16	62 ± 6	27	62 ± 5	18	65 ± 5	144	62 ± 6	223	63 ± 6	191	61 ± 8	290	64 ± 6	34	63 ± 6	36	65 ± 6
LV EDV (mL)	14	122 ± 18	16	88 ± 21	27	111 ± 27	18	88 ± 14	144	121 ± 25	223	90 ± 22	191	119 ± 30	290	87 ± 23	34	88 ± 22	36	63 ± 12
LV ESV (mL)	14	46 ± 7	16	33 ± 10	27	42 ± 11	18	31 ± 7	144	46 ± 14	223	34 ± 11	191	46 ± 16	290	32 ± 11	34	32 ± 8	36	22 ± 6
Apical four-chamber view†																				
LV EF (%)	247	63 ± 6	274	63 ± 6	363	61 ± 7	478	62 ± 8	235	58 ± 7	383	60 ± 9	96	60 ± 7	163	60 ± 8	21	59 ± 5	18	60 ± 6
LV EDV (mL)	247	136 ± 29	274	106 ± 23	363	131 ± 28	478	99 ± 23	235	118 ± 28	383	84 ± 20	96	115 ± 29	163	82 ± 18	21	110 ± 24	18	74 ± 15
LV ESV (mL)	247	51 ± 13	274	39 ± 11	363	51 ± 14	478	37 ± 11	235	50 ± 16	383	34 ± 12	96	47 ± 16	163	33 ± 12	21	45 ± 12	18	29 ± 7
Biplane‡																				
LV EF (%)	29	62 ± 5	39	63 ± 4	34	61 ± 4	34	63 ± 4	45	62 ± 5	82	64 ± 4	55	63 ± 5	116	64 ± 5	38	63 ± 5	48	65 ± 6
LV EDV (mL)	29	118 ± 25	39	87 ± 18	34	114 ± 22	34	82 ± 13	45	107 ± 20	82	77 ± 13	55	101 ± 21	116	73 ± 14	38	98 ± 21	48	68 ± 11
LV ESV (mL)	29	46 ± 11	39	32 ± 8	34	44 ± 10	34	31 ± 6	45	41 ± 10	82	28 ± 6	55	38 ± 9	116	26 ± 6	38	36 ± 9	48	24 ± 6
LV stroke volume (mL)	29	73 ± 17	39	55 ± 12	34	69 ± 15	34	52 ± 8	45	66 ± 12	82	49 ± 9	55	64 ± 15	116	46 ± 10	38	62 ± 14	48	44 ± 8
Normalized to BSA																				
Apical two-chamber view*																				
LV EDV (mL/m <sup>2</sup> )	14	59 ± 8	16	50 ± 9	27	56 ± 14	18	50 ± 8	144	61 ± 13	223	52 ± 12	191	60 ± 14	290	51 ± 13	34	45 ± 11	36	37 ± 7
LV ESV (mL/m <sup>2</sup> )	14	22 ± 4	16	19 ± 5	27	21 ± 6	18	18 ± 4	144	23 ± 7	223	19 ± 6	191	23 ± 8	290	19 ± 6	34	16 ± 4	36	13 ± 3
Apical four-chamber view†																				
LV EDV (mL/m <sup>2</sup> )	247	70 ± 14	274	63 ± 13	363	67 ± 13	478	59 ± 13	235	60 ± 13	383	50 ± 11	96	59 ± 13	163	49 ± 10	21	56 ± 11	18	44 ± 8
LV ESV (mL/m <sup>2</sup> )	247	26 ± 6	274	23 ± 6	363	26 ± 7	478	22 ± 6	235	26 ± 8	383	20 ± 7	96	24 ± 14	163	20 ± 7	21	22 ± 5	18	17 ± 4
Biplane‡																				
LV EDV (mL/m <sup>2</sup> )	29	62 ± 10	39	52 ± 9	34	57 ± 11	34	49 ± 6	45	54 ± 9	82	45 ± 7	55	52 ± 9	116	43 ± 7	38	50 ± 10	48	40 ± 7
LV ESV (mL/m <sup>2</sup> )	29	24 ± 5	39	19 ± 4	34	22 ± 5	34	18 ± 4	45	21 ± 5	82	16 ± 3	55	19 ± 4	116	15 ± 3	38	18 ± 4	48	14 ± 3

Data sources.

\*Asklepios, CARDIA5, Flemehgho.

†Flemehgho, CARDIA25; Asklepios10.

‡Asklepios10, Flemehgho, Padua.



**Supplemental Table 5** LV size and function by race and gender

Parameter	Black				White			
	Male		Female		Male		Female	
	n	Mean $\pm$ SD	n	Mean $\pm$ SD	n	Mean $\pm$ SD	n	Mean $\pm$ SD
Apical two-chamber view*								
LV EF (%)	65	61 $\pm$ 7	74	64 $\pm$ 6	345	62 $\pm$ 7	509	64 $\pm$ 6
LV EDV (mL)	65	130 $\pm$ 28	74	99 $\pm$ 23	345	114 $\pm$ 28	509	85 $\pm$ 22
LV ESV (mL)	65	51 $\pm$ 16	74	36 $\pm$ 10	345	44 $\pm$ 14	509	31 $\pm$ 11
Apical four-chamber view†								
LV EF (%)	244	63 $\pm$ 6	192	64 $\pm$ 6	770	60 $\pm$ 7	1072	61 $\pm$ 8
LV EDV (mL)	244	135 $\pm$ 29	192	106 $\pm$ 23	770	125 $\pm$ 29	1072	91 $\pm$ 23
LV ESV (mL)	244	50 $\pm$ 12	192	38 $\pm$ 11	770	50 $\pm$ 15	1072	36 $\pm$ 12
Normalized to BSA								
Apical two-chamber view*								
LV EDV (mL/m <sup>2</sup> )	65	66 $\pm$ 13	74	55 $\pm$ 11	345	57 $\pm$ 14	509	50 $\pm$ 12
LV ESV (mL/m <sup>2</sup> )	65	26 $\pm$ 8	74	20 $\pm$ 6	345	22 $\pm$ 7	509	18 $\pm$ 6
Apical four-chamber view†								
LV EDV (mL/m <sup>2</sup> )	244	70 $\pm$ 14	192	62 $\pm$ 13	770	64 $\pm$ 14	1072	54 $\pm$ 13
LV ESV (mL/m <sup>2</sup> )	244	26 $\pm$ 6	192	22 $\pm$ 6	770	26 $\pm$ 7	1072	21 $\pm$ 7

Data sources.

\*Asklepios, CARDIA5, Flemengho.

†Flemengho, CARDIA25; Asklepios10.

**Supplemental Table 6** Normal LV strain values from meta-analysis and individual recent publications using specific vendors' equipment and software

vendor	Software	n	Mean	SD	LLN	Reference from list below
Varying	Meta-analysis	2597	−19.7%		NA	1
GE	EchoPAC BT 12	247	−21.5%	2.0%	−18%	2
	EchoPAC BT 12	207	−21.2%	1.6%	−18%	3
	EchoPAC BT 12	131	−21.2%	2.4%	−17%	4
	EchoPAC 110.1.3	333	−21.3%	2.1%	−17%	5
Philips	QLAB 7.1	330	−18.9%	2.5%	−14%	5
Toshiba	Ultra Extend	337	−19.9%	2.4%	−15%	5
Siemens	VVI 1.0	116	−19.8%	4.6%	−11%	6
	VVI 1.0	82	−17.3%	2.3%	−13%	7
Esaote	Mylab 50	30	−19.5%	3.1%	−13%	8

**References**

1. Yingchoncharoen T, Agarwal S, Popovic ZB, Marwick TH. Normal ranges of left ventricular strain: a meta-analysis. *J Am Soc Echocardiogr* 2013;26:185-91.
2. Kocabay G, Muraru D, Peluso D, Cucchini U, Mihaila S, Padayattil-Jose S, et al. Normal left ventricular mechanics by two-dimensional speckle-tracking echocardiography. Reference values in healthy adults. *Rev Esp Cardiol (Engl Ed)*. 2014;67:651-8.
3. Kouznetsova T, Staessen J, Department of Cardiology, Catholic University Leuven, personal communication.
4. Barbier P, University Milano, personal communication.
5. Takigiku K, Takeuchi M, Izumi C, Yuda S, Sakata K, Ohte N, et al. Normal range of left ventricular 2-dimensional strain: Japanese Ultrasound Speckle Tracking of the Left Ventricle (JUSTICE) study. *Circ J* 2012;76:2623-32.
6. Rodríguez-Bailón I, Jiménez-Navarro MF, Pérez-González, García-Orta R, Morillo-Velarde E, de Teresa-Galvána E. Left ventricular deformation and two-dimensional echocardiography: Temporal and other parameter values in normal subjects. *Rev Esp Cardiol*. 2010;63:1195-9.
7. Saleh HK, Villarraga HR, Kane GC, Pereira NL, Raichlin E, Yu Y, et al. Normal left ventricular mechanical function and synchrony values by speckle-tracking echocardiography in the transplanted heart with normal ejection fraction. *J Heart Lung Transplant* 2011;30:652-8.
8. Bussadori C, Moreo A, Di Donato M, De Chiara B, Negura D, Dall'Aglio E, et al. A new 2D-based method for myocardial velocity strain and strain rate quantification in a normal adult and paediatric population: assessment of reference values. *Cardiovascular Ultrasound* 2009;7:8. <http://dx.doi.org/10.1186/1476-7120-7-8>.

**Supplemental Table 7** Numbers of studies and subjects used to derive the reference values for RV chamber size and function

Parameter	Studies	n
RV basal diameter (mm)	12	695
RV mid-cavity diameter (mm)	14	1938
RVOT PLAX proximal diameter (mm)	11	380
RVOT SAX proximal diameter (mm)	5	193
RVOT SAX distal diameter (mm)	4	159
RV wall thickness (mm)	9	527
RV EDA (cm <sup>2</sup> )		
Men	2	909
Women	2	971
RV EDA indexed to BSA (cm <sup>2</sup> /m <sup>2</sup> )		
Men	2	909
Women	2	971
RV ESA (cm <sup>2</sup> )		
Men	1	533
Women	1	600
RV ESA indexed to BSA (cm <sup>2</sup> /m <sup>2</sup> )		
Men	1	533
Women	1	600
RV EDV indexed to BSA (mL/m <sup>2</sup> )		
Men	2	257
Women	2	285
RV ESV indexed to BSA (mL/m <sup>2</sup> )		
Men	2	257
Women	2	285
TAPSE (mm)	68	4803
Pulsed Doppler S wave (cm/s)	69	4752
Color Doppler S wave (cm/s)	9	409
RV fractional area change (%)	57	3606
RV free wall 2D strain (%)	18	782
RV 3D EF (%)	15	1162
Pulsed Doppler MPI	23	853
Tissue Doppler MPI	13	746
E wave deceleration time (ms)	30	1637
E/A	56	2829
e'/a'	33	1230
e'	43	3081
E/e'	8	545

CI, Confidence interval; EDA, end-diastolic area; ESA, end-systolic area; PLAX, parasternal long-axis view; RVOT, RV outflow tract; MPI, myocardial performance index.

Values are expressed as mean (95% CI), while normal limit is expressed as lower reference value (95% CI) and/or \*upper reference value (95% CI) where appropriate.

**Supplemental Table 8** Normal ranges for 3D echocardiographic RV size and function by gender and age decade (from Maffessanti *et al.*<sup>75</sup>)

Age (y)	n (women, men)	RV EDV (mL/m <sup>2</sup> )		RV ESV (mL/m <sup>2</sup> )		RV EF (%)	
		Women	Men	Women	Men	Women	Men
<30	102 (45, 57)	53 (38, 78)	66 (42, 100)	20 (8, 45)	28 (16, 52)	60 (43, 82)	56 (42, 68)
30–39	96 (50, 46)	50 (38, 77)	58 (35, 85)	18 (11, 38)	23 (12, 38)	63 (50, 78)	60 (47, 74)
40–49	96 (53, 43)	50 (34, 65)	54 (36, 78)	18 (8, 27)	21 (11, 33)	65 (49, 80)	59 (51, 75)
50–59	88 (47, 41)	49 (37, 69)	53 (36, 76)	18 (11, 29)	19 (10, 37)	62 (46, 76)	62 (45, 74)
60–69	69 (39, 30)	46 (26, 64)	52 (37, 86)	17 (8, 26)	19 (10, 36)	61 (50, 79)	63 (49, 79)
≥70	37 (23, 14)	43 (25, 62)	54 (31, 68)	12 (7, 21)	18 (7, 28)	71 (57, 82)	65 (55, 76)

Data are expressed as median (5th, 95th percentile).



**Supplemental Table 9** Normal values of LA size

	Women	Men
AP dimension (cm)	2.7–3.8	3.0–4.0
AP dimension index (cm/m <sup>2</sup> )	1.5–2.3	1.5–2.3
A4C area index (cm <sup>2</sup> /m <sup>2</sup> )	9.3 ± 1.7	8.9 ± 1.5
A2C area index (cm <sup>2</sup> /m <sup>2</sup> )	9.6 ± 1.4	9.3 ± 1.6
A4C volume index MOD (mL/m <sup>2</sup> )	25.1 ± 7.2	24.5 ± 6.4
A4C volume index AL (mL/m <sup>2</sup> )	27.3 ± 7.9	27.0 ± 7.0
A2C volume index MOD (mL/m <sup>2</sup> )	26.1 ± 6.7	27.1 ± 7.9
A2C volume index AL (mL/m <sup>2</sup> )	28.0 ± 7.3	28.9 ± 8.5